THE JOURNAL OF CHEMICAL PHYSICS

VOLUME 15 NUMBER 4

APRIL, 1947

Published by the
AMERICAN INSTITUTE OF PHYSICS
Lancaster, Pa. and New York, N. Y.

THE JOURNAL OF CHEMICAL PHYSICS

BOARD OF EDITORS

Editor

Associate Editors

Term ending December 31, 1947

CHARLES D. CORYELL
F. O. RICE
L. H. THOMAS
G. W. WHELAND
E. BRIGHT WILSON, JR.

Term ending December 31, 1948

K. J. MCCALLUM
A. L. PATTERSON
HERTHA SPONER
GEORGE UHLENBECK
BRUNO H. ZIMM

...cation of research and as a ... and carefully edited assemblage of pertinent ...

...for Contributors

... should be submitted to ... Chemical Laboratory, University ... Illinois. Papers are published in ... responsible for the publication manuscript ... original copy and carbon copy, typed ... with wide margins. References ... be numbered only and should be numbered ... Footnotes should be ... numbered consecutively throughout the ... Figure captions should be ... given here. ... to indicate for tables and ... should be complete ... intelligible by the ... article. ... mathematical expressions ... should be separated from ... Fats and ... be used to avoid room-wasting ... to avoid ...

... should be complete ... Fractional exponents should be written ... The solidus (/) should be used wherever ... possible for fractions.

All illustrations should accompany manuscript and should always be referred to in the text. Line drawings should be made with India ink on plain white paper or on tracing cloth. Coordinate paper is not desirable, but if used must be blue-lined with all coordinates to be reproduced drawn with India ink. Lettering should be of sufficient size to be legible after reduction.

Proof and all correspondence concerning papers in the process of publication should be addressed to the Publications Manager, American Institute of Physics, 57 East 55 Street, New York 22, New York.

Subscription Price

The United States and Possessions, Canada and Mexico $10.00
Elsewhere 11.00

Back Numbers

Complete set: Vol. 1, 1933—Vol. 14, 1946 ..... $140.00
Yearly rate: $11.00.
Single copies: $1.00 each.

Subscriptions and orders for single copies should be addressed to Prince and Lemon Streets, Lancaster, Pennsylvania, or to the American Institute of Physics, 57 East ... Street, New York 22, New York.

Changes of address should be sent to the Business Manager, American Institute of Physics.

... at Prince and Lemon Streets, Lancaster, Pennsylvania.

... at Lancaster, Pa., under the Act of August 24, 1912. Acceptance for ... 1918, embodied in paragraph 4, Section 412, P. L. & R. authorised

THE JOURNAL
OF
CHEMICAL PHYSICS

VOLUME 15, NUMBER 4 APRIL, 1947

The Experimental Determination of the Intensities of Infra-Red Absorption Bands

II. Measurements on Ethylene and Nitrous Oxide

A. M. THORNDIKE,* A. J. WELLS,** AND E. BRIGHT WILSON, JR.
Mallinckrodt Chemical Laboratory, Harvard University, Cambridge, Massachusetts

(Received January 23, 1947)

The absolute intensities of the chief infra-red absorption bands of ethylene and nitrous oxide have been determined experimentally to be (in cycles per centimeter at N.T.P.):

Ethylene	Nitrous oxide
950 cm^{-1} band: 1540×10^{10}	590 cm^{-1} band: 120×10^{10}
1444 cm^{-1} band: 210×10^{10}	1285 cm^{-1} band: 1150×10^{10}
3050 cm^{-1} band: 840×10^{10}	2224 cm^{-1} band: 5600×10^{10}

From these intensities it is possible to calculate the dipole moments, μ, of bonds between vibrating atoms and also the rates of change of dipole moment with inter-nuclear distances, $\partial\mu/\partial r$. The values of μ obtained are all of the order of magnitude of 0.5×10^{-18} c.g.s. unit, while values of $\partial\mu/\partial r$ are of the order of 1×10^{-10} c.g.s. unit. The results are in agreement with available data on infra-red dispersion and on atomic polarization within the limits of experimental error, which are estimated to be approximately ±10 percent.

IN a recent paper[1] a method has been described for measuring the intensities of infra-red vibrational absorption bands. The integrated apparent absorption coefficient per molecule is measured at several partial pressures of absorbing gas and extrapolated to zero partial pressure. This limit can normally be expected to equal the true integrated absorption coefficient. The use of a non-absorbing gas to broaden the individual lines composing the band assures that the limit will be approached closely for measurable values of the absorption. This pressure broadening need not be so great as to merge completely the rotational lines, but must reduce the variations of $\alpha(\nu)$ across the spectrometer slit until the observed absorption by a given amount of gas is not appreciably increased by a further increase of non-absorbing foreign gas pressure. It has long been known that the addition of a non-absorbing gas causes, in some cases, an increase in the measured absorption. The increase caused by the first increment of foreign gas is considerable, but further additions produce smaller and smaller effects.[2] The pressure required in practice varies from zero to about 50 atmos., depending primarily upon the spacing between the rotational lines of the absorbing gas.

The experimental procedure is simplest for molecules whose lines are adequately broadened by one atmosphere total pressure. N_2O and

* National Research Council Predoctoral Fellow.
** Now at Experimental Station, E. I. du Pont de Nemours and Company, Wilmington, Delaware.
[1] E. Bright Wilson, Jr. and A. J. Wells. J. Chem. Phys. **14**, 578 (1946).
[2] See, for example, E. von Bahr, Ann. d. Physik **29**, 780 (1909); **33**, 585 (1910).

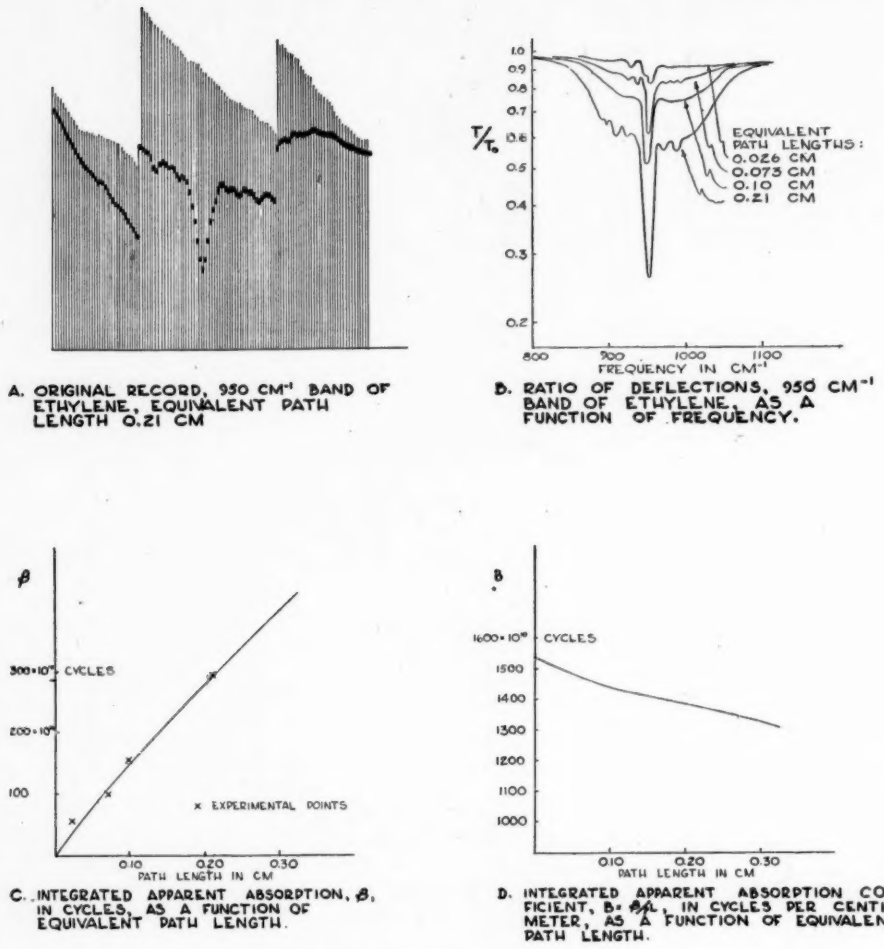
A. ORIGINAL RECORD, 950 CM⁻¹ BAND OF ETHYLENE, EQUIVALENT PATH LENGTH 0.21 CM
B. RATIO OF DEFLECTIONS, 950 CM⁻¹ BAND OF ETHYLENE, AS A FUNCTION OF FREQUENCY.
EQUIVALENT PATH LENGTHS: 0.026 CM 0.073 CM 0.10 CM 0.21 CM
FREQUENCY IN CM⁻¹
C. INTEGRATED APPARENT ABSORPTION, β, IN CYCLES, AS A FUNCTION OF EQUIVALENT PATH LENGTH.
× EXPERIMENTAL POINTS
PATH LENGTH IN CM
D. INTEGRATED APPARENT ABSORPTION COEFFICIENT, B= β/L, IN CYCLES PER CENTIMETER, AS A FUNCTION OF EQUIVALENT PATH LENGTH.
CYCLES

FIG. 1. Steps in calculating the intensity from experimental data (950 cm^{-1} band of ethylene).

C_2H_4 were chosen as fulfilling this requirement[2] without having unduly complicated spectra. This paper describes measurements of the intensities of their fundamental bands.

EXPERIMENTAL PROCEDURE

The absorption of the gas under study is measured as a function of frequency for various partial pressures of absorbing gas, at a fixed total pressure, and the intensity is obtained from the extrapolation previously described.[1] An automatic recording prism spectrograph was employed[3] whose effective slit width varied from about 5 cm^{-1} to 25 cm^{-1} depending upon frequency. The sample was enclosed in a cell 30 cm long, with NaCl or KBr windows. Air was added as a broadening gas to a total pressure of about one atmosphere. The partial pressure of the sample was varied from nearly an atmosphere down to about 0.1 mm Hg for an intense band. The data for low pressures (that is, those which lead to a maximum observed absorption not greater than about 30 percent) are most important in determining the intensity. The lower limit to the partial pressures employed was set by the fact that absorptions of less than about 10 percent were too small to be determined precisely from the record obtained.

The first measurements, made in 1940–41, have been repeated in 1946 with special emphasis on the low partial pressures.

The basic data were obtained as a record on

[3] The instrument is that described by Gershinowitz and Wilson, J. Chem. Phys. 6, 197 (1938). Improved slits and a more sensitive thermocouple were used, and an off-axis parabolic mirror has replaced the original spherical one for the more recent of the measurements here discussed.

photographic paper of galvanometer deflections for sample (T) and blank cells (T_0) at frequency intervals averaging about 5 cm^{-1}. The ratio of these deflections was then plotted as a function of frequency on semi-logarithmic graph paper, and the area between the curve for zero pressure of absorbing gas and that for pressure p was measured to give the integrated apparent absorption, defined by (1), below:

$$\mathfrak{B} = pLB = \int \ln(T_0/T)d\nu \qquad (1)$$

where L is the cell length and ν the frequency. The integration is over the band.

While it is the integrated apparent absorption *coefficient*, B, that is extrapolated[1] to obtain the true intensity, A, this quantity is liable to fluctuate considerably if calculated directly from experimental data. It was most convenient to plot the integrated apparent absorption, $\mathfrak{B}$, draw a smooth curve through the experimental points and select smoothed values of $\mathfrak{B}$ from which to calculate B for extrapolation. These steps are illustrated by data for the 950 cm^{-1} band of C_2H_4 in Fig. 1.

EXPERIMENTAL DATA

The integrated apparent absorption, $\mathfrak{B}$, is obtained from the basic data by unambiguous arithmetical reduction, whereas quantities obtained through smoothing and extrapolation involve individual judgment. The plotted values of $\mathfrak{B}$ in Figs. 2 and 3 are, therefore, a summary of the basic data, but the values of the intensities given in Table I involve judgment as well.

Data for N_2O are presented in Fig. 2, and those for C_2H_4 in Fig. 3. The case of N_2O is clear-cut, but that of C_2H_4 has some unsatisfactory aspects. In the first place, 1941 and 1946 data are not in agreement for the 950 cm^{-1} band, and the discrepancy is more than the expected limits of experimental error (see discussion below). In addition, both 3050 cm^{-1} and 950 cm^{-1} "bands" actually involve absorption by two vibrational modes which are not resolved. The separate contributions can only be estimated in these cases.

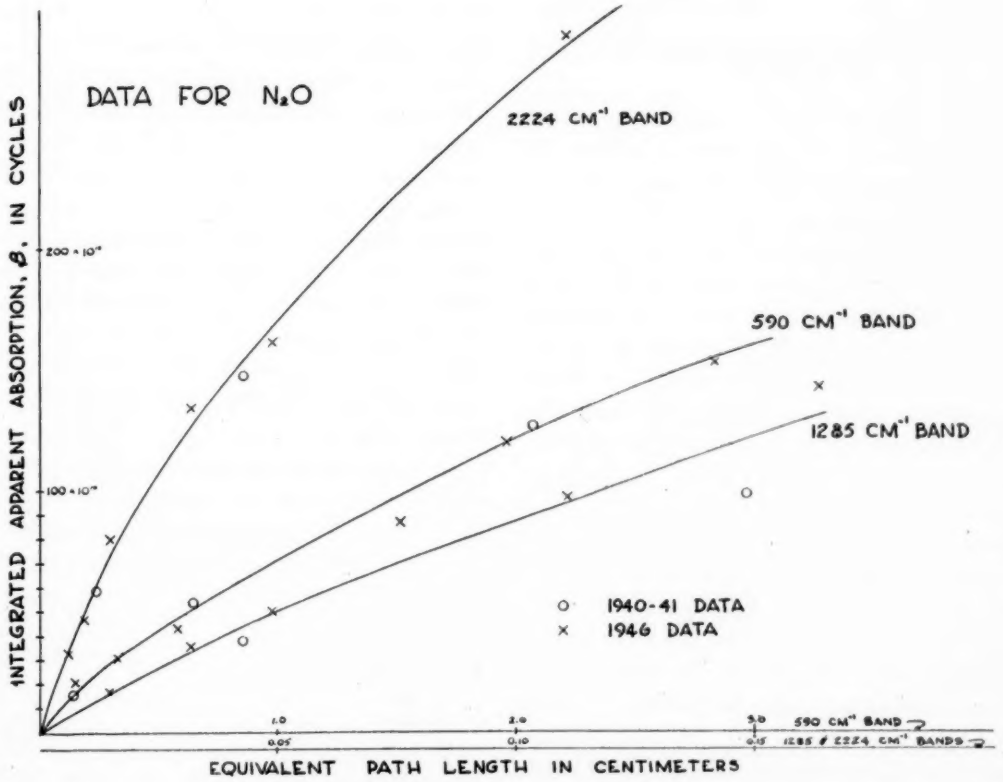

FIG. 2. Experimental results for N_2O.

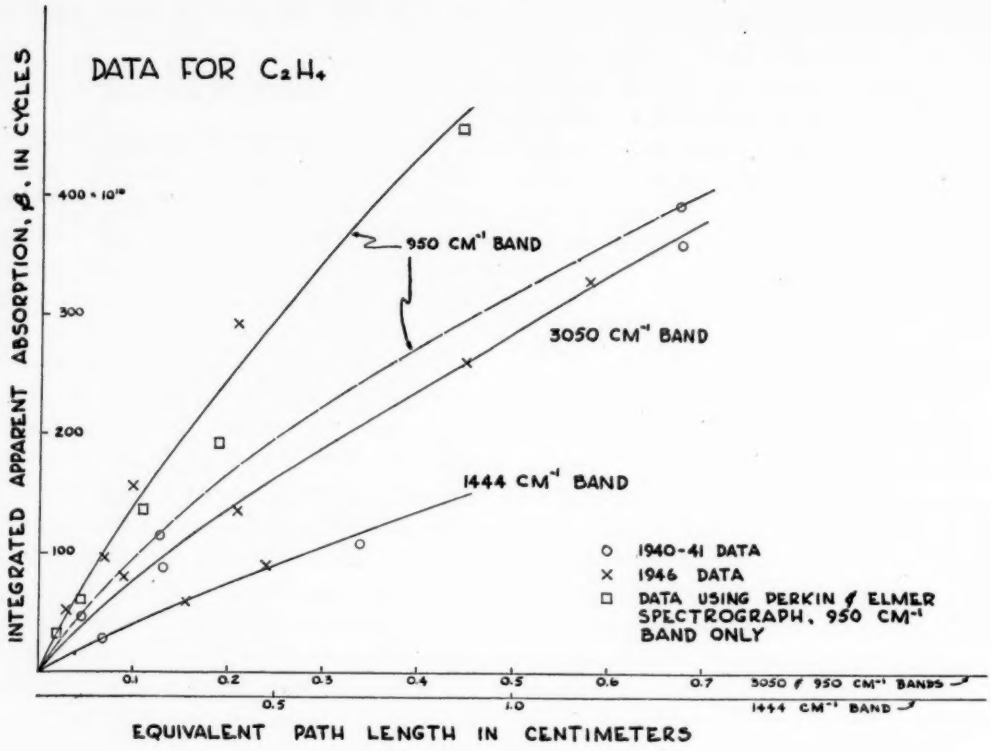

FIG. 3. Experimental results for C_2H_4.

ACCURACY OF RESULTS AND LIMITATIONS OF METHOD

The most serious general limitation of the method is the critical importance of the low pressure measurements where a small absolute error results in a large percentage error. Inaccuracies in measuring records, and in determining the ratio of sample to blank deflections in the absence of absorbing gas, may be responsible for errors of 5–10 percent. By taking a very large number of measurements the error in the smoothed curve could be made less than this, but it is believed that the intensities given in Table I may be in error by about 10 percent.

A number of other sources of error may be minimized by proper procedure. Stray light must be corrected for, and this correction becomes a serious potential source of error if the contribution of stray light to the deflections is 20 percent or more. In the above data only the N_2O 590 cm^{-1} band was low enough in frequency to have appreciable stray (about 40 percent). Rapid fluctuations in the intensity of the incident beam, due to absorption by atmospheric CO_2 and H_2O, are a potential source of error,[1] even if accurate ratios of transmission through the filled and blank cells are obtained. During the 1946 measurements an attempt to eliminate this absorption was made in the case of the 1444 cm^{-1} band of C_2H_4, the only one of the bands studied which lies in a region of strong atmospheric absorption. While the H_2O absorption was by no means eliminated, it was much reduced. Data on this band show good agreement between 1941 and 1946 data, suggesting that the errors due to atmospheric absorption are not serious in this case.[4]

A final source of error which is difficult to eliminate is that of "envelope effect" in the Q-branches of perpendicular bands, since these branches may be intense and narrower than the slit width of low resolving power spectrographs. To give the Q-branch a half-width of 10 cm^{-1} by pressure broadening (assuming it to be effectively a single line) would require about 100 atmos-

[4] One would expect atmospheric absorption to have no effect if randomly distributed in frequency, but to have a serious effect if the lines are spaced regularly in relation to those of the absorbing gas.

pheres broadening gas pressure. To eliminate the envelope effect by extrapolation to zero equivalent path length may require measurements at impracticably low absorptions. This type of difficulty may well account for the difference between 1941 and 1946 data on the 950 cm^{-1} band of C_2H_4, since this band is the only one of those measured which has prominent multiple Q-branches (spaced about 10 cm^{-1} apart), and the resolution of the spectrograph was considerably better in 1946 than in 1941.

In order to ascertain whether the resolution of the spectrograph in 1946 (about 10 cm^{-1} effective slit width in this region) was adequate, a series of measurements was made on an instrument of considerably higher resolving power (a Perkin and Elmer spectrograph at Brown University).[5] While the fine structure was very much more pronounced on these records, the values of integrated apparent absorption were in good agreement with our 1946 data, and the extrapolated intensities very nearly the same. We may conclude that errors due to envelope effect are not serious in this case.

On the basis of these estimates of errors, it is considered that the results above may be in error by about 10 percent, but that certainly in no case should errors exceed 25 percent. In order to achieve this accuracy, considerable care must be employed in measuring the records and a sufficient number of pressures must be used.

The preliminary results,[6] published in 1941, were satisfactory for N_2O but were based on too few points to give good agreement with our final results on ethylene, even when adjusted to N.T.P.

INTERPRETATION OF RESULTS

The integrated intensity A_i is related to the matrix elements of the electric moment by

$$A_i \equiv \int_i \alpha(\nu)d\nu = (8\pi^3 N\nu_i/3hc) \times\{|\mu_{ix}^{1,0}|^2+|\mu_{iy}^{1,0}|^2+|\mu_{iz}^{1,0}|^2\}, \quad (2)$$

in which the integration covers the ith band, of frequency ν_i. $\alpha(\nu)$ is the true absorption coefficient, N is the number of molecules per cc, h is Planck's constant, and c the velocity of light. $\mu_{ix}^{1,0}$ etc., are the matrix elements of the components of the electric moment for a transition between the ground state and first-excited state of the ith normal mode.[7] This quantity may be calculated on the basis of various simple models.

If, for example, we assume the wave equation to have been separated in normal coordinates, Q_i, we can, to a first approximation, express the (vector) dipole moment, $\mathfrak{y}$, as a linear function of the Q_i:

$$\mathfrak{y}-\mathfrak{y}_0=\textstyle\sum_i (\partial\mathfrak{y}/\partial Q_i)Q_i, \quad (3)$$

whence

$$\mathfrak{y}_i^{1,0}=(\partial\mathfrak{y}/\partial Q_i)Q_i^{1,0}. \quad (4)$$

$Q_i^{1,0}$ is the matrix element of Q_i for the 0–1 transition in question; $\mathfrak{y}_0$ is the constant part of the dipole moment. Each normal coordinate may be treated as a harmonic oscillator coordinate for which

$$Q_i^{1,0}=(h/8\pi^2\nu_i)^{\frac{1}{2}}. \quad (5)$$

Substituting (4) and (5) in (2) yields a simple relation between the observed intensity and the coefficient in Eq. (3):

$$A_i=(N\pi/3c)\{|\partial\mu_x/\partial Q_i|^2 +|\partial\mu_y/\partial Q_i|^2+|\partial\mu_z/\partial Q_i|^2\}. \quad (6)$$

In order to explain the observed values of the A_i with a smaller number of constants we might

TABLE I. Intensities obtained by extrapolation.

Substance	Band	Intensity (cycles per centimeter at N.T.P.)
N_2O	590 cm^{-1}	120×10^{10}
N_2O	1285 cm^{-1}	1150×10^{10}
N_2O	2224 cm^{-1}	5600×10^{10}
C_2H_4	950 cm^{-1}	1540×10^{10}[a, b]
C_2H_4	1444 cm^{-1}	210×10^{10}
C_2H_4	1890 cm^{-1} (combination)	67×10^{10}
C_2H_4	3050 cm^{-1}	840×10^{10}[c]

[a] The intensity of 1540×10^{10} for the 950 cm^{-1} "band" is based on 1946 data only. On account of better resolving power it is considered to be more accurate than that obtained in 1940–41.

[b] This includes a contribution from the weak 995 cm^{-1} band. From the observed asymmetry of this pair of overlapping bands we estimate that the total intensity should be apportioned as follows. 950 cm^{-1}: 1390×10^{10} cycles; 995 cm^{-1}: 150×10^{10} cycles.

[c] There are two overlapping bands here, at 2990 and 3105 cm^{-1}. Using the relative intensities observed by Levin and Meyer, J. Opt. Soc. Am. 16, 137 (1928), we tentatively divide this observed intensity as follows. 2990 cm^{-1}: 270×10^{10} cycles; 3105 cm^{-1}: 570×10^{10} cycles.

[5] We are indebted to Professor Paul C. Cross, Professor Donald H. Hornig, and Mr. Earl Wilson of Brown University for their cooperation with these measurements.

[6] A. J. Wells and E. B. Wilson, Jr., J. Chem. Phys. 9, 659 (1941).

[7] G. Herzberg, *Infrared and Raman Spectra of Polyatomic Molecules* (D. Van Nostrand Company, New York, 1945), p. 261.

TABLE II. Normal coordinates for ethylene.

Mode	Symmetry	Frequency*	Normal coordinate
ν_{11}	B_{2u}	2989.5	$Q_{11}=12.6\times10^{-13}S_4-1.95\times10^{-6}S_5$
ν_{12}	B_{3u}	1443.5	$Q_{12}=-1.12\times10^{-13}S_4+90.8\times10^{-6}S_6$
ν_9	B_{2u}	3105.5	$Q_9=-12.2\times10^{-13}S_6+0.72\times10^{-6}S_7$
ν_{10}	B_{2u}	995	$Q_{10}=+0.91\times10^{-13}S_6+93.1\times10^{-6}S_7$
ν_7	B_{1u}	949.2	$Q_7=126\times10^{-6}S_{11}$

* See reference 7.

endeavor to reproduce the intensities by assigning fixed "effective charges" to each type of atom, and taking the form of the normal modes into account. Such a simplification would be too drastic, however, since the intensities calculated in this manner do not agree well with those observed. It is more satisfactory to assume, as has been done, for example, by Rollefson and Havens,[8] and Wolkenstein,[9] that the electric moments of the bonds are additive. Then the intensities of the stretching vibrations depend on $d\boldsymbol{\mu}/dr$, and those of the bending vibrations depend on $\boldsymbol{\mu}$, r being the bond length.

This relation can be written explicitly since the normal coordinates, Q_i, are linearly related to the internal coordinates, R_k (e.g., changes in inter-atomic distances, etc.), by the transformation

$$R_k=\sum_i L_{ki}Q_i, \quad Q_i=\sum_k (L^{-1})_{ik}R_k. \qquad (7)$$

But the dipole moment of the molecule is related to the coordinates, Q_i, by the $\partial\boldsymbol{\mu}/\partial Q_i$ as in (3). From (3) and (7) we obtain

$$\begin{aligned}\boldsymbol{\mu}-\boldsymbol{\mu}_0&=\sum_i (\partial\boldsymbol{\mu}/\partial Q_i)Q_i\\ &=\sum_{ik} (\partial\boldsymbol{\mu}/\partial Q_i)(L^{-1})_{ik}R_k\\ &=\sum_k (\partial\boldsymbol{\mu}/\partial R_k)R_k,\\ \partial\boldsymbol{\mu}/\partial R_k&=\sum_i (\partial\boldsymbol{\mu}/\partial Q_i)(L^{-1})_{ik}. \qquad (8)\end{aligned}$$

Since the transformation L^{-1} is easy to normalize,[10] this is a convenient method of determining the behavior of bond dipole moments with respect to stretching, bending, or other internal coordinates from the observed absorption intensities.[11]

[8] R. Rollefson and R. Havens, Phys. Rev. **57**, 710 (1940).
[9] M. W. Wolkenstein, J. Phys. USSR, **5**, 185 (1941).
[10] E. Bright Wilson, Jr., J. Chem. Phys. **9**, 76 (1941).
[11] For symmetrical molecules it may be convenient to introduce internal symmetry coordinates, $\mathcal{R}$, as an intermediate step, determining first the $\partial\boldsymbol{\mu}/\partial\mathcal{R}$ as in (8) and then the $\partial\boldsymbol{\mu}/\partial R_k$.

TABLE III. Experimentally determined characteristics of bond moments of C_2H_4 (c.g.s. units).

Bond	Bands involved	μ	μ/s	$\partial\mu/\partial r$
CH	ν_{11} out-of-plane bending	0.77×10^{-18}	0.72×10^{-10}	—
CH	ν_7 in-plane bending	0.52×10^{-18}	0.48×10^{-10}	—
CH	ν_5 in-plane bending	0.37×10^{-18}	0.33×10^{-10}	—
CH	ν_4 stretching	—	—	$+0.70\times10^{-10}$ or -0.60×10^{-10}
CH	ν_6 stretching	—	—	$+0.57\times10^{-10}$ or -0.53×10^{-10}

This procedure involves one serious difficulty, however, arising from the fact that it is the squares of $\partial\mu_x/\partial Q_i$, $\partial\mu_y/\partial Q_i$, and $\partial\mu_z/\partial Q_i$ that enter into (6). The signs of these coefficients are, therefore, undetermined, and can be either positive or negative. When they are substituted in Eq. (8) a large number of combinations of signs are possible, each leading to a different value of $\partial\boldsymbol{\mu}/\partial R_k$. Other arguments must be introduced in order to eliminate as many of them as possible.

Following this procedure bond moments and their rates of change were calculated from the intensities given in Table I. In order to obtain the $(L^{-1})_{ik}$ coefficients normal coordinate treatments of N_2O and C_2H_4 were carried out using the methods previously described.[10]

Ethylene

In the case of C_2H_4 the normal coordinates were calculated from the observed frequencies on the assumption that the dependence of the potential energy upon the infra-red active symmetry coordinates can be expressed without interaction terms as

$$V=\tfrac{1}{2}\{f_{44}S_4^2+f_{55}S_5^2+f_{66}S_6^2+f_{77}S_7^2+f_{11\ 11}S_{11}^2\},$$

TABLE IV. Normal coordinates for N_2O.

f_{12}	f_1[a]	f_2[a]	$(L^{-1})_{11}$	$(L^{-1})_{12}$	$(L^{-1})_{21}$	$(L^{-1})_{22}$
in units of 10^5			in units of 10^{-12}			
0.50	15.47	14.05	−2.30	+1.65	+3.24	+3.78
1.36	17.91	11.36	−2.72	+1.13	+2.89	+3.95
2.72	20.32	10.29	−3.03	+0.613	+2.48	+4.07
5.00	22.94	9.884	−3.42	−0.017	+2.05	+4.22
10.00	26.51	11.38	−3.85	−1.14	+1.05	+4.01

[a] There are, of course, two algebraic solutions for f_1 and f_2 with each value of f_{12} assumed, of which only one is tabulated. The other leads, in each case, to a solution with f_1 smaller than f_2, and was discarded since the 2½-fold NN bond must surely be stiffer than the 1½-fold NO bond.

TABLE V. Characteristics of bond moments of N_2O (c.g.s. units).

f_{12}	$(\partial\mu/\partial r)_{NN}$	$(\partial\mu/\partial r)_{NO}$	μ_{NN}	μ_{NO}	μ_{NN}/s	μ_{NO}/s
1.0	-2.9×10^{-10}	-7.5×10^{-10}	-0.50×10^{-18}	-0.67×10^{-18}	-0.45×10^{-10}	-0.56×10^{-10}
2.0	-4.1×10^{-10}	-6.6×10^{-10}				
3.0	-5.0×10^{-10}	-5.9×10^{-10}				
5.0	-6.2×10^{-10}	-4.6×10^{-10}				
7.0	-7.1×10^{-10}	-3.4×10^{-10}				
10.0	-8.2×10^{-10}	-1.6×10^{-10}				

where

$$\left.\begin{aligned} S_4&=\tfrac{1}{2}\{r_1+r_2-r_3-r_4\},\\ S_5&=\tfrac{1}{2}rR\{\gamma_1+\gamma_2-\gamma_3-\gamma_4\},\end{aligned}\right\}\text{Along C}-\text{C axis}$$

$$\left.\begin{aligned} S_6&=\tfrac{1}{2}\{r_1-r_2+r_3-r_4\},\\ S_7&=\tfrac{1}{2}rR\{\gamma_1-\gamma_2+\gamma_3-\gamma_4\},\end{aligned}\right\}\text{Perpendicular to C}-\text{C axis}$$

$$S_{11}=[(-rR\cos\gamma)/\sqrt{2}]\{\delta_a+\delta_b\}.$$

The internal coordinates r_i and γ_i are changes in CH bond lengths and C−C−H bond angles, respectively, and δ_a and δ_b are out-of-plane bending angles of the H−C−H planes with respect to the C−C bond.

The force constants were determined to be

$$f_{44}=5.07\times10^5 \text{ dynes/cm},$$

$$f_{55}=6.33\times10^{20} \text{ dynes/cm}^3/\text{radian}^2,$$

$$f_{66}=5.08\times10^5 \text{ dynes/cm},$$

$$f_{77}=3.07\times10^{20} \text{ dynes/cm}^3/\text{radian}^2,$$

$$f_{11\ 11}=5.11\times10^{20} \text{ dynes/cm}^3/\text{radian}^2.$$

The corresponding normal coordinates are given in Table II.

The results for C_2H_4 are presented in Table III. Values are given for μ, $\partial\mu/\partial r$, and μ/s, where s is the equilibrium inter-atomic distance. (It is assumed throughout that the dipole moments are directed along the bond in question.) μ/s and $\partial\mu/\partial r$ have the dimensions of charge, and may be compared with the charge of -4.8×10^{-10} for an electron.

In Table III considerations of the electronegativities of the atoms have been employed to determine the signs when possible. Since hydrogen is less electronegative than carbon, negative values for the CH bond moment would be unreasonable, and this restriction allows us to select the proper sign for three of the five $\partial\mu/\partial Q$'s for C_2H_4. The remaining two must have opposite signs, leaving two possibilities which lead to the two values of $\partial\mu/\partial r$ for ν_{11} and ν_9. If the $\partial\mu/\partial Q$'s had the same signs, these two CH-stretching vibrations would involve values for $\partial\mu/\partial r$ of opposite sign, which seems quite impossible.

Nitrous Oxide

The case of N_2O is made more complicated by the existence of resonance between the two structures

$$\text{(a) } \overset{-}{\text{N}}=\overset{+}{\text{N}}=\text{O}, \quad \text{(b) } \text{N}\equiv\overset{+}{\text{N}}-\overset{-}{\text{O}}.$$

The potential energy must be expressed as

$$V=\tfrac{1}{2}\{f_1r_1^2+2f_{12}r_1r_2+f_2r_2^2+f_3\gamma^2\},$$

where r_1=NN stretch, r_2=NO stretch, and γ=NNO bending. The interaction coefficient cannot be evaluated from the two observed frequencies, but is probably large (and positive) since a stretch of the NO bond will favor structure (b) which has the greater NO distance and thereby stiffen the NN bond considerably.

It was, therefore, necessary to calculate normal coordinates as a function of the variable f_{12}. The results of these calculations are summarized in Table IV, the indices being selected so that:

$$\nu_1=2224 \text{ cm}^{-1}, \quad Q_1=(L^{-1})_{11}r_1+(L^{-1})_{12}r_2.$$
$$\nu_2=1285 \text{ cm}^{-1}, \quad Q_2=(L^{-1})_{21}r_1+(L^{-1})_{22}r_2.$$

For the normal coordinates corresponding to each possible choice of f_{12} there are four possible combinations of signs for the $\partial\mu/\partial Q$'s that must be considered. The values are:

$$\partial\mu/\partial Q_1=\pm244, \quad \partial\mu/\partial Q_2=\pm111.$$

The choice is restricted, however, by the fact that stretching the NO bond will favor structure (b) above, and, therefore, give the molecule a dipole moment directed to the left, whereas

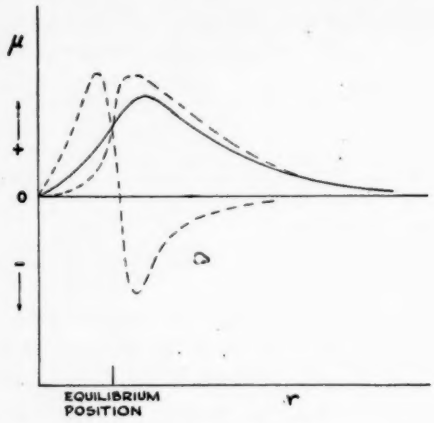

FIG. 4. Hypothetical curves for dipole moment, μ, as a function of internuclear distance, r.

stretching the NN bond will favor structure (a) and give a dipole moment directed to the right. Substitution of the above values for $\partial\mu/\partial Q_1$ and $\partial\mu/\partial Q_2$ with those from Table IV in Eq. (8) shows that this restriction is satisfied only if $\partial\mu/\partial Q_1$ and $\partial\mu/\partial Q_2$ are both positive. Possible values of $\partial\mu/\partial r_1$ (NN bond), and $\partial\mu/\partial r_2$ (NO bond), are given in Table V as a function of f_{12}. A positive contribution to the dipole moment on the part of the NN bond is defined as one which is directed from the central nitrogen to the end nitrogen. Similarly a positive contribution by the NO bond will be directed from nitrogen to oxygen.

Table V also includes values for the dipole moments themselves, determined from the intensity of the bending mode. These signs are also uniquely determined. Since oxygen is more electronegative than nitrogen, the moment of the NO bond must be negative. It will be assumed that the molecular dipole moment is directed toward the nitrogen end and that it has the value[12] 0.17×10^{-18}. These two conditions and the observed intensity determine the NO and NN bond moments using the hypothesis of additivity, though it should be remembered that in a resonant molecule any separation into individual bonds is somewhat artificial.

Behavior of Bond Dipole Moments

As might be expected, values of μ/s and $d\mu/dr$ vary from about 0.1 to 2.0 times the charge of an electron. The slope, $d\mu/dr$ is in most cases greater than μ/s, but the values for CH are consistent with a simple curve such as that shown solid in Fig. 4. The values for NN and perhaps NO seem to require a steeper form like one or the other of the dotted curves. The value of μ for CH obtained from the 950 cm^{-1} band is almost twice that obtained from the 1444 cm^{-1} or 995 cm^{-1} bands. Apparently the electric moment behaves differently for this out-of-plane bending than for the in-plane modes because of some interaction with neighboring atoms.

COMPARISON WITH OTHER DATA

There are very few other measurements of infra-red intensities, and they are not directly comparable with those reported here. Bourgin[13] obtained 0.86×10^{-10} for $d\mu/dr$ in HCl, and Matheson[14] obtained 3.92×10^{-10} for CO. Foley[15] has given the "dipole moment" of the bending mode of HCN as 0.147×10^{-18}, from which we calculate the CH bond moment as 0.57×10^{-18}, $\mu/s=0.54\times10^{-10}$. This is intermediate between our values for in-plane and out-of-plane modes in C_2H_4.

The conventional value for the CH bond moment obtained from molecular moments[16] on

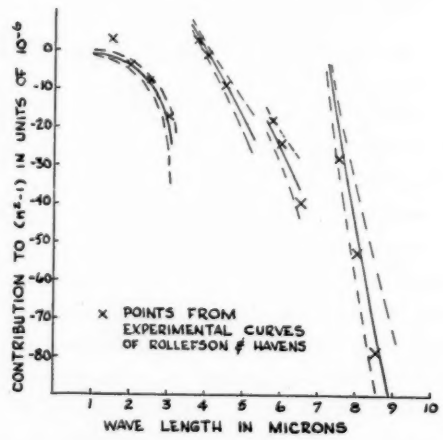

FIG. 5. Dispersion curve for ethylene calculated from intensity data and compared with experimental points from Rollefson and Havens. Dotted curves show limits of 20 percent error.

[12] J. H. Van Vleck, *Electric and Magnetic Susceptibilities* (Clarendon Press, Oxford, 1932), Chap. III.

[13] D. G. Bourgin, Phys. Rev. **29**, 794 (1927); **32**, 237 (1928).

[14] L. A. Matheson, Phys. Rev. **40**, 813 (1932).

[15] H. M. Foley, Phys. Rev. **69**, 628 (1946).

[16] C. P. Smyth, *Dielectric Constant and Molecular Structure* (Chemical Catalogue Company, New York, 1931), p. 117.

the basis of additivity is 0.4×10^{-10}, agreeing well with our in-plane moment.

Measurements of infra-red dispersion also lead to values for bond dipole moments. In the case of methane Rollefson and Havens[8] concluded that $\mu=0.307\times10^{-18}$, and $\partial\mu/\partial r=\pm0.562\times10^{-10}$, in fair agreement with our in-plane moment and our values for $\partial\mu/\partial r$. Rollefson and Havens have also very kindly furnished us with some unpublished data on the index of refraction of ethylene, and we find that our values for the intensities reproduce their observed dispersion curve quite closely if the combination band at 1890 cm^{-1} is taken into account, as shown in Fig. 5. The agreement is well within an assumed maximum experimental error of 20 percent shown by the dotted curves except at the highest frequencies where contributions from electronic transitions should be taken into account.

TABLE VI. Atomic polarizations.

Substance	Calculated from intensity data	From visible index and dielectric constant[a]
C_2H_4	0.40 cc	0.39 cc
N_2O	0.55 cc	0.41 cc (0.46[b])

[a] H. E. Watson and K. L. Ramaswamy, Proc. Roy. Soc. London, **A156**, 144 (1936).
[b] E. Czerlinsky, Zeits. f. Physik **88**, 515 (1934).

A final comparison can be made with the atomic polarization obtained from measurements of dielectric constant. Table VI shows the contribution of infra-red vibration bands to the molar polarization as calculated from our intensities and from the difference of extrapolated visible indices of refraction and measured dielectric constants.[12] Again the agreement is good.

THE JOURNAL OF CHEMICAL PHYSICS VOLUME 15, NUMBER 4 APRIL, 1947

On the Theory of Accidental Predissociation*

I. Kovács and A. Budó
Department of Theoretical Physics, University of Budapest, Budapest, Hungary
(Received November 11, 1946)

Applying the results of quantum electrodynamics we investigate the case of perturbation between two discrete and one continuous term series. Even though no interaction between the first discrete and the continuous states exists, a considerable predissociation may arise for some spectrum lines in case of coincidence or close proximity between the levels of the two discrete terms belonging to the same rotational quantum number. The predissociation occurring in the first discrete term is caused by the second. This phenomenon is called accidental predissociation. Our results are in excellent agreement with the results obtained in the γ-bands of NO molecule by Schmid and Gerö.

THE phenomenon of accidental predissociation was first discovered by Coster, Brons, and van der Ziel[1] in the so-called II positive band system of N_2. A short theoretical interpretation was subsequently given by Ittmann.[2] A similar effect has been observed recently by Schmid and Gerö in the initial states of the γ bands of NO.[3] The interpretation of these experimental data renders the extension and generalization of the theory necessary.

The states of the system of the molecule and of the radiation field can be described according to Dirac[4] with a normalized wave function:

$$\psi(N_1, N_2, \cdots N_\rho, \cdots; q_1, q_2, \cdots; t); \quad \int |\psi|^2 = 1. \tag{1}$$

Here $q_1, q_2, \cdots$ are the space and spin coordinates of the electrons and nuclei, $N_1, N_2, \cdots$ are the numbers of light quanta in the first, second, $\cdots$ monochromatic plane wave, from which field, the radiation, is formed as a linear combination. Let us denote the wave functions of the molecular states without radiation field by φ_l, where l is the totality of the quantum numbers related to the energy values. Since the φ_l's (depending only on the space and spin coordinates of the particles) form an orthogonal, normalized complete system, we may write[5]

$$\psi(N_1, N_2, \cdots N_\rho, \cdots; q_1, q_2, \cdots; t) = \sum_l a_l(N_1, N_2, \cdots N_\rho, \cdots; t)\varphi_l(q_1, q_2, \cdots); \quad \sum_{N_\rho, l} |a_l|^2 = 1 \tag{2}$$

where the a_l coefficients depend, apart from the time and the N_ρ quantum numbers of the radiation field also on the totality of the energy quantum numbers of the particles.

Let us denote with $H_{op}^{(0)}$ the operator corresponding to the separable part of the wave equation of the molecule and with $G_{op}^{(0)}$ the energy operator of the radiation field, furthermore let $H_{op}^{(1)}$ be the perturbation between the different levels within the molecule, which was neglected in setting up the function φ_l, and let $G_{op}^{(1)}$ be the small perturbing operator describing the interaction of the molecule and the radiation field. Then we have the time dependent wave equation as follows:

$$[H_{op}^{(0)} + G_{op}^{(0)} + H_{op}^{(1)} + G_{op}^{(1)}]\psi = -\frac{h}{2\pi i}\frac{\partial \psi}{\partial t}. \tag{3}$$

* Lecture delivered by one of the authors (Kovács) on September 25, 1946 in the Physics Section of the Hungarian Sciences Association.

[1] C. Coster, F. Brons, and A. v. d. Ziel, Zeits. f. Physik **84**, 304 (1933).
[2] G. P. Ittmann, Naturwiss. **22**, 118 (1934).
[3] R. Schmid and L. Gerö, Math. u. Naturwiss. Anz. d. Ung. Akad. der Wiss. **62**, 408 (1943).
[4] P. A. M. Dirac, Proc. Roy. Soc. London **A114**, 243 (1927).
[5] H. A. Kramers, *Theorien des Aufbaues der Materie II. Quantentheorie des Elektrons und der Strahlung* (1938), p. 462.

Substituting the expression for ψ from Eq. (2) into Eq. (3) and multiplying from the left by φ_k^* and integrating, we obtain the following expressions:

$$\int \varphi_k^* H_{op}^{(0)} \sum_l a_l \varphi_l d\tau = a_k E_k, \tag{4a}$$

$$\int \varphi_k^* G_{op}^{(0)} \sum_l a_l \varphi_l d\tau = h(\nu_1 N_1 + \nu_2 N_2 + \cdots + \nu_\rho N_\rho + \cdots) a_k, \tag{4b}$$

$$\int \varphi_k^* H_{op}^{(1)} \sum_l a_l \varphi_l d\tau = \sum_l H_{kl} a_l, \tag{4c}$$

$$\int \varphi_k^* G_{op}^{(1)} \sum_l a_l \varphi_l d\tau = \sum_\rho \sum_l G_{kl}^{(\rho)} [(N_\rho+1)^{\frac{1}{2}} a_l(N_1, \cdots, N_\rho+1, \cdots) + (N_\rho)^{\frac{1}{2}} a_l(N_1, \cdots, N_\rho-1, \cdots)], \tag{4d}$$

$$\int \varphi_k^* \left(-\frac{h}{2\pi i} \frac{\partial}{\partial t} \sum_l a_l \varphi_l \right) d\tau = -\frac{h}{2\pi i} \dot{a}_k, \tag{4e}$$

where E_k are the unperturbed molecular energies belonging to the totality of the quantum numbers, $\sum_\rho h\nu_\rho N_\rho$ is the eigenvalue of the radiation field, $H_{kl} = \int \varphi_k^* H_{op}^{(1)} \varphi_l d\tau$ is the perturbing matrix element of the non-radiating molecule and finally

$$G_{kl}^{(\rho)} = \int \varphi_k^* G_{op}^{(\rho)}(q_1, q_2, \cdots) \varphi_l d\tau. \tag{4f}$$

Here the operator $G_{op}^{(\rho)}$ designates the part of $G_{op}^{(1)}$ which depends on the space coordinates related to the vector potential of the ρth plane wave.[6] With the help of the expressions mentioned above we have, from the wave equation,

$$-\frac{h}{2\pi i} \dot{a}_k = [E_k + h \sum_\rho \nu_\rho N_\rho] a_k + \sum_l H_{kl} a_l + \sum_\rho \sum_l G_{kl}^{(\rho)} [(N+1)^{\frac{1}{2}} a_l(N_1, \cdots N_\rho+1, \cdots) + (N_\rho)^{\frac{1}{2}} a_l(N_1, \cdots N_\rho-1, \cdots)]. \tag{5}$$

For accidental predissociation, according to the experiments, we take into consideration the interaction $H_{AB}^{(1)}$ between the two discrete term series denoted by A and B, furthermore the interaction $H_{BC}^{(1)}$ between the discrete states B and the continuous states C. We neglect the immediate interaction between A and C. This means that the A state, in spite of the presence of the continuous state C, does not predissociate into C. The reason for this may be, e.g., that one of Kronig's conditions on which the existence of the interaction depends is not satisfied. Further we make the supposition that an emission transition from the discrete term series A to a lower discrete term series denoted by D may exist. (See Fig. 1.) These assumptions mean that in Eq. (2) a_k differs from zero only in the following cases:

$$\begin{aligned} &k=A, \quad N_1=N_2=\cdots=N_\rho=\cdots=0, \\ &k=B, \quad N_1=N_2=\cdots=N_\rho=\cdots=0, \\ &k=C, \quad N_1=N_2=\cdots=N_\rho=\cdots=0, \\ &k=D, \quad N_1=N_2=\cdots=N_{\rho-1}=N_{\rho+1}=\cdots=0, \quad N_\rho=1, \end{aligned} \tag{6}$$

[6] V. Weisskopf and E. Wigner, Zeits. f. Physik **63**, 60 (1930).

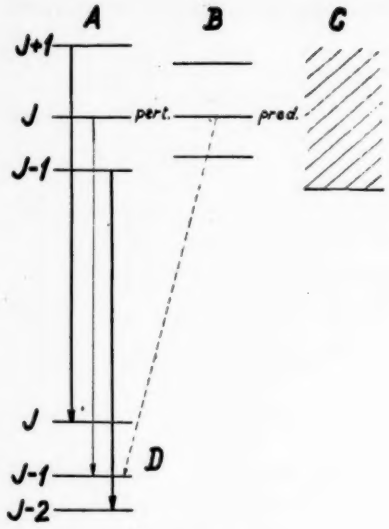

FIG. 1.

TABLE I.

	$\left\|\frac{E_A-E_B}{hc}\right\|$	$\int \Sigma_\rho \|a_{D1}^{(\rho)}\|^2 d\nu$	$\int \Sigma_\rho \|a d_2^{(\rho)}\|^2 D\nu$
$\frac{H_{AB}}{hc}=0.2$ cm^{-1}	0 cm^{-1}	0.06	1.5×10^{-7}
	2 cm^{-1}	0.08	1.25×10^{-7}
	10 cm^{-1}	0.24	3.2×10^{-8}
	20 cm^{-1}	0.5	10^{-8}
$\frac{H_{AB}}{hc}=0.1$ cm^{-1}	0 cm^{-1}	0.22	3.5×10^{-8}
	5 cm^{-1}	0.34	1.9×10^{-8}
	10 cm^{-1}	0.56	0.8×10^{-8}
	20 cm^{-1}	0.8	0.25×10^{-8}

furthermore

$$E_A-E_D-h\epsilon<h\nu_\rho<E_A-E_D+h\epsilon.$$

With respect to the continuity of the state C we obtain from Eqs. (2) and (6) for ψ:

$$\psi=a_A(\overset{1}{0},\overset{2}{0},\cdots\overset{\rho}{0},\cdots;t)\varphi_A+a_B(\overset{1}{0},\overset{2}{0},\cdots\overset{\rho}{0},\cdots;t)$$
$$+\int a_C(\overset{1}{0},\overset{2}{0},\cdots\overset{\rho}{0},\cdots E;t)\varphi_C(E)dE+\sum_\rho a_D{}^{(\rho)}(\overset{1}{0},\overset{2}{0},\cdots,\overset{\rho}{1},\cdots;t)\varphi_D. \quad (7)$$

Our problem is solved, if we succeed in computing explicitly the a_k coefficients, because $|a_k|^2$ represents the probability of the realization of each state and if $k=D$, it gives the rate of decrease of the intensity itself. Substituting the expressions for ψ given by Eq. (7) into Eqs. (3), (4a), and (4e), respectively, Eq. (5) gives for the calculation of the a_k's the following system of linear differential equations:

$$-\frac{h}{2\pi i}\dot{a}_A=E_Aa_A+H_{AB}a_B+\sum_\rho G_{AD}{}^{(\rho)}a_D{}^{(\rho)}(0\cdots1\cdots), \quad (8a)$$

$$-\frac{h}{2\pi i}\dot{a}_B=H_{BA}a_A+E_Ba_B+\int H_{BC}(E)a_C(E)dE, \quad (8b)$$

$$-\frac{h}{2\pi i}\dot{a}_C(E)=H_{CB}(E)a_B+Ea_C(E), \quad (8c)$$

$$-\frac{h}{2\pi i}\dot{a}_D{}^{(\rho)}(0\cdots1\cdots)=G_{DA}{}^{(\rho)}a_A+[E_D+h\nu_\rho]a_D{}^{(\rho)}(0\cdots1\cdots). \quad (8d)$$

We shall attempt to solve this system of equations mentioned above by the following assumptions:

$$a_A=S_Ae^{-2\pi at};\quad a_B=S_Be^{-2\pi at}, \quad (9)$$

where S_A, S_B, and a are still to be determined. Substituting a_A into Eq. (8d), a_B into Eq. (8c) with the

assumption that $a_D^{(\rho)}=a_C(E)=0$, when t is also 0 (that is, when only A and B states are excited) we obtain

$$a_D^{(\rho)}=S_A G_{DA}^{(\rho)}\frac{1-\exp\left(2\pi i\left[\frac{E_D}{h}+\nu_\rho+ia\right]t\right)}{h\left[\frac{E_D}{h}+\nu_\rho+ia\right]}\cdot\exp\left(-\frac{2\pi i}{h}[E_D+h\nu_\rho]t\right);$$

$$a_C(E)=S_B\cdot H_{CB}(E)\frac{1-\exp\left(\left[\frac{2\pi}{i\frac{h}{h}}E-2\pi a\right]t\right)}{\frac{h}{2\pi i}\left[\frac{2\pi}{i\frac{h}{h}}E-2\pi a\right]}\cdot\exp\left(-\frac{2\pi i}{h}E\cdot t\right). \tag{10}$$

For the evaluation of S_A, S_B, and the exponent a let us substitute Eqs. (9) and (10) into Eqs. (8a) and (8b). The summation over ρ in Eq. (8a), may be replaced, to a good approximation, by an integration over ν between $\nu_D{}^{A'}-\epsilon<\nu<\nu_D{}^{A'}+\epsilon$.[7] Considering that, according to the experimental results about accidental predissociation, the perturbed terms are hardly displaced from their original unperturbed places (in any case within the limits of experimental error), we may put $|G_{AD}{}^{(\rho)}|^2$ before the integral sign with the value taken at $\nu=\nu_D{}^A$ (and not at $\nu=\nu_D{}^{A'}$). Integrating in this way we have[8]

$$-i\frac{h}{4\pi}V_{AD}e^{-2\pi at}, \tag{11a}$$

where

$$V_{AD}=\frac{4\pi^2}{h^2}|G_{AD}(\nu_D{}^A)|^2. \tag{11b}$$

The physical significance V_{AD} is the number of transitions from the A term into D per molecule per unit time (*viz.*, the reciprocal of T_{AD}, the average lifetime of A without predissociation).

Proceeding in the same way, we obtain for the integration occuring in Eq. (8b)[9]

$$-\frac{h}{4\pi}V_{BC}e^{-2\pi at}, \tag{11c}$$

where

$$V_{BC}=\frac{4\pi^2}{h}|H_{BC}(E_B)|^2. \tag{11d}$$

V_{BC} means the number of transitions from the B term into C without radiation per molecule per unit time (*viz.*, the reciprocal of T_{BC}, the average lifetime of B without transition to a lower term).

With these results we obtain from Eqs. (8a) and (8b)

$$\left.\begin{aligned}S_A\left[\frac{i}{h}E_A+\frac{V_{AD}}{4\pi}-a\right]+S_B\cdot\frac{i}{h}H_{AB}=0,\\ S_A\cdot\frac{i}{h}H_{BA}+S_B\left[\frac{i}{h}E_B+\frac{V_{BC}}{4\pi}-a\right]=0.\end{aligned}\right\} \tag{12}$$

[7] A' is the perturbed value of the A term.
[8] See reference 6, p. 63.
[9] See H. A. Kramers, *Theorien des Aufbaues der Materie. I. Die Grundlagen der Quantentheorie* (1933), p. 219.

Equation (12) represents a system of homogeneous linear equations for the computation of S_A, S_B. The condition of its solubility is that the determinant should vanish, *viz.*,

$$\begin{vmatrix} \frac{i}{h}E_A+\frac{V_{AD}}{4\pi}-a & \frac{i}{h}H_{AB} \\ \frac{i}{h}H_{BA} & \frac{i}{h}E_B+\frac{V_{BC}}{4\pi}-a \end{vmatrix}=0. \tag{13}$$

Evaluating a, we have

$$2\pi a_{1,2}=\frac{V_{AD}+V_{BC}}{4}\mp\Delta(r)+\frac{2\pi i}{h}\left[\frac{E_A+E_B}{2}\mp\operatorname{sign}\epsilon_A{}^B\cdot\Delta(i)\right],^{10} \tag{14a}$$

where

$$\Delta(r)=\frac{1}{\sqrt{2}}\left\{w^2-\frac{4\pi^2}{h^2}\left[\left(\frac{\epsilon_A{}^B}{2}\right)^2+|H_{AB}|^2\right]\right.$$
$$\left.+\left(\left[w^2+\frac{4\pi^2}{h^2}\left(\left(\frac{\epsilon_A{}^B}{2}\right)^2+|H_{AB}|^2\right)\right]^2-\frac{16\pi^2}{h^2}|H_{AB}|^2\cdot w^2\right)^{\frac{1}{2}}\right\}^{\frac{1}{2}}, \tag{14b}$$

$$\Delta(i)=\frac{1}{\sqrt{2}}\left\{\left(\frac{\epsilon_A{}^B}{2}\right)^2+|H_{AB}|^2-\left(\frac{h}{2\pi}w\right)^2\right.$$
$$\left.+\left(\left[\left(\frac{\epsilon_A{}^B}{2}\right)^2+|H_{AB}|^2+\left(\frac{h}{2\pi}w\right)^2\right]^2-4|H_{AB}|^2\left(\frac{h}{2\pi}w\right)^2\right)^{\frac{1}{2}}\right\}^{\frac{1}{2}}, \tag{14c}$$

$$\epsilon_A{}^B=E_B-E_A;\quad w=\frac{V_{BC}-V_{AD}}{4}. \tag{14d}$$

Employing Eqs. (14a)–(14d), we obtain from Eq. (12) for the S's (taking account of the conditions of normalization)

$$S_{A1}=S_{B2}=(\tfrac{1}{2}[1+(1-\rho^2)^{\frac{1}{2}}])^{\frac{1}{2}};\quad S_{B1}=-S_{A2}=(\tfrac{1}{2}[1-(1-\rho^2)^{\frac{1}{2}}]^{\frac{1}{2}}, \tag{15a}$$

where

$$\rho^2=\frac{|H_{AB}|^2}{[\Delta(i)]^2+\left(\frac{h}{2\pi}w\right)^2}. \tag{15b}$$

With the help of these equations we can determine the coefficients a_k after some transformations in the exponent

$$a_{A1}=S_{A1}e^{-\alpha_1 t};\quad a_{A2}=S_{A2}e^{-\alpha_2 t}, \tag{16a}$$

$$a_{B1}=S_{B1}e^{-\alpha_1 t};\quad a_{B2}=S_{B2}e^{-\alpha_2 t}, \tag{16b}$$

---

[10] More exactly we should have to write $\operatorname{sign}(\epsilon_A{}^B\cdot w)$, but in our case, predissociation of the B state being complete, $V_{BC}\gg V_{AD}$, *viz.*, $w>0$, we may neglect w.

$$a_{C1}(E)=S_{B1}\cdot\frac{2\pi i}{h}H_{CB}(E)\frac{1-\exp\left[\left(\frac{2\pi i}{h}E-\alpha_1\right)t\right]}{\frac{2\pi i}{h}E-\alpha_1}\cdot\exp\left(-\frac{2\pi i}{h}Et\right);$$

$$a_{C2}(E)=S_{B2}\cdot\frac{2\pi i}{h}H_{CB}(E)\frac{1-\exp\left[\left(\frac{2\pi i}{h}E-\alpha_2\right)t\right]}{\frac{2\pi i}{h}E-\alpha_2}\cdot\exp\left(-\frac{2\pi i}{h}Et\right), \tag{16c}$$

$$a_{D1}^{(\rho)}=S_{A1}\cdot\frac{2\pi i}{h}G_{DA}^{(\rho)}\frac{1-\exp\left(\left[\frac{2\pi i}{h}(E_D+h\nu_\rho)-\alpha_1\right]t\right)}{\frac{2\pi i}{h}(E_D+h\nu_\rho)-\alpha_1}\cdot\exp\left(-\frac{2\pi i}{h}[E_D+h\nu_\rho]t\right);$$

$$a_{D2}^{(\rho)}=S_{A2}\cdot\frac{2\pi i}{h}G_{DA}^{(\rho)}\frac{1-\exp\left(\left[\frac{2\pi i}{h}(E_D+h\nu_\rho)-\alpha_2\right]t\right)}{\frac{2\pi i}{h}(E_D+h\nu_\rho)-\alpha_2}\cdot\exp\left(-\frac{2\pi i}{h}[E_D+h\nu_\rho]t\right), \tag{16d}$$

where

$$\alpha_1=\tfrac{1}{2}(S_{A1}{}^2V_{AD}+S_{B1}{}^2V_{BC})+\frac{2\pi i}{h}\left[\frac{E_A+E_B}{2}-\operatorname{sign}\epsilon_A{}^B\cdot\Delta(i)\right],$$

$$\alpha_2=\tfrac{1}{2}(S_{A2}{}^2V_{AD}+S_{B2}{}^2V_{BC})+\frac{2\pi i}{h}\left[\frac{E_A+E_B}{2}+\operatorname{sign}\epsilon_A{}^B\cdot\Delta(i)\right]. \tag{17}$$

In the expression (7) for ψ the values of a_k given in Eq. (16) are to be substituted. The $|a_k|^2$, that is, the probabilities of realization of each φ_k state, will be as follows:

$$|a_{A1}|^2=S_{A1}{}^2\exp(-[S_{A1}{}^2V_{AD}+S_{B1}{}^2V_{BC}]t);\quad |a_{A2}|^2=S_{A2}{}^2\exp(-[S_{A2}{}^2V_{AD}+S_{B2}{}^2V_{BC}]t), \tag{18a}$$

$$|a_{B1}|^2=S_{B1}{}^2\exp(-[S_{A1}{}^2V_{AD}+S_{B1}{}^2V_{BC}]t);\quad |a_{B2}|^2=S_{B2}{}^2\exp(-[S_{A2}{}^2V_{AD}+S_{B2}{}^2V_{BC}]t). \tag{18b}$$

I will give a detailed computation for one of the coefficients,

$$\int|a_{C1}(E)|^2dE=S_{B1}{}^2\frac{2\pi}{h}\int_{-\infty}^{+\infty}|H_{CB}(E)|^2\frac{1-2\cdot\cos yt\cdot e^{-st}+e^{-2st}}{y^2+s^2}dy$$

$$=S_{B1}{}^2\frac{V_{BC}}{2\pi}\cdot\frac{2\pi}{2s}(1-e^{-2st})=\frac{S_{B1}{}^2V_{BC}}{S_{A1}{}^2V_{AD}+S_{B1}{}^2V_{BC}}[1-\exp(-[S_{A1}{}^2V_{AD}+S_{B1}{}^2V_{BC}]t)],$$

where

$$y=\frac{2\pi}{h}\left[E-\frac{E_A+E_B}{2}+\operatorname{sign}\epsilon_A{}^B\cdot\Delta(i)\right];\quad s=\tfrac{1}{2}(S_{A1}{}^2V_{AD}+S_{B1}{}^2V_{BC});\quad dy=\frac{2\pi}{h}dE.$$

By a similar method we obtain for all the four coefficients

$$\int |a_{C1}(E)|^2 dE = \frac{S_{B1}^2 V_{BC}}{S_{A1}^2 V_{AD} + S_{B1}^2 V_{BC}} [1 - \exp(-[S_{A1}^2 V_{AD} + S_{B1}^2 V_{BC}]t)];$$

$$\int |a_{C2}(E)|^2 dE = \frac{S_{B2}^2 V_{BC}}{S_{A2}^2 V_{AD} + S_{B2}^2 V_{BC}} [1 - \exp(-[S_{A2}^2 V_{AD} + S_{B2}^2 V_{BC}]t)], \tag{18c}$$

$$\int \sum_\rho |a_{D1}^{(\rho)}|^2 d\nu = \frac{S_{A1}^2 V_{AD}}{S_{A1}^2 V_{AD} + S_{B1}^2 V_{BC}} [1 - \exp(-[S_{A1}^2 V_{AD} + S_{B1}^2 V_{BC}]t)];$$

$$\int \sum_\rho |a_{D2}^{(\rho)}|^2 d\nu = \frac{S_{A2}^2 V_{AD}}{S_{A2}^2 V_{AD} + S_{B2}^2 V_{BC}} [1 - \exp(-[S_{A2}^2 V_{AD} + S_{B2}^2 V_{BC}]t)]. \tag{18d}$$

DISCUSSION OF RESULTS

1. At the beginning of the time measurement ($t=0$), we have:

$$|a_{A1}|^2 = S_{A1}^2; \qquad |a_{A2}|^2 = S_{A2}^2, \tag{19a}$$

$$|a_{B1}|^2 = S_{B1}^2; \qquad |a_{B2}|^2 = S_{B2}^2, \tag{19b}$$

$$\int |a_{C1}(E)|^2 dE = 0; \qquad \int |a_{C2}(E)|^2 dE = 0, \tag{19c}$$

$$\int \sum_\rho |a_{D1}^{(\rho)}|^2 d\nu = 0; \qquad \int \sum_\rho |a_{D2}^{(\rho)}|^2 d\nu = 0, \tag{19d}$$

and consequently

$$\psi_1 = S_{A1}\varphi_A + S_{B1}\varphi_B; \quad \psi_2 = S_{A2}\varphi_A + S_{B2}\varphi_B. \tag{20}$$

Disregarding the probability of the transition of the A term into D and of the B term into C (*viz.*, $V_{AD} = V_{BC} = 0$), Eqs. (20) means nothing else but the time-independent solution of the wave equation for the case of common perturbation between the A and B states. Namely in this case in Eq. (15b) the expression of ρ and $\Delta(i)$ will be:

$$\rho^2 = \frac{|H_{AB}|^2}{|\Delta(i)|^2}; \quad \Delta(i) = \left(\left(\frac{\epsilon_A{}^B}{2}\right)^2 + |H_{AB}|^2\right)^{\frac{1}{2}} \tag{21}$$

which are well-known results.[11]

2. In order to be able to compute the intensity decrease of the emitted light, we have to investigate our solutions for the case $t = \infty$. Then we have:

$$|a_{A1}|^2 = 0; \qquad |a_{A2}|^2 = 0, \tag{21a}$$

$$|a_{B1}|^2 = 0; \qquad |a_{B2}|^2 = 0, \tag{21b}$$

$$\int |a_{C1}(E)|^2 dE = \frac{S_{B1}^2 V_{BC}}{S_{A1}^2 V_{AD} + S_{B1}^2 V_{BC}}; \qquad \int |a_{C2}(E)|^2 dE = \frac{S_{B2}^2 V_{BC}}{S_{A2}^2 V_{AD} + S_{B2}^2 V_{BC}}, \tag{21c}$$

$$\int \sum_\rho |a_{D1}^{(\rho)}|^2 d\nu = \frac{S_{A1}^2 V_{AD}}{S_{A1}^2 V_{AD} + S_{B1}^2 V_{BC}}; \qquad \int \sum_\rho |a_{D2}^{(\rho)}|^2 d\nu = \frac{S_{A2}^2 V_{AD}}{S_{A2}^2 V_{AD} + S_{B2}^2 V_{BC}}. \tag{21d}$$

[11] G. P. Ittmann, Zeits. f. Physik **71**, 623 (1931). A. Budó and I. Kovács, Zeits. f. Physik **109**, 393 (1938).

Equations (21c) gives the percentage of the initial molecules which are transferred without radiation (predissociation) from the two perturbed states into C. As we may see, although at the beginning predissociation came only from one of the two unperturbed states, namely from $B(V_{BC}\neq 0)$, now both of the two perturbed states are predissociated.

Equations (21d) gives the percentage of the initial molecules which are transferred with radiation from the two perturbed states into the lower state D. Though at the beginning, transition was possible only from one of the two unperturbed states, namely from $A(V_{AD}\neq 0)$, now each of the two perturbed states furnishes a spectrum line.

Let us now consider what kind of numerical results can be deduced from our formulae for the decrease of the intensity. From other considerations it follows that under normal conditions we have $V_{AD}=10^{8}$ (that is $T_{AD}=10^{-8}$), and in the case of a complete predissociation $V_{BC}=10^{12}$ (that is, $T_{BC}=10^{-12}$). In the case of an accidental predissociation, according to the experimental results, we have to assume the H_{AB} matrix element to be so small that no displacements of the lines are observable. Thus, in the first case H_{AB} should be 0.2 cm^{-1}, in the second case 0.1 cm^{-1} (both measured in wave numbers). Calculated for different term differences and using the above mentioned H_{AB} values, we get the results given in Table I.

From the data collected in the table it is obvious that the intensity of the lines corresponding to the perturbing state designated by the subscript 2 (corresponding to B) is negligible, while the decrease of the intensity of the lines arising from the perturbed state designated by the subscript 1 (corresponding to A) can take any values between 0.06–1.00 depending on the energy difference.

COMPARISON WITH EXPERIMENT

Schmid and Gerö[12] photographed and analyzed the spectrum of the NO molecule between 1950–2700A with large dispersion and great intensity. They found that near the intersection of the $v'=0$ level of the so-called β-bands with that of the γ-bands (using the (0, 0), (0, 1), (0, 2), (0, 3), (0, 4) γ-bands), there is no irregularity to be found, a behavior which can be explained by the small value of the matrix element of interaction. We find the same situation at the intersection of level $v'=1$ of the β-bands with the level $v'=0$ of the γ-bands at about $J\approx 50$. However the intensities of the lines belonging to $K=48$ and $K=65$, respectively, of the $v'=1$ and $v'=0$ levels of the γ-bands, *are smaller* than the intensities of the lines belonging to the neighboring quantum numbers; whereas while the wave numbers of these lines do not show any irregularities. These two lines correspond to levels just at the place where the $v'=2$ and $v'=3$ β-term series, which are already predissociated at this energy, cross the γ-term series, leading to an accidental predissociation. Considering that even here the wave numbers of the lines exhibit no irregularity, we have to assume the matrix element to be very small, which seems to be a general property at these intersections corresponding to the case above mentioned (compare the crossing of $v'=0$ of γ and $v'=0$ of β, and that of $v'=0$ of γ and $v'=1$ of β) This example is more convincing than that of Coster, since here the terms (the β-terms) causing the accidental predissociation were in fact observed below the limits of their own predissociation (50,000–51,000 cm^{-1}).

---

[12] The work of Schmid and Gerö quoted under reference 3 will be published later elsewhere. Furthermore see: K. Ballenegger, Mat. és Fiz. Lapok, Budapest **51** (1944).

THE JOURNAL OF CHEMICAL PHYSICS VOLUME 15, NUMBER 4 APRIL, 1947

Physical Properties and Cation Arrangement of Oxides with Spinel Structures

I. Cation Arrangement in Spinels

E. J. W. VERWEY AND E. L. HEILMANN*
Natuurkundig Laboratorium der N. V. Philips' Gloeilampenfabrieken, Eindhoven, Nederland
(Received November 29, 1946)

By means of a detailed x-ray study of a large number of oxides having a spinel structure, it has been established whether they crystallize in the "normal" spinel-type structure, XY_2O_4, or in the "inversed" type of structure, $Y(XY)O_4$, discovered by Barth and Posnjak. Certain rules can be derived which are also applicable to more complicated spinels or to solid solutions of different spinel oxides. Madelung constants have been calculated for different spinel types in order to investigate their stability on the basis of an ionic concept of the chemical bond (Born's lattice theory). The experimental results are only partially explainable on this basis. All exceptions to the electrostatic principles can be understood by assuming that Fe^{3+}, Ga^{3+}, In^{3+}, Zn^{2+}, and Cd^{2+} favor a configuration having the coordination number 4, because of a considerable covalent contribution to the chemical bond for that configuration.

1. INTRODUCTION

THERE are a great many oxides having the general formula XY_2O_4 which crystallize with the same general crystal structure as the mineral spinel, $MgAl_2O_4$. Certain groups of spinels show remarkable electrical and magnetic properties. The spinels are, therefore, of considerable interest from a technical point of view. They may be readily synthesized so that their properties, which are composition-sensitive, may be controlled within varying limits.

The spinel structure is cubic with a large unit cell containing 8 X, 16 Y, and 32 oxygen atoms. The positions of the oxygen atoms are more or less fixed but the arrangement of the cations varies considerably within certain limits. The

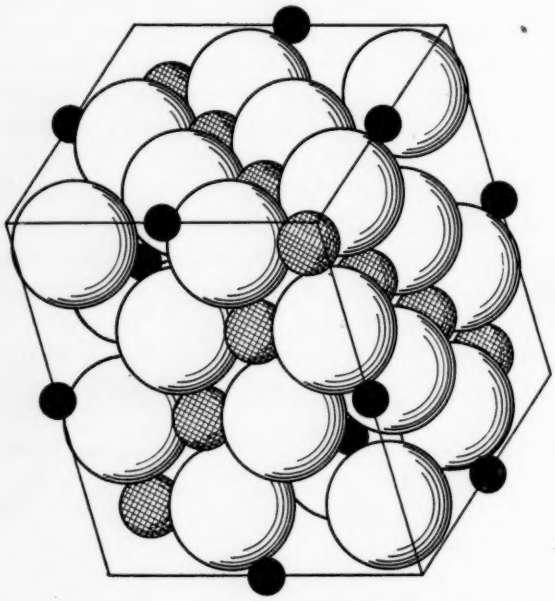

FIG. 1. Arrangement and packing of atoms in unit cell of ideal spinel-type ($u=0.375$) containing $8[XY_2O_4]$. Large spheres represent oxygen, small black spheres represent fourfold coordination position and cross-hatched spheres sixfold coordination position.

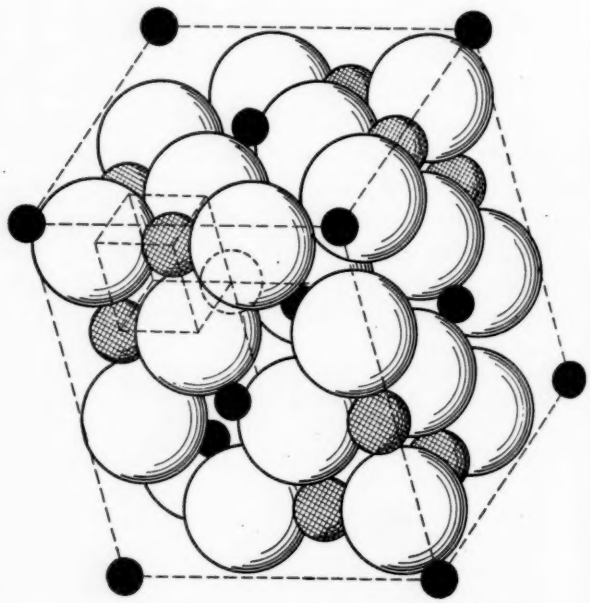

FIG. 2. Same as Fig. 1 but with unit cell shifted by one-half a cube edge. Small dashed-line cube shows NaCl-type structural motif with the cross-hatched ion in an octahedral interstice.

* Deported to a concentration camp in the eastern part of Germany (July 1944), from which he never returned.

variations in distribution of cations in the X and Y positions cause marked changes in some of the physical properties. One of these is the electrical conductivity which will be considered in a following paper (II). Equivalent lattice points may be occupied by different cations distributed statistically throughout the crystal. The permutations are often more complicated than those found in ordinary primary solid solutions.

We have investigated a large number of these compounds during the past few years. The present paper describes a detailed study of the structure of the oxide spinels. It contains the crystallographic results for those compounds in which we have established the arrangement of the cations and a general discussion of the factors determining their arrangement.

2. DISCUSSION OF THE SPINEL STRUCTURE

In most oxidic structures the oxygen ions are appreciably larger than the metallic ions and the spinel structure can be approximated by a cubic close packing of O^{2-} ions in which the Mg^{2+} and Al^{3+} ions occupy certain interstices. Each unit cell contains 8 $[MgAl_2O_4]$ and, therefore, 32 O^{2-} ions. This close packing contains 64 interstices surrounded by 4 O^{2-} ions (coordination number 4, tetrahedral) and 32 interstices surrounded by 6 O^{2-} ions (coordination number 6, octahedral). In the spinel structure, 8 of these tetrahedral holes and 16 of the octahedral holes are occupied. Unit cells of the "ideal" spinel structure are shown in Fig. 1 and Fig. 2; the only difference between them is that the cell unit has been shifted over one-half of the cube edge a in one of the three cubic cube edge directions in the crystal. It is convenient to subdivide the unit cell in 8 octants. The structure then may be described as a face-centered compilation of A- and B-cubes, where the A-cubes comprise a group Mg_2O_4 (Mg in 4-coordination) and the B-cubes a group Al_4O_4 (Al in 6-coordination).[1]

In all spinel-like substances the parameter u has a value in the neighborhood of 0.375. For $u=0.375$, the case corresponding to Figs. 1–3, the arrangement of the O^{2-} ions equals exactly a cubic close packing. In actual spinel lattices this ideal pattern is slightly deformed, usually, corresponding to $u>0.375$, in such a way that the oxygen tetrahedron in the A-cubes is somewhat expanded and the oxygen tetrahedron in the B-cubes is slightly contracted. Accordingly, in that case, the octahedrons formed by the 6 O^{2-} ions directly surrounding the positive ions in these B-cubes deviate somewhat from regular octahedrons.

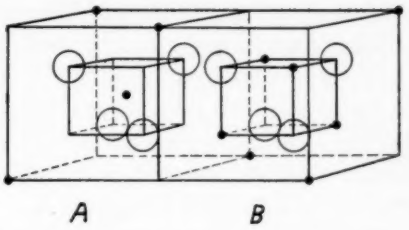

FIG. 3. Two octants of a unit cell. Spinel structure is a three-dimensional packing of A- and B-cubes in a checkerboard arrangement.

In simple spinels the valencies of the cations may be either

$$X=2+, \quad Y=3+,$$

or

$$X=4+, \quad Y=2+.$$

The third possibility, $X=6+$, $Y=1+$, is very rare. In the present work, separate examples of the two common possibilities and their combinations in more complicated spinels are studied.

Originally, in accordance with classical principles of crystallography, it was assumed that in the spinels the X atoms or ions occupied the eightfold position (the tetrahedral holes of the A-cubes indicated in Fig. 3) and the Y atoms or ions were in the 16-fold positions (the octahedral interstices of the B-cubes). However, Barth and Posnjak[2] pointed out a second possibility of distributing the cations while retaining cubic symmetry; *viz.*, one in which the tetrahedral interstices are occupied by half of the Y ions, the octahedral holes by the X ions, and the other half of the Y ions are distributed at random at these lattice points. For the sake of convenience, the first arrangement will be indicated as characteristic for "*normal spinels*," the Barth and Posnjak arrangement as that of "*inversed spinels*." A number of examples for both groups have

[1] E. J. W. Verwey, Zeits. f. Krist. **91A**, 65 (1935).

[2] T. F. W. Barth and E. Posnjak, Zeits. f. Krist. **82**, 325 (1932).

already been given by Barth and Posnjak, who based their conclusions upon a detailed discussion of the intensities of x-ray diffraction pictures. In addition to these two arrangements, there is the possibility of some intermediate arrangement with an averaged distribution of all ions about all spinel cation positions. As a matter of fact, this contingency constitutes in effect an infinite series of possibilities, as this type of distribution will generally occur in such a way that certain ions show a definite preference for one type of interstice according to a certain distribution factor. Machatschki[3] has described such an intermediate case ($MgGa_2O_4$).

3. CONSIDERATION OF THE STABILITY OF DIFFERENT ARRANGEMENTS BASED ON CALCULATIONS OF MADELUNG POTENTIALS

Before passing to an extension of the experimental facts and an attempt to find general rules as to the most stable arrangement in a given case as a function of the properties of the participating ions, it is useful to consider first what might be expected from a purely heteropolar point of view.

The chemical bonding in these spinel oxides can be treated to a first-order approximation as an ionic bond, in which the state of affairs is described by an equilibrium of Coulomb forces and Born repulsion forces. Comparing states with the same crystal structure, the former forces are described by the Madelung potential; the latter are roughly determined by the size of the different ions. The ionic radii will not vary over a very wide range, because the spinel structure is stable only if the cations are rather medium sized and, in addition, the radii of the different ionic species in the same compound do not differ too much. The ionic dimensions will have an influence upon the value of the parameter u; large values of u can be expected if the tetrahedral interstices are occupied by comparatively large ions. Values for this parameter, however, have been determined in only a few cases (where they were usually about 0.380). Accurate values are rather difficult to obtain and only very few are available.

Madelung summation constants have been calculated for spinels with the following values of the valencies, where p and q are the valencies of the ions at tetrahedral and octahedral interstices, respectively:

(a) $p=4$, $q=2$,
(b) $p=2$, $q=3$,
(c) $p=3$, $q=2\frac{1}{2}$.

Case (a) will then give the Madelung constant of a normal 4-2 spinel, $X^{4+}Y_2^{2+}O_4$, and case (b) that of a normal 2-3 spinel, $X^{2+}Y_2^{3+}O_4$. In the inversed 4-2 spinel $Y^{2+}(X^{4+}Y^{2+})O_4$, the 16-fold position contains an averaged distribution of 4-valent and 2-valent ions and the corresponding Madelung constant will approximately be given by case (b) as the valency of the ions in the 16-fold position is on the average 3. In the inversed 2-3 spinel $Y^{3+}(X^{2+}Y^{3+})O_4$, the valency between the brackets is on the average $2\frac{1}{2}$ and the Madelung constant will be approximated by case (c).

The calculations have been carried out for different values of u in order to establish the effect of this parameter upon the stability.

The calculations have been done by a combination of the Ewald[4] and the Evjen[5] methods, for the following reasons. As a consequence of the large number of ions per unit cell the calculations are rather laborious, especially in those cases where the parameter u differs from 0.375 and the oxygen ionic lattice shows small deviations from the ideal face-centered cubic compilation.

Evjen's method, a direct summation over a restricted number of unit cells where electroneutrality is maintained by counting the ions in the outside planes $\frac{1}{2}$, etc., appears to lead to results accurate within 1 percent when the summation is carried out over a cube of 8 unit cells, with the ion under consideration in the corner common to all 8 cells (this has been checked by extending the calculations in one case over 27 and 64 cells). Accordingly, this method has been used for a calculation of the Madelung constant M for $u=0.375$, 0.380, 0.385, and 0.390. In some cases, including the present one, however, the Evjen method leads to M values which contain a constant error due to

[3] F. Machatschki, Zeits. f. Krist. **82**, 348 (1932).

[4] P. P. Ewald, Ann. d. Physik **64**, 253 (1921); Zeits. f. Krist. **56**, 129 (1921).

[5] H. M. Evjen, Phys. Rev. **39**, 675 (1932).

the circumstance that the outer part of the crystal fraction cut out of the crystal in this way gives rise to an electrical dipole layer. As this constant error will be independent of u, it is sufficient to eliminate it by calculating for the ideal parameter value $u=0.375$, the Madelung constant according to an alternative method avoiding this constant error. For this calculation Ewald's method has been chosen. According to this method the summation over the infinitely large lattice is carried out by transforming the infinite series into the elliptical theta-functions, so that again a rapid convergency is obtained.

Calculating in this way the electrical potential at a tetrahedral lattice point, an octahedral lattice point, and an O-point, we find for the total Coulomb energy per "molecule" XY_2O_4:

$$V=-\tfrac{1}{2}\cdot(e^2/a)(pM_{tetra.}+2qM_{oct.}+8M_O)$$
$$=-M\cdot(e^2/a)$$

where a = the length of the unit cell. The data obtained for the Madelung constant M are given in Table I. Hence, on the basis of the ionic picture of spinels, assuming that the cube edge of the unit cell is not altered by the inversion (we will see later on that this is not entirely true, but sufficiently true for our following conclusions), and also assuming that the Born repulsion potential is a constant fraction, amounting to about 10 percent of the Coulomb potential, we should arrive at the following results concerning the stability of different cation arrangements.

1. The normal 2-3 spinel (case (b)) is more stable than the inversed 2-3 spinel (case (c)), but the inversed 4-2 spinel (again case (b)) is more stable than the normal 4-2 spinel (case (a)).

2. This conclusion is not altered by the influence of the parameter, as the M values do not cross within the range of practically occurring u values.

The first conclusion can also roughly be explained on the basis of the principle of maximal charge neutralization; in both cases we find that the most stable arrangement is that in which the cations with the highest charge occupy the interstices with the highest coordination number.

Similarly it can easily be understood that the Madelung potential of a normal 4-2 spinel is increased by a decrease of u and that of a normal 2-3 spinel by an increase of u, as both variations of u correspond to a contraction of the oxygen ions around the cations with the highest charges.

TABLE I.

	(a) $p=4$; $q=2$	(b) $p=2$; $q=3$	(c) $p=3$; $q=2\frac{1}{2}$
$u=0.375$	142.1	150.3	143.6
$=0.380$	139.9	153.1	143.8
$=0.385$	137.7	155.7	144.1
$=0.390$	135.6	158.2	144.3

It is also understood that the intermediate case ($p=3$, $q=2\frac{1}{2}$) is less sensitive to variations of the parameter.

In the following section the extent of the agreement between the predictions given above concerning the relative stability of different arrangements and the cation distributions actually found will be shown.

4. X-RAY INVESTIGATION OF VARIOUS SPINELS

A large number of spinel oxides were prepared by mixing the pure oxides ("pro-analysis" quality) in the proper ratio, pressing the mixture into bars and heating the latter for several hours in an electric furnace at a constant temperature. The sintering temperature varied with the nature of the constituent oxides; for easily sintering samples it was mostly 1200°C, for oxides sintering with greater difficulty it was 1300°C, or even 1400°C (as in the case of $MgCr_2O_4$). Only in the instance last mentioned was it necessary to carry out the heating process in an atmosphere of oxygen; in the other cases air was sufficient to prevent reduction. The samples with Fe^{2+} form an exception to this rule and require special precautions to obtain the iron completely in the desired valency state.

The determination of the cation arrangement and, consequently, also of the detailed pattern of the oxygen ions (the latter described by the parameter u) was made in the usual way with the aid of x-ray powder diagrams.* The intensities of a great number of diffraction lines were measured and the observed values were compared with the calculated reflection intensities** for different arrangements and different

* We wish to thank Dr. J. F. H. Custers and Mr. C. G. J. Jansen, both from this Laboratory, for the preparation of these x-ray pictures under carefully controlled, checked conditions.

** The intensities were measured visually by comparison with an intensity scale. In the calculations the usual angle-dependent factors were taken into account, including absorption.

TABLE II. Intensities.

Plane	Cu	$Cu_{0.4}Zn_{0.6}$	$Cu_{0.4}Zn_{0.6}$	Zn
(111)	5	4	3	1–
(220)	15	20	20	30
(311)	100	100	100	100

values of u. In several cases the difference in the scattering power of the constituent metal ions for arbitrarily chosen wave-length of x-radiation was too small to allow a decision between different arrangements. In that case it was often possible to arrive at the desired result by a special choice of the irradiating wave-length. The scattering power of an element is comparatively low for the characteristic $K\alpha$-radiation of the metal having an atomic number one higher than the scattering metal atom, as a consequence of the proximity of the absorption edge. Thus, the scattering power of Fe is reduced by about 20 percent for the same values of $\sin\theta/\lambda$ when Co $K\alpha$-radiation is used instead of, for instance, Cu $K\alpha$-radiation. Hence, we must replace the usual theoretical scattering factor by the experimental values, which in this case have been determined by Bradley and Hope.[6] In this way it was possible, for instance, to determine the arrangement in samples containing both Cu and Fe which normally would have been impossible to determine.

The following substances were investigated: $MgCr_2O_4$, $NiCr_2O_4$, $CdCr_2O_4$, $CuFe_2O_4$, $ZnFe_2O_4$, $Cu_xZn_{1-x}Fe_2O_4$, $CdFe_2O_4$, $TiZn_2O_4$, $SnZn_2O_4$, $SnCo_2O_4$, $Fe^{2+}Fe^{3+}AlO_4$, $LiAl_5O_8$, and a large number of solid solutions containing these and other spinels.

The following are the results obtained with the simpler spinels.

$MgCr_2O_4$. Radiation Cu $K\alpha$. Lattice dimension $a=8.312$A. Intensities exclude the arrangement $Cr_8(Mg_8Cr_8)O_{32}$ and point definitely to $Mg_8Cr_{16}O_{32}$, hence all Mg in eightfold position (tetrahedral holes), and all Cr in 16-fold position (octahedral holes). Comparison of experimental and calculated intensities does not permit very accurate conclusions as to the value of u; the calculations were made with differences of 0.5/60. The best agreement is found for $u=23/60$ though also $u=23.5/60$ cannot be excluded. Hence $u=0.38_5\pm0.01$.

$NiCr_2O_4$. Radiation Cr $K\alpha$. $a=8.299$A. For the scattering power of Cr for Cr $K\alpha$ a correction was made in view of the vicinity of the absorption edge. Arrangement definitely $Ni_8Cr_{16}O_{32}$. Intensities do not permit a decision between $u=23/60$ and $u=23.5/60$, hence $u=0.38_5$ to 0.39 ± 0.01.

$CdCr_2O_4$. Radiation Cu $K\alpha$. $a=8.567$A. Arrangement $Cd_8Cr_{16}O_{32}$. Best u value 23/60 though 23.5/60 cannot be excluded. Hence $u=0.38_5\pm0.01$.

$CuFe_2O_4$. Radiation Co $K\alpha$. $a=8.37$A. Very good agreement for inversed spinel arrangement: $Fe_8(Cu_8Fe_8)O_{32}$ with $u=0.38_0\pm0.005$.

$ZnFe_2O_4$. Radiation Co $K\alpha$. $a=8.416$A. Very good agreement for normal spinel positions: $Zn_8Fe_{16}O_{32}$ with $u=0.38_0\pm0.005$.

$Cu_{0.5}Zn_{0.5}Fe_2O_4$. Radiation Co $K\alpha$. $a=8.388$A. Arrangement $Zn_4Fe_4(Cu_4Fe_{12})O_{32}$ with $u=0.380\pm0.005$.

$Cu_{0.4}Zn_{0.6}Fe_2O_4$. $a=8.402$A. Arrangement $Zn_{4.8}Fe_{3.2}(Cu_{3.2}Fe_{12.8})O_{32}$ with $u=0.380\pm0.005$.

It is not possible to distinguish between Cu and Zn. However, the gradual transition between the inversed spinel (copper) and the normal spinel (zinc), with each Zn and Cu keeping its own position, can very well be followed in the gradual change of the intensities as one goes from $CuFe_2O_4$ to $ZnFe_2O_4$. For example, the relative increase of the intensity of (220) or decrease of (111), in comparison with (311), which was a strong reflection arbitrarily set equal to 100 in all films, is shown in Table II.

$CdFe_2O_4$. Arrangement $Cd_8Fe_{16}O_{32}$.

$TiZn_2O_4$. Radiation Cu $K\alpha$. $a=8.445$A. Arrangement $Zn_8(Ti_8Zn_8)O_{32}$ with $u=0.380\pm0.005$.

$SnZn_2O_4$. Arrangement $Zn_8(Sn_8Zn_8)O_{32}$.

$SnCo_2O_4$. Arrangement $Co_8(Sn_8Co_8)O_{32}$.

$Fe^{2+}Fe^{3+}AlO_4$. Radiation Co $K\alpha$.

Best agreement for the arrangement $Fe_8^{2+}(Al_8Fe_8^{3+})O_{32}$ or $Fe_8^{3+}(Al_8^{3+}Fe_8^{2+})O_{32}$, with $u=0.385\pm0.01$, though small deviations remain which can be explained by a small percentage of Al in eightfold position (less than 10 percent). The presence of a weak (111) reflection might even suggest that Fe^{2+} is at the 16-fold position, as for small reflection angles the scattering power of Fe^{2+} will be appreciably larger than that of Fe^{3+}.

[6] A. J. Bradley and R. A. H. Hope, Proc. Roy. Soc. 136, 283 (1932).

$LiAl_5O_8$. The x-ray data used in the investigation of this substance were those found in the literature.[7] Of the two possible arrangements, $Al_8(Li_4Al_{12})O_{32}$ or $(Li_4Al_4)Al_{16}O_{32}$, the intensities are definitely in favor of the former, though the best agreement is obtained by assuming that the actual distribution is an intermediate one, with a small contribution of the second, $u=0.385 \pm 0.01$. Hence, the most probable arrangement approaches the completely random distribution which would correspond to $(Li_{1\ 1/3}Al_{6\ 2/3})(Li_{2\ 2/3}Al_{13\ 1/3})O_{32}$. As this substance is the only one investigated of the interesting type in which $Li^+ + Al^{3+}$ together take the role of two divalent ions, we merely give the results for this compound; in the following sections, which are concerned only with 2-3 and 4-2 spinels, it will be omitted from further consideration.

5. CONSIDERATION OF LATTICE DIMENSION; DISCUSSION

Including the results of Barth and Posnjak[2] (who found normal spinels with a number of Al spinels, inversed spinels for Mg_2TiO_4, Fe_2TiO_4, $MgFe_2O_4$, and $MgIn_2O_4$) and that of Machatschki ($MgGa_2O_4$ intermediate case), we arrive at the following conclusions:

(a) 4-2 spinels are always found in the inversed arrangement, in complete accordance with the lower Coulomb potential thereby realized.

(b) 2-3 spinels are often found in the normal arrangement, again in accordance with expectation on the basis of electrostatic considerations. Thus, all Al and Cr spinels investigated obey this electrostatic rule. The same holds for $ZnFe_2O_4$ and $CdFe_2O_4$. Obvious exceptions, however, are a number of other Fe spinels ($MgFe_2O_4$, $CuFe_2O_4$) and also $MgIn_2O_4$, $MgGa_2O_4$ (partially inversed).

In connection with these conclusions, it would be interesting to have more information as to the behavior of other Fe spinels, such as those containing Mn, Fe, Co, Ni as the divalent ion. Here, however, the difference in scattering power is so small that no information can be obtained from the x-ray intensities. We have investigated, therefore, whether there are regularities in the values of a, the cube edge of the unit cell, for the different spinels. This is shown in Table III, where most data concerning a were derived from the literature; in those cases for which more than one value was found we used an average value.

Comparing all Al spinels, all Cr spinels, and those Fe spinels for which a normal arrangement was established in the present paper (Zn and Cd), it is seen that the lattice dimensions of these spinels run completely parallel to their composition and, apart from small deviations, go in the sequence to be expected from the divalent ionic radii. One finds an increase of 0.235A (average value maximal deviation only 0.015A) in a as one goes from Al to Cr spinels, and an increase of 0.12A as one goes from Cr to normal Fe spinels. This increase, practically independent of the nature of the divalent ion, can easily be understood on the basis of the different sizes of the Al^{3+}, Cr^{3+}, and Fe^{3+} ions, and it is in agreement with the gradual increase of the ionic radii established from more simple oxide structures.

Making the same comparison, but now with the other Fe spinels, we find the same parallelism and again a constant increase of a between Cr and inversed Fe spinels. Now, however, this increase is only 0.04 to 0.06A and, accordingly, on the average is 0.07A less than that found for the two normal Fe spinels (Zn and Cd). Since the Fe spinels of Cu and Mg were found to be inversed spinels, this may tentatively be considered as an indication *that the* Fe *spinels of* Mn, Fe^{2+}, Co, *and* Ni *are also inversed spinels;* simultaneously one can conclude that the Al and Cr spinels for which the normal arrangement was not established by x-ray intensity considerations are actually all normal spinels.

TABLE III. Cube edge a of unit cell for a number of 2–3 spinels XY_2O_4.

$Y^{3+}=$ / $r_{Y^{3+}}=$	Al^{3+} 0.57		Cr^{3+} 0.64			Fe^{3+} 0.67
X^{2+}	$r_{X^{2+}}$	a	Δ	a	Δ	a
Ni^{2+}	0.78	8.05	0.25	8.30	0.06	8.36
Cu^{2+}	— *	8.07	—	—	—	8.37
Zn^{2+}	0.83	8.07	0.23	8.30	0.12	8.42
Mg^{2+}	0.78	8.07	0.24	8.31	0.05	8.36
Co^{2+}	0.82	8.08	0.24	8.32	0.04	8.36
Fe^{2+}	0.83	8.12	0.22	8.34	0.05	8.39
Mn^{2+}	0.91	8.26	0.23	8.49	(0.06)	(8.55)**
Cd^{2+}	0.97	—	—	8.57	0.12	8.69

* The value of $r_{Cu^{2+}}=1.01$ found in many tables in the literature is obviously incorrect.

** The values for $MnFe_2O_4$ in the literature vary considerably, obviously as a consequence of differences in the valency states of Mn and perhaps also Fe.

[7] E. Kordes, Zeits. f. Krist. 91, 193 (1935).

TABLE IV.

Solid solutions of:	Formula
$Fe^{3+}(Fe^{3+}Fe^{3+})O_4$ and $Fe^{3+}(AlAl)O_4$	$Fe^{3+}(Fe^{2+}Al)O_4$
Fe (Cu Fe)O_4 and Zn (FeFe)O_4	$(Fe_{1/2}Zn_{1/2})(Fe_{3/2}Cu_{1/2})O_4$
Fe (Mg Fe)O_4 and Mg (CrCr)O_4	Fe (Mg Cr)O_4
Zn (Fe Fe)O_4 and Zn (CrCr)O_4	Zn (Fe Cr)O_4
Zn (Ti Zn)O_4 and Fe (MgFe)O_4	Zn $(FeMg_{1/2}Ti_{1/2})O_4$
Mg (Ti Mg)O_4 and Fe (MgFe)O_4	Fe $(Ti_{1/2}Mg_{3/2})O_4$
Zn (Fe Fe)O_4 and $\left\{\begin{matrix}Fe\\ =\gamma\cdot Fe_2O_3\end{matrix}\right.$ (Fe 2/3)O_4	$(Zn_{1/2}Fe_{1/2})Fe_{1\ 5/6}O_4$

Hence, we arrive at the conclusion that, contrary to electrostatic rules, all Fe spinels are inversed spinels, except those of Zn and Cd. The comparison of lattice dimensions is obviously not so conclusive as a direct derivation from the intensities, but our conclusions will be seen to be in complete accordance with other physical properties of the Fe spinels.

The shrinkage of about 0.07A found above for an inversed spinel in comparison with the corresponding normal arrangement must obviously be explained by a more dense structure in the former case. Actually, the arrangement which is electrostatically most stable for a 2-3 spinel, where the comparatively large divalent ions go into the smallest interstices, is not the most favorable one from a geometrical point of view, and a certain contraction of the whole lattice can reasonably be expected if, for some reason, the inversed spinel becomes the most stable configuration (the corresponding contraction is itself a factor in favor of the inversed configuration, but it is so small that its effect is negligible in comparison with the difference between the two Madelung potentials).

Since it is thus made plausible that all Fe spinels, except Zn and Cd, have the inversed cation spinel arrangement, the explanation of this abnormal behavior must obviously be found in the circumstance that these structures cannot be completely understood from a purely ionic point of view. Comparatively important homopolar contributions to the bond must be considered. Apparently the Fe^{3+} ion shows a certain preference for such a homopolar contribution if surrounded by 4 O^{2-} ions, and the same must be true for In^{3+} and Ga^{3+}. The fact that $ZnFe_2O_4$ and $CdFe_2O_4$ show again a normal behavior can then easily be explained, as the Fe^{3+} will find in Cd^{2+} and Zn^{2+} a competitor for the tetrahedral interstices. The preference of Zn^{2+} and Cd^{2+} for a tetrahedral surrounding is well known; e.g., in ZnO, ZnS, Zn_2SiO_4, CdS, CdSe; and has been attributed to homopolar contributions to the chemical bond.[8] Zn^{2+} and Cd^{2+} have a filled *d*-band, and the distance between the *d*-band and the unoccupied *s*-band is only small; hence there is a possibility of hybridization of 3 *d*-electrons and 1 *s*-electron, forming 4 bonds in tetrahedral directions (sp^3 and d^3s form a hybrid with 4 equivalent tetrahedral bonds[9]). The same explanation would probably hold for In^{3+} and Ga^{3+} which have the same electronic configuration as Cd^{2+} and Zn^{2+}.

The general principles underlying the building up of oxidic spinels can thus be summarized as follows:

1. Trivalent and quadrivalent ions, in accordance with electrostatic rules, preferably occupy the octahedral interstices of the 16-fold position.

2. Exceptions are, however, certain trivalent ions: Fe^{3+}, In^{3+}, Ga^{3+} which show a preference for the tetrahedral interstices of the eightfold position.

3. Some divalent ions, Zn^{2+} and Cd^{2+}, show a special preference for occupying the tetrahedral position, which can counteract the tendency mentioned under 2.

These general principles appear to hold their validity in more complicated spinels. The application of these rules may be illustrated with the aid of a few examples given in Table IV.*

The atomic configuration in all these cases has been confirmed by an analysis of the intensities of the x-ray diagram (for the first two cases this has already been given in Section 4 of the present paper) and other means of investigation.

The crystallographic points of view developed here will be used in a series of subsequent papers in which a study of various physical properties of many complicated spinels will be reported.

---

[8] F. A. Kröger, Thesis, Amsterdam, p. 104 (1940).

[9] G. E. Kimball, J. Chem. Phys. **8**, 188 (1940).

* In this and the following paper we use a notation which is slightly different from that in mineralogical work. $Fe(MgFe)O_4$, for instance, expresses that the octahedral position contains together 1 Mg and 1 Fe for each Fe in the tetrahedral position.

THE JOURNAL OF CHEMICAL PHYSICS VOLUME 15, NUMBER 4 APRIL, 1947

Physical Properties and Cation Arrangement of Oxides with Spinel Structures

II. Electronic Conductivity

E. J. VERWEY, P. W. HAAYMAN, AND F. C. ROMEIJN
Natuurkundig Laboratorium der N. V. Philips' Gloeilampenfabrieken, Eindhoven, Nederland
(Received November 29, 1946)

The relations between the electronic conductivity of certain spinels and the arrangement of the cations in the crystal structure (see preceding paper) are studied. Several arguments favor the assumption that Fe_3O_4 contains both divalent and trivalent iron in the 16-fold position. The transition point in the neighborhood of liquid-air temperature is probably associated with an increased degree of order at low temperature in the distribution of the 8 electrons between the 16 Fe-lattice points per unit cell. The considerably increased conductivity below the transition points shows tetragonal anisotropy when the crystal is cooled in a magnetic field. The possible distributions of the electrons in the crystal at low temperature are discussed. In more complicated spinels, containing other metal atoms as well as iron in both the divalent and the trivalent state, the electronic interchange is more or less inhibited by the foreign metal atoms. The higher values of their resistance in comparison to that of Fe_3O_4 can be roughly described by an increased activation energy. The investigation of a number of substances with different arrangements of the cations shows that the activation energy (and therefore the electrical resistance) is lowest for those cases in which the electrons can travel, as in Fe_3O_4, along the Fe of the 16-fold position.

1. CATION ARRANGEMENT OF Fe_3O_4

THE simplest compound for which interesting relations appear to occur between electronic conductivity and the arrangement of the cations is Fe_3O_4.

In paper I of this series,[1] we classified Fe_3O_4 as an inversed Fe spinel $Fe^{3+}(Fe^{2+}Fe^{3+})O_4$, together with the Fe spinels of Mn^{2+}, Co, Ni, Cu, and Mg, as contrasted with the "normal" spinels $ZnFe_2O_4$ and $CdFe_2O_4$. This classification could be made plausible on the basis of a detailed consideration of the values of dimensions of the unit cell of a large number of spinels. Several years ago, however, this "inversed" arrangement had been already proposed by Verwey and de Boer[2] on the basis of the electrical properties of Fe_3O_4. The high electronic conductivity, $\sigma = 200$ ohm^{-1} cm^{-1}, in comparison with that of similar compounds (Mn_3O_4, γ-Fe_2O_3) which have a very low conductivity, was explained on the basis of the continuous interchange of the electrons between Fe^{2+} and Fe^{3+} at the 16-fold position. This picture was corroborated by the behavior of Fe_3O_4 at low temperatures, where below a transition point a sudden decrease of the conductivity was observed which was explained in terms of an order-disorder phenomenon of the Fe^{2+} and Fe^{3+} involved in the electronic conduction.[3]

a. The Value of the Parameter u

As an argument in favor of this inverse arrangement[2] the value of the parameter u had already been used in connection with the ionic radii of the Fe^{2+} and Fe^{3+} ions. This argument can now be further substantiated by the Madelung-potentials calculated in reference 1. This Madelung constant was given there as a function of u, and it is also possible to calculate the Born repulsion between the different iron ions and the surrounding O^{2-} ions as a function of this parameter. The total lattice potential (Coulomb + Born potential) can thus be calculated, for a given (i.e., experimental) value of the lattice constant a, and the value of u for which this total potential is a minimum can be determined.

For the repulsive potential we used the Born Mayer function

$$V_R = b \exp\{(r_+ + r_- - r)/\rho\}$$

with for Fe^{2+} $r_+ = 0.83$, for Fe^{3+} $r_+ = 0.67$, and for a

[1] E. J. W. Verwey and E. L. Heilmann, J. Chem. Phys. 15, 174 (1947).
[2] E. J. W. Verwey and J. H. de Boer, Rec. trav. chim. 55, 531 (1936).
[3] E. J. W. Verwey and P. W. Haayman, Physica 9, 979 (1941).

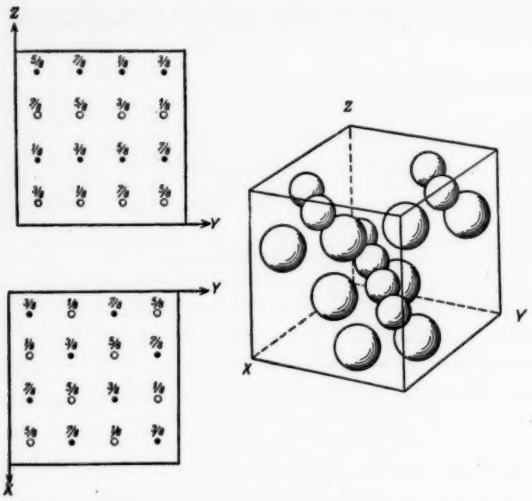

FIG. 1. Unit cell showing possible arrangement at low temperature of Fe^{2+} (large spheres) and Fe^{3+} (small spheres) in 16-fold octahedrally-coordinated position. All 32 oxygens and eight Fe^{3+} in eightfold tetrahedrally-coordinated position are omitted for sake of clarity. Projection of the atoms in the 16-fold position onto the back zy-plane and bottom xy-plane are shown at the left. The numbers indicate the fraction of a above these planes, respectively. The small black dots represent Fe^{3+} and open circles Fe^{2+}.

mixture of Fe^{3+} and Fe^{2+} the average value $r_+=0.75$; for the oxygen ions $r_-=1.40$; $\rho=0.345$A, the usual constant. Substituting $u=\frac{3}{8}+\delta$, we obtain the total repulsive potential per molecule XY_2O_4, on the assumption that the oxygen-oxygen repulsion forms only a small contribution to the potential and can be neglected as a first approximation:

$$V_R=4b\cdot\exp[\{2.07-a\sqrt{3}(\tfrac{1}{8}+\delta)\}/0.345]+12b\cdot\exp[\{2.15-a(\tfrac{1}{4}-\delta)\}/0.345].$$

This function has a minimum value for $\delta=0.002$ or $u=0.377$. The attractive potential, however,

$$V_C=-Me^2/a$$

is also a function of u or δ, as can be seen from Table I in reference 1. After eliminating the constant b with the aid of the equilibrium condition $(dV/da)=0$ for the experimental value of a, the total potential $V=V_C+V_R$ appears to have its minimum for $u=0.379$. The experimental value found by Claassen[4] is $u=0.379$, from the x-ray intensities determined with the aid of an ionization chamber for a large crystal of Fe_3O_4. For the normal spinel $Fe^{2+}(Fe^{3+}Fe^{2+})O_4$ we would have calculated a much larger value of u, in the neighborhood of $u=0.390$ (here the mutual repulsion of the oxygens cannot be neglected, owing to the much larger deformation of the close packing of the oxygen ions corresponding to the larger value of u). The calculation shows that the larger values of u to be expected for normal 2–3 spinels (and actually found for all Al spinels, etc.) are mainly caused by the Coulomb potential, the absolute value of which increases considerably with increasing value of u.

b. Further Experiments on the Conductivity

Assuming for Fe_3O_4 the inversed spinel arrangement, the distribution of 8 Fe^{2+} and 8 Fe^{3+} about the 16 lattice points of the octahedral position can be described as a distribution of 8 electrons about 16 Fe^{3+} ions. Above the transition temperature this will approach a statistical distribution, because of the continual electronic interchange. Below this temperature, however, these conducting electrons will tend to arrange themselves according to some regular pattern. Without resorting to a larger unit cell this pattern of order can no longer be of cubic symmetry. The most probable pattern is one having a tetragonal cell and is shown in Fig. 1.

Hence the pattern of order can be described as being built up by continuous rows, consisting alternately of either Fe^{2+} or Fe^{3+} only, in the xy-plane. The Fe^{2+} rows are all parallel to each other, as are the Fe^{3+}, but in a direction perpendicular to the Fe^{2+} rows. If the Fe^{2+} ions in the plane $z=\frac{5}{8}$ occupy the lattice points $\frac{1}{8}, \frac{1}{8}$; $\frac{3}{8}, \frac{3}{8}$; $\frac{5}{8}, \frac{5}{8}$; $\frac{7}{8}, \frac{7}{8}$; the Fe^{2+} ions in the plane $z=\frac{1}{8}$ occupy the points $\frac{5}{8}, \frac{1}{8}$; $\frac{7}{8}, \frac{3}{8}$; $\frac{1}{8}, \frac{5}{8}$; $\frac{3}{8}, \frac{7}{8}$ etc.

If this description of the order-disorder transition at low temperature is correct, one should expect that the electronic conduction below the transition temperature would be different in different directions. This will be measurable only if the direction of the tetragonal axis can be fixed. Ching Hsien Li[5] has found that a single crystal of Fe_3O_4 becomes magnetically anisotropic at low temperature. Hence it seems possible to fix the tetragonal axis with the aid of a magnetic field. We did not have a single crystal of Fe_3O_4 of sufficient purity to show the transition at low

[4] A. Claassen, Proc. Phys. Soc. **38**, 482 (1925–26).

[5] Ching Hsien Li, Phys. Rev. **40**, 1012 (1932).

temperatures. In a previous paper[3] we have shown that the transition phenomenon is entirely suppressed by a small amount of oxygen in excess of stoichiometric proportions; small amounts of impurities dissolved in the lattice have the same detrimental effect as a deviation from the stoichiometric composition. We had to use, therefore, sintered bars of pure Fe_3O_4, consisting of agglomerates of small crystals oriented in all directions, where the expected effect will be reduced considerably. The following experiment, therefore, has only qualitative significance.

A sintered bar was cooled in a magnetic field, once in a direction parallel to the field, a second time in a direction perpendicular to the field. In the first case the electrical conductivity of the bar at liquid air temperature was 7.19×10^{-3} ±0.02 ohm^{-1} cm^{-1}, in the second case 6.18×10^{-3} ±0.02 ohm^{-1} cm^{-1}. After the bar had passed the transition temperature in the magnetic field the conductivity below this temperature was not altered perceptibly by the presence of the field, as could be established by changing its direction, switching it off, etc. The conductivity when the bar was cooled in the absence of a magnetic field was 6.45×10^{-3} ohm^{-1} cm^{-1}.

Hence there is a definite effect of the magnetic field orientation upon the electronic conductivity. The phenomenon can be explained by assuming that at the transition temperature the disorder-order transformation occurs preferentially in such a way that the tetragonal axis is that cubical axis of the high temperature crystal which lies nearest to the direction of the magnetic field. The electrical conductivity will then be highest in directions where Fe^{2+} and Fe^{3+} alternate, and lowest in directions where one meets either only Fe^{2+} or only Fe^{3+} ions. Hence it is to be expected that the conductivity will be highest parallel to the magnetic field; that is, more or less parallel to the directions in which the *c*-axis has been "frozen in." The picture of the disorder-order transition is in qualitative agreement with these experiments, which therefore corroborate the picture of Fe_3O_4 given here. They show at the same time that the ionic picture according to which the electrons are thought to be added entirely to one-half of the Fe^{3+} ions is much too simple. A low transition temperature is very rare for a crystal lattice in which the atoms are held together by strong bonds, and has generally only been found for lattices in which *molecules* are held together by weak van der Waals-London bonds. In the present case the transition can occur at such a low temperature because it is an electronic transition between different atoms. The low transition temperature also proves that the energy of order is very small. The entropy of order is R ln 2 per atom, and accordingly $T\Delta S$ is of the order of 0.01 ev (T is of the order of 100°K). Neglecting the polarization and the displacement of the oxygen ions, one would calculate an energy of the order of a few electron volts (each Fe^{2+} ion is surrounded by 4 Fe^{3+} and 2 Fe^{2+} ions in a first sphere of radius $r=\frac{1}{4}a\sqrt{2}$, by 4 Fe^{2+} and 8 Fe^{3+} ions in a second sphere of radius $r=\frac{1}{4}a\sqrt{6}$, by 6 Fe^{2+} ions at a distance $\frac{1}{2}a\sqrt{2}$, etc.). The actual energy will probably be several (say 5) times smaller due to the polarization of the surrounding medium. This, however, is obviously far too high, and suggests that the wave functions of the electrons extend over several atomic distances.

2. MORE COMPLICATED SPINELS

(a) Fe_2AlO_4

The x-ray investigation[1] has revealed that this substance can be described as consisting for the main part of $Fe(FeAl)O_4$, with Al in the octahedral holes. The intensity of the reflection with the lowest diffraction angle and the general rules derived in the preceding paper suggest that the Fe in the tetrahedral hole is the Fe^{3+} ion:

$$Fe^{3+}(Fe^{2+}Al)O_4$$

so that the substance belongs to the "inversed" spinels, with an averaged distribution of divalent and trivalent ions about the 16-fold positions. Hence the substance appears to be analogous to Fe_3O_4

$$Fe^{3+}(Fe^{2+}Fe^{3+})O_4$$

with the Fe^{3+} in the 16-fold position replaced by Al.

As already indicated by the x-ray intensities, the cation arrangement is not entirely that corresponding to the formula given above, and the best agreement with x-ray data was obtained by assuming that a small fraction of the Al has replaced Fe in the eightfold position. The sub-

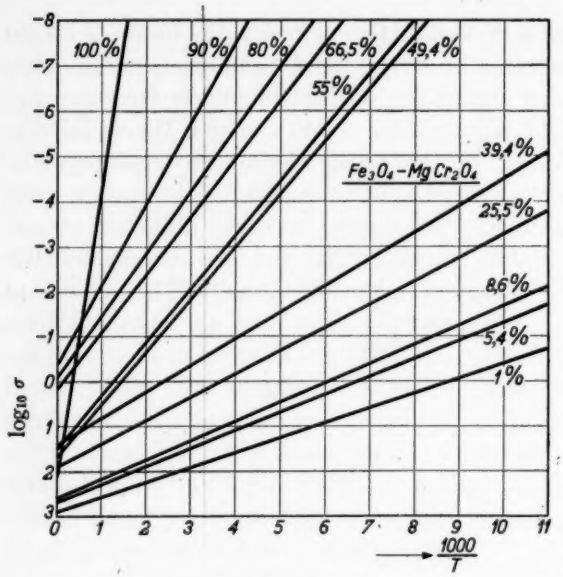

FIG. 2.

stance was prepared by heating an intimate mixture of iron and aluminum oxides in a suitable gas atmosphere, and it is therefore always possible that at the high temperature of preparation the energy difference between the two arrangements is insufficient to outweigh the gain of entropy accompanying a more uniform distribution of the Al about both positions.

These conclusions are corroborated by the electrical properties of the substance. If the substance were pure $Fe^{3+}(Fe^{2+}Al)O_4$ (or $Fe^{2+}(Fe^{3+}Al)O_4$) it would be a rather poor electronic conductor, as it does not contain Fe^{3+} and Fe^{2+} in equivalent lattice points. There might be a possibility of electronic transfer between Fe in the tetrahedral holes and Fe in the octahedral interstices, but this would only occur if the electronic levels in the two different positions were practically identical, which would be rather accidental.

The electrical conductivity of the substance appears to be about 10^3 times smaller than that of Fe_3O_4: *viz.* 0.2 ohm^{-1} cm^{-1}. This is, however, several powers of 10 greater than would be expected for the pure substance, even if we take into account that the sample showed a small deviation from stoichiometric proportions (for 1 Al ion it contained 1.005 Fe^{3+} and 0.995 Fe^{2+} ions). If the assumption that this residual conductivity is caused by a small fraction of Fe^{3+} in the 16-fold position is correct, one would expect the conductivity to be very sensitive to the heat treatment. Actually we found that by annealing the sample in a small (evacuated and closed) quartz tube at a temperature of 850°C for ½ hour, the conductivity decreased by a factor of 55, the new specific conductivity being 0.0037 ohm^{-1} cm^{-1}. Obviously, as a consequence of this heat treatment at a temperature well below the formation temperature (1300°C), more Al has gone over to the position of lower energy, and the formula $Fe^{3+}(Fe^{2+}Al)O_4$ of the pure material has been more closely realized.

This behavior is rather exceptional, as the conductive properties of other substances (to be described below) of similar type proved to be very insensitive to similar heat treatment, and such substances have even found technical application in cases for which a high thermal stability is required.

(b) Solid Solutions of Fe_3O_4 and $MgCr_2O_4$

$MgCr_2O_4$ is a very poor conductor and can even be called an insulator ($\sigma < 10^{-10}$ ohm^{-1} cm^{-1}). Solid solutions with Fe_3O_4 were prepared in the following way.

An intimate mixture of Fe_2O_3, MgO, and Cr_2O_3 in the proper proportions was pressed into bars of about 3 cm length and 0.3 to 0.4 cm diameter. These bars were preheated at 1200°C in a stream of pure CO_2, with the result that most of the Fe was reduced to the oxidation level of Fe_3O_4. Then the CO_2 was replaced by very pure N_2 and the temperature was raised to 1300°C. This temperature was maintained for one hour. After that the carrier with the bars was shifted to a cooler part of the furnace and the substance was allowed to cool in the same atmosphere. For preparations containing more than 50 percent $MgCr_2O_4$ the heating was conducted at about 1400°C, in order to obtain well-sintered bars. In this case the

TABLE I.

% $MgCr_2O_4$	ϵ in ev	σ_∞ in ohm^{-1} cm^{-1}
0.9	0.06_5	700
5.4	$.07_9$	550
8.6	$.08_7$	450
25.5	$.10_3$	100
39.4	$.12_9$	35
49.4	$.21_1$	35
54.6	$.23_0$	35
67.4	$.30_5$	8
80	$.33_4$	5
90	$.35_6$	0.05

atmosphere must be less reducing in order to prevent a deviation from stoichiometric proportions in the direction of FeO. Satisfactory results were obtained by heating at 1400°C in N_2 containing 1 percent of O_2. The content of ferrous ions was checked by dissolving a sample in chlorine-free hydrochloric acid under exclusion of atmospheric oxygen and determining the amount of Fe^{2+} in the solution by a titration with 0.01 normal ceric sulphate solution.

The electrical resistance of a series of bars with varying composition was measured over a wide range of temperatures. The results are given in Table I and summarized in Fig. 2.

These results show initially that there is a gradual transition from Fe_3O_4, with a high conductivity and a low temperature coefficient, to $MgCr_2O_4$, with a very low conductivity and a high temperature coefficient. The curves of $\log\sigma$ against $1/T$ are straight lines to a first approximation, with a slope continually increasing from Fe_3O_4 to $MgCr_2O_4$. The conductivity as a function of temperature can be described for each sample by the equation

$$\sigma = \sigma_\infty \exp(-\epsilon/kT),$$

and the gradual decrease of the conductivity at room temperatures with increasing content of $MgCr_2O_4$ is obviously mainly determined by the gradual increase of the "activation energy" ϵ, although the values of σ_∞ found by extrapolation, formally the conductivities at $T=\infty$, vary appreciably.

The theory for the electronic conductivity of the oxides of these "transition elements" is still not very satisfactory.[6] It has been suggested[2] that the high conductivity of Fe_3O_4 must be explained by the fact that, in an averaged distribution of Fe^{2+} and Fe^{3+} about equivalent lattice points (here those of the 16-fold spinel position), an interchange of electrons must be possible without requiring an appreciable amount of added energy. Hence the electrons would travel with a very low activation energy along the lattice points containing both Fe^{2+} and Fe^{3+}, and the effect of the different ions Mg^{2+} and Cr^{3+} in solid solutions of Fe_3O_4 with $MgCr_2O_4$ must, as a first result, be

[6] J. H. de Boer and E. J. W. Verwey, Proc. Phys. Soc. 49, 59 (1937). N. F. Mott and R. W. Gurney, *Electronic Processes in Ionic Crystals* (Oxford University Press, New York, 1940), p. 167.

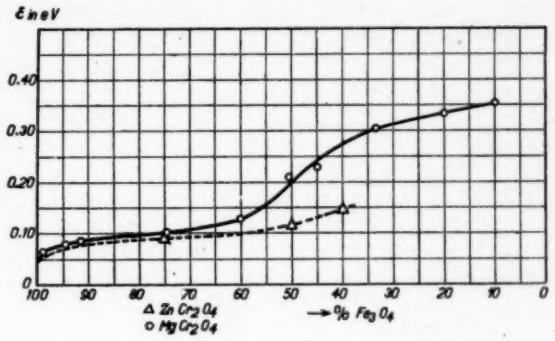

FIG. 3.

the blocking up of this irregular $Fe^{2+}-Fe^{3+}$ pattern. It therefore follows that with increasing $MgCr_2O_4$ content the electrons are forced to follow narrow and complicated channels to an increasing extent. These blocking barriers will be different from point to point in the crystal lattice of the solid solutions. Nevertheless, this dilution of Fe^{2+} and Fe^{3+} by the different ions of $MgCr_2O_4$ can be described up to a temperature of about 400°C with the aid of a single "activation energy." This behavior shows again that the conduction mechanism cannot be described completely with the aid of wave functions of the conduction electrons belonging to a single Fe^{2+} ion. On the other hand, the picture of the lattice wave functions (Wilson's theory of semi-conductors) fails entirely to explain the absence of conduction in these oxidic substances containing the transition elements Cr, Mn, Fe, Co, etc., and it is rather obvious that a better understanding of this case can be obtained only by introducing into the theory the interaction between a traveling electron and the positive hole left behind; i.e., by going again in the direction of localized wave functions.

Upon examining the curves of Fig. 2 more closely we observe a peculiar anomaly. It is interesting to consider this point in some detail, as it is directly connected with the cation arrangement in these solid solutions and may throw some more light on the conduction mechanism in these materials.

This anomaly is most easily demonstrated by plotting the activation energy of the different samples as a function of the composition (see Fig. 3).

Starting from the building principles derived in reference 1 for the cation distribution in

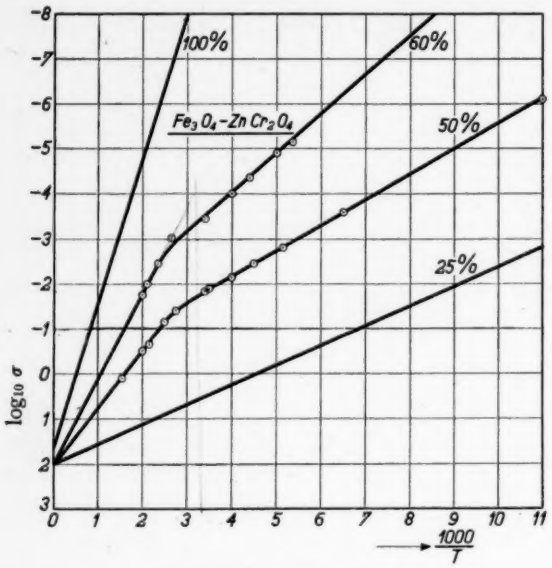

FIG. 4.

spinels, we would expect that the different cations in these solid solutions would have the distributions about the cation lattice points shown in Table II (we only give the compositions with 25, 50, and 75 molecular percent $MgCr_2O_4$).

Hence from 0 to 50 percent content of $MgCr_2O_4$ there are both Fe^{3+} and Fe^{2+} ions in the 16-fold positions, and the electronic conduction will occur along planes containing both of these ions. At 50 percent $MgCr_2O_4$, however, the preference of Fe^{3+} for the eightfold position results in a separation of the Fe^{3+} and the Fe^{2+} ions. Hence a rapid increase of the "activation energy" can be expected if we approach this composition. There are a number of possibilities for the mechanism of electronic conduction for compositions containing more than 50 percent of $MgCr_2O_4$. This depends on the distribution of the divalent ions in the region 50 to 100 percent $MgCr_2O_4$, for which two possibilities are given in Table II, but for which an intermediate distribution between these two extremes might also be possible. X-ray evidence supports arrangement IIIa, but the differences in the calculated intensities corresponding to IIIa and IIIb are rather small, so that an intermediate distribution cannot be ruled out and is even highly probable in view of the small energy differences which can be expected to exist between the two extreme arrangements. Hence for compositions containing more than 50 percent of $MgCr_2O_4$ the conduction mechanism will be either an interchange of electrons between Fe^{3+} and a small amount of Fe^{2+} along the lattice points of the eightfold position, or an exchange of electrons between Fe^{3+} and Fe^{2+} from different positions. In both cases the "activation energy" will be increased; in the first case because of the blocking action of the Mg^{2+} ions and the large distance between the tetrahedral interstices ($\frac{1}{4}a\sqrt{3}=0.43a$), in the second case because of the difference between the energy levels at the octahedral and the tetrahedral lattice positions, respectively, although the distance is slightly shorter ($\frac{1}{8}a11^{\frac{1}{2}}=0.41a$, both distances to be compared with the shortest distance between two octahedral interstices, $\frac{1}{4}a\sqrt{2}=0.35a$). The latter seems to be the less probable case. For example, in the case of $AlFe_2O_4$ (Section 2(a)) there were no indications in favor of such a mechanism, which would only be possible if the difference between the two energy levels happens to be small.

TABLE II. Arrangement of cations in solid solutions of $Fe_3O_4+MgCr_2O_4$.

Composition Fe_3O_4: $MgCr_2O_4$	Eightfold position (tetrahedral interstices)	16-fold position (octahedral interstices)
I 75:25	Fe^{3+}	$\frac{1}{4}Fe^{3+}$, $\frac{3}{4}Fe^{2+}$, $\frac{1}{4}Mg$, $\frac{1}{2}Cr$
II 50:50	Fe^{3+}	$\frac{1}{2}Fe^{2+}$, $\frac{1}{2}Mg$, Cr
III 25:75	(a) $\frac{1}{4}Fe^{3+}$, $\frac{1}{2}Mg$	$\frac{1}{4}Fe^{2+}$, $\frac{1}{4}Mg$, $\frac{3}{4}Cr$
	(b) $\frac{1}{4}Fe^{3+}$, $\frac{1}{4}Fe^{2+}$, $\frac{1}{4}Mg$	$\frac{1}{2}Mg$, $\frac{3}{4}Cr$

(c) Solid Solutions of Fe_3O_4 and $ZnCr_2O_4$

It is interesting to compare the behavior of these solid solutions of Fe_3O_4 and $MgCr_2O_4$ with those of Fe_3O_4 and $ZnCr_2O_4$. Here the different ions will be distributed over the different positions indicated in Table III. The Zn ions always occupy the eightfold position and are replaced by Fe^{3+} when the Fe_3O_4 content is increased. Simultaneously the Cr ions in the 16-fold position are replaced by $\frac{1}{2}Fe^{2+}+\frac{1}{2}Fe^{3+}$. Accordingly, there

TABLE III. Arrangement of cations in solid solution of $Fe_3O_4+ZnCr_2O_4$.

Composition Fe_3O_4: $ZnCr_2O_4$	Eightfold position (tetrahedral interstices)	16-fold position (octahedral interstices)
75:25	$\frac{3}{4}Fe^{3+}$, $\frac{1}{4}Zn$	$\frac{3}{4}Fe^{2+}$, $\frac{3}{4}Fe^{3+}$, $\frac{1}{2}Cr$
50:50	$\frac{1}{2}Fe^{3+}$, $\frac{1}{2}Zn$	$\frac{1}{2}Fe^{2+}$, $\frac{1}{2}Fe^{3+}$, Cr
25:75	$\frac{1}{4}Fe^{3+}$, $\frac{1}{4}Zn$	$\frac{1}{4}Fe^{2+}$, $\frac{1}{4}Fe^{3+}$, $\frac{3}{4}Cr$

are always equivalent amounts of Fe^{2+} and Fe^{3+} in the octahedral position, and there is no reason for a discontinuous increase of ϵ with increasing $ZnCr_2O_4$ content.

The corresponding $\log\sigma$ *vs.* $1/T$ curves are given in Fig. 4. At high temperatures the preparations containing large amounts of $ZnCr_2O_4$ show a break in the curves, suggesting that at these temperatures a second conduction mechanism covers the $Fe^{2+}-Fe^{3+}$ conduction prevailing for lower temperatures. The curves can be represented by

$$\sigma=\sigma_\infty \exp(-\epsilon/kT)+\sigma_\infty' \exp(-\epsilon'/kT).$$

As the specific conductivity of $ZnCr_2O_4$ is much greater than that of $MgCr_2O_4$ this phenomenon is most probably caused by the conductivity of $ZnCr_2O_4$ itself, so that at higher temperatures the conduction is taken over by Zn (or by Zn and Cr ions jointly) as a consequence of the higher temperature coefficient of this conduction mechanism.

In Fig. 3, therefore, where ϵ has again been plotted against the composition, the value of ϵ corresponding to the low temperature part of the curves has been used. The plot shows a continuous increase of ϵ with increasing $ZnCr_2O_4$ content.

We wish to acknowledge the valuable assistance of Mr. A. Bol in the preparation of specimens and the measurements.

THE JOURNAL OF CHEMICAL PHYSICS VOLUME 15, NUMBER 4 APRIL, 1947

Integral Equations between Distribution Functions of Molecules

JOSEPH E. MAYER
Institute of Nuclear Studies, University of Chicago, Chicago, Illinois

(Received February 18, 1947)

Integral equations are derived that relate variations in the potentials of average force between molecules of a system at two different densities or activities. These permit the calculation of the change in thermodynamic properties, or of the change in the distribution of molecules in space, in a liquid or crystalline phase, if either the temperature is varied, or if the the mutual potentials between the molecules is assumed to change. The equations are in a somewhat complex, but still distinguishable, matrix form. A matrix operates on the variations in potential occurring at one activity and transforms them into those occurring at a second activity. The matrix elements are combinations of the distribution functions at the second activity, to which the transformation is made, multiplied by powers of the difference of the two activities. The matrix approaches the unit matrix in value as this activity difference approaches zero. The product of the two matrices, one which transforms from activity α to activity β, with that which transforms from activity β to α, is the unit matrix. This leads to an integral (matrix) equation between the distribution functions at any two activities.

The calculation of one element of this matrix product leads to a cell type equation for the computation of the activity, or free energy, of a system in terms of the potential between a single molecule and the molecules that immediately surround it in the system.

The transformation matrices have solutions, at certain values of the activity difference y, corresponding to variations in the potentials of average force, which are transformed into zero variations at the new activity. The activities at which such variations can occur are those of the phase transitions in the systems. The solutions at these special values of the activity are differences of combinations of the distribution functions in the two pure phases that can coexist at these activities.

INTRODUCTION

ONE may define "distribution functions" for a given number, n, of molecules as being proportional to the probability density of finding n molecules in a certain configurational position, averaged over all positions of the other molecules of the system. These functions are the exponent of minus the potential of average force between the molecules, divided by kT. The distribution functions of a given system at constant tem-

perature, but at two different densities, are then related to each other by equations which can be obtained by a simple extension of the concept of the Gibbs grand canonical ensemble. The special case of most general interest is that for which one of the two densities is the limit of zero density. At zero density the distribution function for a classical system is the exponent of minus the potential energy divided by kT, and may be regarded as known.

Although the equations relating the distribution functions of a liquid or solid to those at infinite dilution are rigorous and exact, they are not susceptible of numerical solution, since they involve integration over the coordinates of the number of molecules in a macroscopic portion of the system. It is, however, possible to consider a variational method which leads to certain integral equations involving integrations over fewer numbers of molecules.

The variational method discussed in this paper is essentially as follows: We consider the potentials of average force at one density, say those at infinite dilution, to be capable of some continuous variation. This, of course, causes a variation in the potentials at some other density, say that of the liquid. By assuming the variation in the potentials of zero density to be of the sort induced by a change in the mutual potentials between pairs, or between some relatively small number of molecules, the equations for the variation in the potentials of average force in the liquid can first be integrated over all but the molecules for which the change in potential is being computed, and the few with which these are interacting. One thus obtains a set of integral equations giving the variations in the liquid potentials as the sum of integrals of kernels times the variations in the potentials of zero density. The kernels are combinations of the unvaried distribution functions in the liquid.

One of the purposes of this paper is merely the formal attainment of these equations. Their use is not further discussed in the body of this article, but will be dealt with in a subsequent paper. By considering variations due to changes in temperature, or other physically meaningful changes, one has a tool for the calculation of the thermodynamic properties of the system in terms of the distribution functions.

However, certain formal mathematical relationships that follow from these equations appear to be of interest. The discussion of these relationships occupies the main body of the paper.

NOTATION

Owing to the relatively complex equations involved, it is desirable to use a special symbolism in order to attain some brevity of expression. The final equations are in no way more complicated if a system of many components is considered than if a single component system is handled. We deal with an infinite system containing σ types of molecular species, and use the subscript s (or r) to refer to a special species of type s (or r). Symbols ρ, z, without subscripts refer to a set of quantities:

$$\rho = \rho_1, \rho_2, \cdots, \rho_s, \cdots \rho_\sigma, \tag{1}$$

$$z = z_1, z_2, \cdots, z_s, \cdots z_\sigma. \tag{2}$$

The symbol ρ_s indicates the average concentration of molecules of species s, in molecules per unit volume, and z_s is the activity or fugacity, defined by the equation:

$$z_s = \lim_{\rho_0 \to 0} [\rho_{0s} \exp(\mu_s - \mu_{0s})/kT], \tag{3}$$

in which μ_s is the chemical potential of species s in the system, and the limit is taken as all concentrations, ρ_0, approach zero, with μ_{0s} the chemical potential, and ρ_{0s} the concentration, of species s, in this limit at which the system approaches a perfect gas in properties. Thus z_s is proportional to the exponent of the chemical potential μ_s, divided by kT, with the proportionality constant so chosen that z_s/ρ_s becomes unity in the perfect gas at infinite dilution of the system:

$$\lim \rho \to 0 [z_s/\rho_s] = 1. \tag{4}$$

The letters k, m, n, κ, μ, ν, λ, etc., when written without subscripts, will be used to indicate sets of integers:

$$k = k_1, k_2, \cdots, k_s, \cdots k_\sigma, \tag{5}$$

of k_s molecules of type s. The shorthand notation:

$$k! = k_1! k_2! \cdots k_s! \cdots k_\sigma!, \tag{6}$$

$$\rho^k = \rho_1^{k_1} \rho_2^{k_2} \cdots \rho_s^{k_s} \cdots \rho_\sigma^{k_\sigma},$$
$$z^k = z_1^{k_1} z_2^{k_2} \cdots z_s^{k_s} \cdots z_\sigma^{k_\sigma}, \tag{7}$$

will be employed. With this notation the equations for the σ component system become identical with those for a single component system of activity z, or concentration ρ, in which k, m, n, etc., is used to indicate the number of molecules of the single component. The reader will probably find the ensuing discussion simpler if the one component case only is kept in mind.

The coordinates of the ith molecule of type s are indicated by

$$(i_s) = x_{is}, y_{is}, z_{is}, q_{1is}, \cdots q_{fis}, \tag{8}$$

including any internal coordinates, q, and the volume element, calculated in the Cartesian space of the constituent atoms by

$$d(i_s) = dx_{is}dy_{is}dz_{is}\begin{bmatrix} q \\ x \end{bmatrix} dq_{is}\cdots dq_{fis}, \tag{9}$$

with $\begin{bmatrix} q \\ x \end{bmatrix}$ the Jacobian transformation to the Cartesian volume. The introduction of the internal coordinates causes no change in the ensuing equations. The reader will probably find the visualization of the operations easier if the case that no internal coordinates are present is kept in mind. The coordinates of k_s molecules of type s are indicated by

$$\{k_s\} = (1_s), (2_s), \cdots, (k_s), \tag{10}$$

and the volume element by

$$d\{k_s\} = d(1_s)d(2_s)\cdots d(k_s), \tag{11}$$

whereas the coordinates of the set k of molecules are,

$$\{k\} = \{k_1\}, \{k_2\}, \cdots, \{k_s\}, \cdots \{k_\sigma\}, \tag{12}$$

and the volume element is

$$d\{k\} = d\{k_1\}d\{k_2\}\cdots d\{k_s\}\cdots d\{k_\sigma\}. \tag{13}$$

A function, $\Psi_n\{n\}$, of the coordinates of the set $\{n\}$ of molecules may happen to be simply expressible as a sum of functions of the coordinates $\{\nu\}_n$ of small subsets of molecules out of the set n. The typical component function, $\psi_\nu\{\nu\}_n$, composing a member of this sum, say for example, $\psi_2((i_s)(j_s))$, of the coordinates of the i_sth and j_sth molecule, will, if Ψ_n is symmetrical in permutations of identical molecules, have the same functional dependence on the coordinates that the function $\psi_2((j_s)(k_s))$ has upon the coordinates of the j_sth and k_sth molecule, but the two functions are distinct in the sum and have, in general, different values for some arbitrary value $\{n\}$ of the coordinates of the set n of molecules. The summation symbol, $(\sum\{\nu\}_n)$, will be used to indicate summation of functions of such subsets, $\{\nu\}_n$, over all subsets, for all values of ν, $0 \leq \nu_s \leq n_s$, including a single (constant) term for which all $\nu_s = 0$. It will be noted that there are $n!/(n-\nu)!\nu!$ different distinct subsets, $\{\nu\}_n$, for each value of the set of numbers, $\nu = \nu_1, \cdots, \nu_s, \cdots$, so that in the trivial case that the function is a constant, $(-1)^\nu$, for all νs, then

$$(\sum\{\nu\}_n)(-)^\nu = 0 \text{ if } n > 0, \tag{14}$$

$$(\sum\{\nu\}_n)(-)^\nu = 1 \text{ if } n = 0. \tag{15}$$

Thus if Ψ_n is one of a set of functions of the coordinates $\{n\}$, symmetrical in permutations of identical molecules, defined for all values of n including $n=0$, for which the function, Ψ_0, is a constant,

$$\Psi_n = \Psi_n\{n\}, \tag{16}$$

then we may define functions ψ_ν by

$$\psi_\nu = (\sum\{n\}_\nu)(-)^{\nu-n}\Psi_n, \tag{17}$$

and, in view of (14) and (15) we have that,

$$\Psi_n = (\sum\{\nu\}_n)\psi_\nu, \tag{18}$$

since then on inserting (17) in (18) we obtain the identity:

$$\begin{aligned}\Psi_n &= (\sum\{\nu\}_n)(\sum\{\kappa\}_\nu)(-)^{\nu-\kappa}\Psi_\kappa \\ &= (\sum\{\kappa\}_n)(\sum\{\nu-\kappa\}_{n-\kappa}(-)^{\nu-\kappa})\Psi_\kappa \\ &= \Psi_n.\end{aligned}$$

THE DISTRIBUTION FUNCTION EQUATION

With this notation we now define distribution functions $F_n(\rho, T, \{n\})$, of the coordinates of a set n of molecules, by the statement that in a system of infinite extent ($V \gg n_s/\rho_s$ for all s) at the temperature T, and concentration ρ, the probability that there are an appropriate set n of molecules at the coordinates $\{n\}$ within the volume element $d\{n\}$ is equal to $\rho^n F_n(\rho, T, \{n\})d\{n\}$. It is to be

noted that with this definition the functions F_n are so normalized that,

$$\lim_{V\to\infty}\left[\frac{1}{V^n}\int\int\cdots_V F_n d\{n\}\right]=1. \tag{19}$$

We arbitrarily include $F_0\equiv 1$ in the set of functions so defined.

In a previous paper[1] it has been shown that for two sets of concentrations ρ_α and ρ_β, for which the pressures are P_α and P_β, and for which the fugacity sets are z_α and z_β, respectively, the distribution functions are related by the equation set:

$$[\exp(P_\alpha V/kT)][\rho_\alpha/z_\alpha]^n F_n(\rho_\alpha, T, \{n\})$$
$$=\sum_{m\geq 0}\frac{(z_\alpha-z_\beta)^m}{m!}\int\int\cdots_V\int e^{P_\beta V/kT}\left[\frac{\rho_\beta}{z_\beta}\right]^{n+m}F_{n+m}(\rho_\beta, T, \{n+m\})d\{m\}. \tag{20}$$

This actually represents two sets of equations for each pair of concentrations ρ_α and ρ_β, since obviously the subscripts on the right and left can be interchanged. Thus if we define:

$$G_n=e^{P_\alpha V/kT}\left[\frac{\rho_\alpha}{z_\alpha}\right]^n F_n(\rho_\alpha, T, \{n\}), \tag{21}$$

$$G_n^*=e^{P_\beta V/kT}\left[\frac{\rho_\beta}{z_\beta}\right]^n F_n(\rho_\beta, T, \{n\}), \tag{21'}$$

$$z=z_\alpha-z_\beta, \tag{22}$$

we may write (20) as,

$$G_n=\sum_{m\geq 0}\frac{z^m}{m!}\int\int\cdots_V\int G^*_{n+m}d\{m\}, \tag{23}$$

or as,

$$G_n^*=\sum_{m\geq 0}\frac{(-z)^m}{m!}\int\int\cdots_V\int G_{n+m}d\{m\}. \tag{23'}$$

THE VARIATIONAL METHOD

Without regard, at first, to the physical interpretation of the functions G_n and G_n^* we shall now proceed to carry out some mathematical manipulations which lead us to a set of integral equations that are of considerable interest in interpreting the relationships between these two sets of functions. The only mathematical limitations which must be imposed upon the functions G_n and G_n^* are to require that they be symmetrical in permutations of identical molecules, and of such a form that the series (23) and (23′) converge absolutely. These conditions are assuredly fulfilled for the physical case. The symmetry in permutations of the coordinates of identical molecules is obvious. In addition we have that G_n and G_n^* are positive definite, from their definitions in terms of probability functions, and for repelling molecules G_n and G_n^* approach zero in value for all values of the coordinates $\{n\}$ within a finite volume V as n/V approaches infinity.

We now assume that G_n, and therefore through (23′) G_n^*, depend on a parameter y, defining:

$$\Psi_n=d\ \ln G_n/dy, \tag{24}$$

$$\Psi_n^*=d\ \ln G_n^*/dy. \tag{24'}$$

For instance, we may take y to be the temperature T, in which case, from (21) and (24) one could relate the Ψ's to the various temperature derivatives of the system. The function $F_n(0, T, \{n\})$, for $\rho\equiv 0$, is $\exp-(U_n/kT)$, with U_n the potential energy, if the system is classical. One might, for

[1] W. G. McMillan, Jr. and J. E. Mayer, J. Chem. Phys. **13**, 276 (1945) and for component systems, J. E. Mayer, J. Chem. Phys. **10**, 629 (1942).

instance, consider that U_n is $U_n^0 - yU_n^{(1)}$ with $U_n^{(1)}$ some sort of perturbation potential. In this case, if G_n^* referred to $\rho \equiv 0$, the functions Ψ_n^* would be $1/kT$ times the perturbation potential for the set n of molecules. The functions Ψ_n could then be related to the derivatives of the system with respect to this perturbation.

We may now define the functions ψ_ν and ψ_ν^* by (17) and by,

$$\psi_\nu^* = (\sum \{n\}_\nu)(-)^{\nu-n}\Psi_n^*, \tag{25}$$

so that (18), and,

$$\Psi_n^* = (\sum \{\nu\}_n)\psi_\nu^*, \tag{26}$$

are valid.

We now proceed to derive Eq. (29) by which the function ψ can be calculated as a sum of integrals of kernels multiplied by the functions ψ^*. The kernels are given by Eq. (30) as combinations of the functions G. A similar reciprocal set of equations, (29′) and (30′), can be used to compute the functions ψ^* by integration over kernels formed from the G^*'s multiplied by the functions ψ. These equations are obtained by differentiation of both sides of (23) with respect to y, obtaining:

$$\begin{aligned} G_n\Psi_n &= \frac{d}{dy}G_n = \frac{d}{dy}\sum_{m\geq 0}\frac{z^m}{m!}\int\int\cdots\int G_{n+m}^* d\{m\} \\ &= \sum_{m\geq 0}\frac{z^m}{m!}(\sum\{\nu\}_n, \{\mu\}_m)\int\int\cdots\int_V \psi_{\nu+\mu}^* G_{n+m}^* d\{m\} \\ &= \sum_{\mu\geq 0}\frac{z^\mu}{\mu!}(\sum\{\nu\}_n)\int\int\cdots\int_V \psi_{\nu+\mu}^*\left[\sum_{k\geq 0}\frac{z^k}{k!}\int\int\cdots\int_V G_{n+\mu+k}^* d\{k\}\right]d\{\mu\} \\ &= \sum_{\mu\geq 0}\frac{z^\mu}{\mu!}(\sum\{\nu\}_n)\int\int\cdots\int_V \psi_{\nu+\mu}^* G_{n+\mu} d\{\mu\}. \end{aligned} \tag{27}$$

In this the second line follows from the first by the use of (24′) and (26) and by considering that

$$(\sum\{\nu\}_{n+m}) = (\sum\{\nu\}_n)(\sum\{\mu\}_m) = (\sum\{\nu\}_n\{\mu\}_m),$$

where the last notation means summation over all subsets $\{\nu\}_n$ and $\{\mu\}_m$ including $\nu \equiv 0$, and $\mu \equiv 0$. For any given value of the set m one may arbitrarily call $m-\mu=k$, and, remembering that there are $m!/\mu!k!$ different subsets $\{\mu\}_m$ for any given *value* of the set m and μ, one may multiply by this and sum over μ and k rather than m and $\{\mu\}_m$. This leads to the third line. The fourth line follows by using equation (23).

We thus have:

$$\Psi_n = \sum_{\mu\geq 0}\frac{z^\mu}{\mu!}(\sum\{\nu\}_n)\int\int\cdots\int_V \psi_{\nu+\mu}^*\frac{G_{n+\mu}}{G_n}d\{\mu\}. \tag{28}$$

To this equation we apply the operation of equation (17) to both sides, and obtain,

$$\psi_k = \sum_{m\geq 0}\frac{z^m}{m!}(\sum\{\kappa\}_k)\int\int\cdots\int_V \psi_{\kappa+m}^* K_{k,\kappa,m} d\{m\}, \tag{29}$$

in which the kernels, $K_{k,\kappa,m}$, are defined by the equation:

$$K_{k+n,n,m} = (\sum\{\kappa\}_k)(-)^{k-\kappa}\frac{G_{\kappa+n+m}}{G_{\kappa+n}}. \tag{30}$$

The application of the equivalent series of operations to Eq. (23′), instead of (23), leads to the equations:

$$\psi_k^* = \sum_{m\geq 0}\frac{(-z)^m}{m!}(\sum\{\kappa\}_k)\int\int\cdots\int_V \psi_{\kappa+m} K_{k,\kappa,m}^* d\{m\}, \tag{29′}$$

with,

$$K^*_{k+n,\,n,\,m}=(\sum\{\kappa\}_k)(-)^{k-\kappa}\frac{G^*_{k+n+m}}{G^*_{k+n}}. \tag{30'}$$

Special values of the kernels follow from (30) and (30′) to be,

$$K_{0,\,0,\,0}=K^*_{0,\,0,\,0}=1, \tag{31a}$$

$$K_{0,\,0,\,m}=G_m/G_0;\quad K^*_{0,\,0,\,m}=G^*_m/G^*_0, \tag{31b}$$

$$K_{k+n,\,n,\,0}=K^*_{k+n,\,n,\,0}=0 \text{ if } k>0, \tag{31c}$$

$$K_{n,\,n,\,0}=K^*_{n,\,n,\,0}=1. \tag{31d}$$

AN OVERSIMPLIFICATION

Equations (29) and (29′) apply for all values of $k\geq 0$. We may choose either the set ψ_k of functions *or* the set ψ_k^* as arbitrary, limited only by the condition that they be symmetrical in permutations of the coordinates of identical molecules.

A special case of the integral equation (29) (or (29′) but not both) has been used by Kirkwood and Monroe[2] to determine distribution functions for liquids. The special case chosen by them may be constructed from our equations as follows. We use (23) with the asterisk, G_n^*, referring to infinite dilution of a one-component system, and G_n referring to the liquid state. Differentiation is then performed with respect to the coordinate of a molecule at a particular position over which the integration is not extended, that is, one of the coordinates of one of the molecules, (i), of the set n in (23). The functions Ψ_n^*kT are then the true forces, and are zero unless n contains the molecule (i). They are symmetrical in the coordinates of all identical molecules except the molecule i. The ψ_n^* are assumed to be zero unless $n=2$. The functions Ψ_nkT are the average forces in the liquid, which are related, by a well-known relationship to the unknown distribution functions G_n, in the liquid. Equation (29) then has unknown ψ_n and kernel K, but a subsidiary relationship between them is known. It then represents a non-linear integral equation, which Kirkwood and Monroe solved approximately with certain assumptions.

The form (29′) for their problem would have presented them with a linear (non-homogeneous) integral equation with known kernel K^* and known function ψ^*, but unknown average force ψ. The possible advantages of this form have not been investigated.

The standard form of a non-homogeneous linear integral equation of the Fredholm type may be written as

$$\psi(x)=\psi^*(x)-z\int K(x,y)\psi^*(y)dy, \tag{32}$$

in which ψ and the kernel $K(x,y)$ are known functions, and ψ^* is the unknown function to be determined from the equation. There exists a reciprocal kernel $K_z^*(x,y)$ depending on the value of the parameter z, such that, independent of ψ,

$$\psi^*(x)=\psi(x)-z\int K_z^*(x,y)\psi(y)dy. \tag{32'}$$

It is, of course, quite unimportant whether the variables x and y are one dimensional or a set of coordinates in multidimensional space.

The reciprocal kernel, K^*, varies continuously with the parameter z between the value $z=0$ (where $K^*=K$) and the first egienvalue, z_γ, for which the homogeneous equation,

$$\psi^*(x)=z_\gamma\int K(xy)\psi^*(y)dy, \tag{33}$$

has a solution. For values of z between z_γ and z_δ, the second eigenvalue, K^* again varies continuously with z. In general the functions which K^* approach as z approaches z_γ from above and below are different.

Now let us consider a special case of (29), namely that there is only one component kind of molecule, and that ψ_k^*, which we can choose arbitrarily, is identically zero except for $k=1$.

[2] John G. Kirkwood and Elizabeth Monroe, J. Chem. Phys. 9, 514 (1941).

There are, then, only two non-zero terms in the sum on the right, that with $\kappa=1$, $m=0$, and that with $\kappa=0$, $m=1$. We consider the case $k=1$, for which the kernel $K_{1,1,0}$ when $\kappa=1$, $m=0$ is unity from (31d). The equation for this case is,

$$\psi_1(i)=\psi_1^*(i)+z\int K_{1,0,1}((i),(j))\psi_1^*(j)d(j), \quad (34)$$

identical in form to (32). *Were we justified in assuming* that $\psi_k=0$ for all values of k except $k=1$ *then* (29′) for $k=1$ *would* be,

$$\psi_1^*(i)=\psi_1(i)-z\int K_{1,0,1}^*((i)(j))\psi_1(j)d(j)! \quad (34')$$

of the same form as (32′). That is *were the assumption correct* then $K_{1,0,1}$ and $K_{1,0,1}^*$ would be simple reciprocal kernels for the parameter z.

We may now examine more closely what the kernels $K_{1,0,1}$ and $K_{1,0,1}^*$ are. Choosing $\rho_\beta=0$, $z_\beta/\rho_\beta=1$, in Eqs. (21) and (21′) defining G and G^*, so that $z_\alpha=z$ from (22), and using (30) and (30′) defining the kernels we have,

$$K_{1,0,1}^*((i),(j))=\frac{F_2^*((i),(j))}{F_1^*(i)}-F_1^*(j), \quad (35)$$

$$K_{1,0,1}((i),(j))=\frac{\rho}{z}\left[\frac{F_2((i),(j))}{F_2(i)}-F_1(j)\right], \quad (35')$$

where the asterisks refer to infinite dilution and the functions F are the distribution functions at concentration ρ. Now if there are no internal coordinates then $F_1^*\equiv 1$, so that,

$$K_{1,0,1}^*=F_2^*-1, \quad (36)$$

which is a function symmetrical in permutations of the coordinates of the two molecules, approaching zero in value as the distance between them becomes large.

At least in the gaseous and liquid phases we also have $F_1=1$, so that for these phases,

$$K_{1,0,1}=\frac{\rho}{z}[F_2-1], \quad (36')$$

which is also symmetrical and approaches zeros for large distances.

The simplicity of the result obtained from this unjustified assumption of identifying $\psi_k=0$ for $k>1$ when $\psi_k^*=0$ for $k>1$ is made particularly intriguing when we consider that the function (36′) will show discontinuities in form as z changes through the eigenvalues of the kernel (36), so that these eigenvalues would be identified with the values of the activity at which phase transitions occur.

The actual situation is far more complicated due to the occurrence of the summations in the original Eqs. (29) and (29′). We have discussed this simple case at some length because of its suggestiveness, and because it appears to represent a simplified caricature of the true case.

THE KERNELS AS OPERATORS

We shall show that Eq. (29) may be regarded as a generalized matrix equation, in which a matrix, of which combinations of the kernels, K, constitute the elements, operate on the set of functions ψ_k^* to transform them to the set ψ_k. The equation (29′) is the reciprocal equation, in which the reciprocal matrix, of elements formed from the kernels K^*, operate on the set of functions ψ_k, transforming them to the set ψ_k^*.

These matrices, which transform from the activity z_β to the activity z_α, are functions of the distribution functions at the activity z_α, and of the difference, $z=z_\alpha-z_\beta$, Eq. (22), in the activity. We can thus consider the matrices, $A_z(y)$, as depending on two parameters, z and y, the matrix consisting of elements composed of the distribution functions at activity z, and transforming the set of functions ψ_k^* corresponding to the activity $z-y$ into the set ψ_k at z. We then obtain the matrix Eqs. (46) between the matrices for different values of z and y.

Let us use the symbol $a(\{k\},\{m\})$ for a function of the coordinates $\{k\}$ and $\{m\}$, defined by,

$$a(\{k\},\{m\})=(\sum\{\kappa\}_k\{\mu\}_m)\,\delta(\{\kappa\}_k,\{\mu\}_m)\frac{z^{m-\mu}}{(m-\mu)!}K_{k,\kappa,m-\mu}, \quad (37)$$

where the summation runs over all subsets, $\{\kappa\}_k$, of the set $\{k\}$, and all subsets, $\{\mu\}_m$, of $\{m\}$, but $\delta(\{\kappa\}_k,\{\mu\}_m)=0$ unless the two subsets contain the same numbers of the same types of molecules, and unless the coordinates of all corresponding molecules of the two sets are identical; and in the latter case the integral of $\delta(\{\kappa\}_k,\{\mu\}_m)$ about the position of identity of the coordinates

is unity. We similarly define:

$$a^*(\{k\}, \{m\}) = (\sum\{\kappa\}_k, \{\mu\}_m) \delta(\{\kappa\}_k, \{\mu\}_m) \frac{(-z)^{m-\mu}}{(m-\mu)!} K^*_{k,\kappa,m-\mu}. \quad (37')$$

With these two quantities we may write Eqs. (29) and (29′) as,

$$\psi_k = \sum_{m\geq 0} \int a(\{k\}, \{m\}) \psi_m^* d\{m\}, \quad (38)$$

$$\psi_k^* = \sum_{m\geq 0} \int a^*(\{k\}, \{m\}) \psi_m d\{m\}. \quad (38')$$

These equations are now in a more conventional form than that of (29) and (29′). If Φ and Φ^* are the sets of functions:

$$\Phi = \psi_0, \psi_1, \cdots, \psi_k, \cdots, \quad (39)$$

$$\Phi^* = \psi_0^*, \psi_1^*, \cdots, \psi_k^*, \cdots; \quad (39')$$

and A and A^* are the matrices of elements $a(\{k\}, \{m\})$ and $a^*(\{k\}, \{m\})$, respectively; then (38) and (38′) may be written as:

$$\Phi = A\Phi^*, \quad \Phi^* = A^*\Phi, \quad (40)$$

$$AA^* = A^*A = E, \quad (41)$$

With E the unit matrix. The matrix multiplication of the two elements involves *both* summation over the middle index *m and* integration over the coordinates $\{m\}$ for each value of the index m. The matrix A is thus a generalized type of matrix with continuous and discrete ranges. Thus we see that the Eqs. (29) and (29′) do correspond to the equations for two reciprocal commutative linear operators whose matrix elements can be represented by the a and a^* of Eqs. (37) and (37′).

Written in terms of these matrix elements equation (41) takes the form:

$$\sum_{m\geq 0} \int\int \cdots_V \int a(\{k\}, \{m\}) a^*(\{m\}, \{n\}) d\{m\}$$

$$= \sum_{m\geq 0} \int\int \cdots_V \int a^*(\{k\}, \{m\}) a(\{m\}, \{n\}) d\{m\}$$

$$= \delta(\{k\}\{n\}). \quad (42)$$

This equation could be used, in principle at least, as a means of determination of the functions G from known functions G^*.

The matrices A and A^* which we have defined by means of their elements in Eqs. (37) and (37′) depend both on the activity set z at which the kernels are determined (z_α for A and z_β for A^* in Eqs. (21) and (21′)), and upon the difference of activity, $z = z_\alpha - z_\beta$, between the two systems. Let us change our nomenclature at this place, and write the matrices as $A_z(y)$ of element,

$$a_z(y, \{k\}, \{m\}) = (\sum\{\kappa\}_k\{\mu\}_m) \delta(\{\kappa\}_k\{\mu\}_m) \frac{y^{m-\mu}}{(m-\mu)!} K_{k,\kappa,m-\mu}(z), \quad (43)$$

in which the kernels are made up according to (30) from the distribution functions at the activity set z.

If y becomes identically zero there remain in (43) only the terms for which $\mu = m$, and from (31c) and (31d) these are zero unless $k = \kappa = \mu = m$, and are then unity. We thus have,

$$\lim_{y\to 0}[A_z(y)] = E, \quad (44)$$

is the unit operator.

Now let $\Phi(z)$ represent the set of functions $\psi_0(z), \psi_1(z), \cdots, \psi_k(z)$ giving the variations in the potentials at the activity z. The transformation equations, (40), then take the form:

$$\Phi(z) = A_z(y)\Phi(z-y). \quad (45)$$

If we operate on this with $A_{z+x}(x)$ we find:

$$\Phi(z+x) = A_{z+x}(x)\Phi(z) = A_{z+x}(x)A_z(y)\Phi(z-y) = A_{z+x}(x+y)\Phi(z-y),$$

or

$$A_{z+x}(x+y) = A_{z+x}(x)A_z(y). \quad (46)$$

Equation (41) is seen to be a special case of (46), namely that for which $x = -y$, in which, from (44), $A_{z+x}(0) = E$, and,

$$A_{z+x}(x)A_z(-x) = E. \quad (46')$$

A SPECIAL EQUATION

Equation (42), which represnts a set of equations, one for each value of k and n, is comparatively awkward to handle for the case of general values of k and n. It can be seen that the equation is trivially satisfied if $n \equiv 0$, as we shall show in this section. If $k \equiv 0$ and $n = 1$, one obtains an expression which leads to an equation

for the activity, z_s, of the single molecule represented in the set $n=1$.

We use the symbol i_s or j_s to represent a single molecule of type s, and (i_s) or (j_s) to represent its coordinates, but use the subscript s to indicate a kernel in which the corresponding set n is a set consisting of one molecule of type s, and $m-s$ when the set is some general set, m, $(m_s \geq 1)$ less one molecule of type s. If n represents a set consisting of a single molecule of type s then $z^n = z_s$ in our notation. Using (37) and (37′), and Eqs. (31a) to (31d) inclusive, for special values of the kernels, we may write:

$$\left.\begin{aligned} a(0, \{m\}) &= (z^m/m!)K_{0,0,m} \\ &= (z^m/m!)G_m/G_0, \\ a^*(\{m\}, 0) &= a(\{m\}, 0) = \delta(m, 0), \\ a^*(\{m\}, (i_s)) &= -z_s K^*_{m,0,s} + \delta(\{m\}, (i_s)). \end{aligned}\right\} \quad (47)$$

Using these, the sum $\sum a(0, \{m\})a^*(\{m\}, 0)$ has only the single term $G_0/G_0 = 1$ when $m \equiv 0$, so that Eq. (42) for the case $k \equiv 0$, $n \equiv 0$, is trivially satisfied. Similarly, all sums

$$\sum a(\{k\}\{m\})a^*(\{m\}, 0)$$

contain no non-zero terms if $k > 0$, from the second of these equations, so that (42) for this case is also trivially satisfied.

The sum $\sum a(0, \{m\})a^*(\{m\}, (i_s)) = 0$, leads to the equation:

$$-z_s \frac{1}{G_0} \sum_{m \geq 0} \frac{z^m}{m!} \int\int \cdots \int G_m K^*_{m,0,s} d\{m\} + z_s \frac{G_s}{G_0} = 0. \quad (48)$$

If, in this, one sets the special case that the functions with asterisks refer to infinite dilution, see Eqs. (21), (21′) and (22), then $z \equiv z_\alpha$, and

$$z^m G_m/G_0 = \rho^m F_m(\rho, T, \{m\}),$$

is the probability density that the set m of molecules will occur at the position $\{m\}$. The functions $K^*_{m,0,s}$ are now, from (30′),

$$K^*_{m,0,s} = (\sum \{\mu\}_m)(-)^{m-\mu} \frac{F^*_{\mu+s}(0, T, \{\{\mu\}_m + (i_s)\})}{F_\mu^*(0, T, \{\mu\}_m)},$$

where the distribution function at zero concentration is:

$$F_\mu^*(0, T, \{\mu\}) = \exp -(U_\mu\{\mu\}/kT), \quad (49)$$

and U_μ is the potential energy of the μ molecules, if the system is classical.

Equation (48) now becomes,

$$\begin{aligned} &(\rho_s/z_s)F_s(\rho, T, (i_s)) \\ &= \sum_{m \geq 0} \frac{\rho^m}{m!} \int\int \cdots \int F_m(\rho, T, \{m\}) \\ &\quad \times \{\exp[(-1/kT)(U_{\mu+s}\{\{\mu\} + (i_s)\} \\ &\qquad - U_\mu\{\mu\})]\} d\{\mu\}, \end{aligned} \quad (50)$$

as a general equation for any system, if U is understood to be defined by (49) when the system is non-classical, in which case it is not a potential energy.

If Eq. (50) is divided by V, and integrated over the coordinates $d(i_s)$, due to the normalization condition (19), one obtains ρ_s/z_s, the inverse of the activity coefficient, on the left-hand side.

Let us assume a more specialized case, and one that is particularly simple. We assume that there are no internal coordinates, or that they have been integrated out of the distribution functions at zero density so that the potential U_μ is a function of the centers of mass, averaged over the internal coordinates. We further consider a single component system, and one existing in the liquid state so that F_s is unity. If, now, it is legitimate to express U_μ as a sum of terms, u_{jk}, each dependent only on the coordinates of the pair of molecules, j and k, then if,

$$f_{ij} = [\exp -(u_{ij}/kT)] - 1, \quad (51)$$

we have that,

$$K^*_{m,0,s} = \prod_{j=1}^{j=m} f_{ij}. \quad (52)$$

The functions f_{ij} approach zero in value if the distance between the molecules i and j become large, since their mutual potential is then zero. Equation (50) now takes the form,

$$\frac{\rho}{z} = \sum_{m \geq 0} \frac{\rho^m}{m!} \int\int \cdots \int F_m(\rho, T, \{m\}) \times \prod_{j=1}^{j=m} f_{ij} d\{m\}. \quad (53)$$

The distribution functions F_m become zero if too many molecules are crowded into too small a space. The product of f_{ij}'s is zero unless *all* of the m molecules are within interacting distance of the molecule i. As m becomes large there are no positions of the coordinates for which the integrand is non-zero, so the sum converges, and, indeed, terms with $m>13$ must be very small.

This equation is essentially a cell type equation in that one computes the activity, and therefore the free energy, by considering only the interactions of one molecule with those others that can approach it at any one time. The equation is exact in the form (50). It is not essentially different from that derived previously by the author with Montroll,[3] although it is cast in an entirely different appearing form.

EQUATIONS BETWEEN THE KERNELS

To use Eq. (42) in the case of general values of k and n, and convert it to a direct summation of integrals of products of the kernels K and K^* is comparatively difficult. One runs into rather awkward summations, which then simplify with considerable labor. The simplest form of these equations can be found more readily by another method. However, we wish to emphasize that the equations derived in this section are actually another form of (42).

We use Eq. (23′), write it for a set $k+n$ of numbers, sum over μ, and divide and multiply each term in the sum by $G_{k+\mu}$, using, however, (23) for $G_{k+\mu}$ in the numerator:

$$G^*_{k+n}=\sum_{\mu\geq 0}\frac{(-z)^\mu}{\mu!}\int\int\cdots\int_V G_{k+n+\mu}d\{\mu\}$$

$$=\sum_{\mu\geq 0}\frac{(-z)^\mu}{\mu!}\int\int\cdots\int_V\frac{G_{k+n+\mu}}{G_{k+\mu}}\left[\sum_{\nu\geq 0}\frac{z^\nu}{\nu!}\int\int\cdots\int G^*_{k+\mu+\nu}d\{\nu\}\right]d\{\mu\}$$

$$=\sum_{\mu\geq 0}\sum_{\nu\geq 0}\frac{z^{\nu+\mu}}{\nu!\mu!}(-)^\mu\int\int\cdots\int\frac{G_{k+n+\mu}G^*_{k+\mu+\nu}}{G_{k+\mu}}d\{\nu\}d\{\mu\}.$$

In this equation we write $\nu+\mu=m$, and sum over all sets of numbers m. Since there are $m!/\nu!\mu!$ different subsets, $\{\mu\}_m$, for every value of the set of numbers m and μ, we may divide by this and sum over all $\{\mu\}_m$. One obtains,

$$G^*_{k+n}=\sum_{m\geq 0}\frac{(-z)^m}{m!}\int\int\cdots\int_V G^*_{k+m}\left[(\sum\{\mu\}_m)(-)^{m-\mu}\frac{G_{k+\mu+n}}{G_{k+\mu}}\right]d\{m\},$$

or with Eq. (30),

$$G^*_{k+n}=\sum_{m\geq 0}\frac{(-z)^m}{m!}\int\int\cdots\int_V G^*_{k+m}K_{m+k,k,n}d\{m\}. \tag{54}$$

If instead we start with (23), the equation,

$$G_{k+n}=\sum_{m\geq 0}\frac{z^m}{m!}\int\int\cdots\int G_{k+m}K^*_{m+k,k,n}d\{m\}, \tag{54′}$$

may be obtained by the corresponding manipulations.

At first sight Eqs. (54) and (54′) appear to be only complications of the relatively simple forms (23) and (23′), but the forms (54) and (54′) have one enormous advantage, namely that the summations converge far more rapidly in these equations than in (23) and (23′). This superiority of convergence will be discussed in greater detail later, and is merely remarked here in passing.

[3] J. E. Mayer and E. Montroll, J. Chem. Phys. 9, 2 (1941), Eq. (70).

We now use (54) to obtain an equation for $K^*_{k,0,m}$, using (30′) defining this kernel as:

$$K^*_{k,,0n}=(\sum\{\kappa\}_k)(-)^{k-\kappa}G^*_{\kappa+n}/G^*_\kappa=\sum_{m\geq 0}\frac{(-z)^m}{m!}\int\int\cdots\int(\sum\{\kappa\}_k)(-)^{k-\kappa}K^*_{\kappa,\kappa,m}K_{m+\kappa,\kappa,n}d\{m\}.$$

However from (30′) we may write,

$$K^*_{\kappa,\kappa,m}=(\sum\{\lambda\}_{\kappa-\mu})K^*_{\lambda+\mu,\mu,m},$$

where $\mu=\{\mu\}_\kappa$ is any subset of κ, and from (30),

$$K_{m+\kappa,\kappa,n}=(\sum\{\mu\}_\kappa)K_{m+\mu,0,n},$$

so that,

$$(\sum\{\kappa\}_k)(-)^{k-\kappa}K^*_{\kappa,\kappa,m}K_{m+\kappa,\kappa,n}=(\sum\{\kappa\}_k\{\mu\}_k\{\lambda\}_{k-\mu})(-)^{k-\kappa}K^*_{\lambda+\mu,\mu,m}K_{m+\mu,0,n}$$

$$=(\sum\{\mu\}_k\{\lambda\}_{k-\mu})(-)^{k-\mu-\lambda}(\sum\{\kappa-\mu-\lambda\}_{k-\lambda-\mu}(-)^{\kappa-\mu-\lambda})K_{\lambda+\mu,\mu,m}K^*_{m+\mu,0,n}$$

$$=(\sum\{\mu\}_k)K^*_{k,\mu,m}K_{m+\mu,0,n},$$

where the last line follows from the fact that the summation in the brackets of the preceding expression is zero unless $\lambda+\mu=k$. One therefore has,

$$K^*_{k,0,n}=\sum\frac{(-z)^m}{m!}(\sum\{\kappa\}_k)\int\int\cdots\int_V K_{k,\kappa,m}K_{m+\kappa,0,n}d\{m\}. \tag{55′}$$

If, instead, (54′) is used, one finds,

$$K_{k,0,n}=\sum_{m\geq 0}\frac{z^m}{m!}(\sum\{\kappa\}_k)\int\int\cdots\int_V K_{k,\kappa,m}K^*_{m+\kappa,0,n}d\{m\}. \tag{55}$$

Now for fixed values of the coordinates $\{n\}$ the kernels $K^*_{k,0,n}$ and $K_{k,0,n}$ are functions of the coordinates $\{k\}$, symmetrical in permutations of the coordinates of identical molecules. It is seen that Eqs. (55) and (55′) are identical to Eqs. (29) and (29′) with $K^*_{k,0,n}$ replaces $\psi_k{}^*$ and $K_{k,0,n}$ replacing ψ_k. That is, the functions $K_{k,0,n}$ and $K^*_{k,0,n}$ for any set of numbers n and any value of the coordinates $\{n\}$, regarded as functions of the coordinates $\{k\}$, form a suitable set ψ_k and the corresponding solutions $\psi_k{}^*$, respectively, to Eqs. (29) and (29′) or (38) and (38′).

THE CONVERGENCE OF THE EQUATIONS

Whether or not the sum in Eqs. (29) or (29′) converge depend on the variation functions ψ_k and $\psi_k{}^*$. We shall assume that the functions $\psi_k{}^*$ are of the type which one might actually wish to handle if one considers variations in the potential energy of the molecules, or variations in temperature. In particular we assume that $\psi_k{}^*$ approaches zero if the coordinates of any pair of the molecules composing the set k are sufficiently distant in the three-dimensional space of their mass centers, and that this approach to zero is more rapid than r^{-2}, so that,

$$\lim_{V\to\infty}\left[V^{-1}\int\int\cdots\int_V\psi_k{}^*d\{k\}\right]=\text{finite}. \tag{56}$$

We shall also assume that the functions ψ_k approach zero in value as $k\to\infty$, or at least that the integral of Eq. (56) approaches zero as $k\to\infty$.

We shall show that the form of the Eq. (30) defining the kernels is such, that, if the functions $\psi_k{}^*$ obey the conditions above, then if the kernels are formed at an activity for which the system can only exist in one phase, the Eq. (29) will converge and the functions ψ_k will also obey the above conditions. If, however, the kernels are formed at an activity for which two phases are stable no such convergence can be expected.

For such values of the activity set z that the system exists in a single phase, we may expect the distribution functions to show certain characteristics. These functions may be written

$F_n = \exp(-W_n/kT)$ where W_n is the potential of average force. We would expect W_n in single phase systems to have no terms corresponding to long range forces. That is, we expect that for two sets of molecules, k and m, if the distances, $r_{k,m}$, between all molecules of the set k and all of the set m are large, then $W_{k+m} = W_k + W_m$. This means that:

$$\lim_{r_{m,k}\to\infty} [F_{k+m}] = F_k F_m. \tag{57}$$

Let us assume that Eq. (57) applies, and that the difference $F_{k+m} - F_k F_m$ approaches zero more rapidly than $r_{k,m}^{-2}$, an assumption that corresponds to having all forces approach zero more rapidly than r^{-3}.

Now let us examine the kernels,

$$K_{k+n,n,m} = \left(\frac{\rho}{z}\right)^m (\sum\{\kappa\}_k)(-)^{k-\kappa}\frac{F_{\kappa+n+m}}{F_{\kappa+n}}, \tag{58}$$

which equation is equivalent to (30) when ρ and z refer to the concentration and activity set for the functions without asterisks, see Eq. (21). Suppose the distances, $r_{k,n+m}$, between all molecules of the set k, and all molecules of $n+m$ are large. Then from (57)

$$F_{\kappa+n+m} = F_\kappa F_{n+m}, \quad F_{\kappa+n} = F_\kappa F_n,$$

and

$$F_{\kappa+n+m}/F_{\kappa+n} = F_{n+m}/F_n.$$

But the sum $(\sum\{\kappa\}_k)(-)^{k-\kappa}$ is zero if $k>0$, Eq. (15). It follows that,

$$\lim_{r_{k,n+m}\to\infty} [K_{k+n,n,m}] = 0, \quad k>0, \tag{59}$$

and the approach to zero is more rapid than $r_{k,n+m}^{-2}$ according to our assumptions.

Let us now look at the product:

$$K_{k+n,n,m}\psi^*_{n+m} \tag{60}$$

which composes the integrand in the general term of the sum (29). If ψ^*_{n+m} approaches zero as any of the distances of the set $n+m$ becomes large, that is it obeys (56), then the integrand is zero unless all molecules of the set $n+m$ are close together. But if the set $n+m$ is far from the set k, then from (59) the kernel is zero, and the integrand is zero. Furthermore, the argument leading to Eq. (59) applies if *any one* of the molecules of the set k is far from all of the set $n+m$. It follows that, within our assumptions, the integrand (60) is zero unless *all* of the molecules of the complete set $k+n+m$ are reasonably close together (within range of molecular forces one to the other) in the three-dimensional space of their centers of mass. It also follows, since we have assumed conditions leading to a sufficiently rapid approach to zero, that the integral of (60) over the coordinates $\{m\}$ leads to a finite result independent of the volume V over which the range of integration is extended.

If we also assume that $\psi_k^* \to 0$ as $k\to\infty$, then we have assured the convergence of (29) since only a finite number of terms have non-zero integrands, and these each converge upon integration. But we have also shown that, within our assumptions, each integrand is zero in (29) unless all the molecules of the set k are close together, so the ψ_k's also obey the condition (56).

Now at such values of the activity set, z, that two phases can coexist in the system, Eq. (57) is not correct. For instance, in the absence of a gravitational field (which would make z a function of position in the system) the distribution function for the system would be:

$$\rho^n F_n = x\rho_a{}^n F_n{}^{(a)} + (1-x)\rho_b{}^n F_n{}^{(b)},$$

where ρ_a, ρ_b are the densities of the two phases, and $F_n{}^{(a)}$ and $F_n{}^{(b)}$ the distribution functions in the pure phases. The number x is the volume fraction of the system in phase a, and is variable at the given z. Functions constructed according to this equation do not obey (57) even if $F_n{}^{(a)}$ and $F_n{}^{(b)}$ do satisfy it singly. We may conclude that, in general, solutions to (29) are not obtainable at such values of the set z that two phases can coexist in the system at the activities at which the kernels are determined. However, satisfactory solutions should be obtainable as z is varied to approach the value of the transition, but the solutions will, in general, be different as this value is approached from the side of one phase or the other.

EIGENVALUES AS THE ACTIVITIES OF PHASE TRANSITION

The first terms in Eqs. (29) and (29′) are those for which $m=0$. From (31c) and (31d) we see that only the term with $\kappa=k$ in those of $m=0$ has a non-zero kernel, and for this term the

kernel is unity. We may consequently write:

$$\psi_k=\psi_k^*+\sum_{m\geq 1}\frac{z^m}{m!}(\sum\{\kappa\}_k)\times\int\int\cdots\int_V K_{k,\kappa,m}\psi^*_{\kappa+m}d\{m\},\quad(61)$$

$$\psi_k^*=\psi_k+\sum_{m\geq 1}\frac{(-z)^m}{m!}(\sum\{\kappa\}_k)\int\int\cdots\int_V K^*_{k,\kappa,m}\psi_{\kappa+m}d\{m\},\quad(61')$$

as modified forms of (29) and (29′). The fact that the terms independent of z in the matrix element were $\delta(\{k\}\{m\})$ has already been noted in the discussion under Eq. (43), and Eq. (61) and (61′) merely repeat this.

If we define a matrix $B_z(y)$ by the equation:

$$B_z(y)=A_z(y)-E,\quad(62)$$

so that, from (44),

$$\lim_{y\to 0}[B_z(y)]=0,\quad(63)$$

then the transformation equation (45) becomes:

$$\Phi(z)=\Phi(z-y)+B_z(y)\Phi(z-y).\quad(64)$$

Let us write this for $z\equiv y$,

$$\Phi(z)=\Phi(0)+B_z(z)\Phi(0),\quad(65)$$

and the reciprocal equation,

$$\Phi(0)=\Phi(z)+B_0(-z)\Phi(z).\quad(65')$$

Suppose that there exists a value of the set z, namely z_γ, for which there is a solution, Φ_γ, to the homogeneous equation obtained by setting $\Phi(0)=0$ in (65′), namely:

$$\Phi_\gamma+B_0(-z_\gamma)\Phi_\gamma=0.\quad(66)$$

This would mean that there would exist a possible variation of the potentials of average force at the activity z_γ which would not be reflected in a change of the distribution functions at zero density. Without regard to the physical interpretation of this let us first examine its implication in our equations. With this Φ_γ for $\Phi(z_\gamma)$ in (65′) we find $\Phi(0)=0$. However, if we insert $\Phi(0)=0$ in (65) we cannot obtain $\Phi(z_\gamma)=\Phi_\gamma\neq 0$ if the matrix Eqs. (61) (or (38)) converge.

Now at such values of the activity set z that the system exists in a single phase only, one expects that the distribution functions be uniquely determined, and that no stable variations would exist that did not require alterations in the potentials at zero density. One also expects that no long range average forces be present, and that, therefore, as discussed in the preceding section, the matrix Eq. (61) would converge.

However, at values of the activity set for which two or more phases are present the situation is entirely altered. The distribution functions are *not* uniquely determined by the activity, since the relative fractions of the different phases vary at the constant activity. There *are*, then, variations possible which do not require changes in the potentials at zero density. But also the existence of more than one phase introduces a pseudo long range average force which completely spoils the convergence of the matrix Eq. (61), corresponding to (65).

We may therefore identify the values of z for which the homogeneous Eq. (66) has a solution with the values of the activity set for which more than one phase can coexist in the system.

We have previously[1] identified the occurrence of a phase transition with the divergence of a power series in the activity. That is, one could start with a system of any activity, say activity z, and compute the thermodynamic properties such as pressure, density, or the distribution functions, F_n, at some other activity, say $z+y$, in terms of the same property at z and a power series in y. If y were sufficiently small the power series converges, but if, as y increases, the activity $z+y$ approaches the activity, z_γ, at which a phase transition occurs, the power series diverges.

Now the kernel, reciprocal to that in a Fredholm type integral equation, can be calculated by an iterative process as a power series in the characteristic parameter, y, of the equation, provided the value of y is less than the first eigenvalue of the corresponding homogeneous equation. As y approaches this value, the series diverges.

One may regard Eq. (61′) as an equation for unknown functions ψ_k, and attempt to solve it by using $\psi_k^*=\psi_k$ under the integral as a first approximation, and use the resulting equation as a

second approximation. By reiterating this process one obtains an equation involving integrations of products of the kernels K^* multiplied by ψ^*, and by comparison with (61) one obtains an equation for K as a sum of integrals of products of the kernels K^*. The sum is a power series in z. These equations, so obtained, can be transformed into the equations formerly obtained for the thermodynamic properties and distribution functions as a power series in z.

But the iterative process can only lead to a convergent series for those values of the parameter z which are less than the first eigenvalue of the corresponding homogeneous equation. The two methods of obtaining the phase transitions are thus formally equivalent.

THE SOLUTIONS OF THE HOMOGENEOUS EQUATIONS

It is possible to find the significance of the solutions of the homogeneous Eq. (66) at the values, z_γ, of the activity coefficient for which two phases coexist.

We know, from experience, that the solutions G_n, to Eq. (23), for $n>0$, undergo discontinuous changes as z crosses the values at which phase transitions occur. It is possible to disentangle the mathematical reason for this, and to see that the value of m for the term of maximum value undergoes discontinuous transitions at these values of z. In general, then, there exist two values, $G_n^{(a)}$, and $G_n^{(b)}$, which the sum (23) approaches as z approaches z_γ, depending on whether the approach to the activity of the phase transition occurs from the activities for which phase (a) or phase (b) are stable. At $z=z_\gamma$ any value, $G_n=xG_n^{(a)}+(1-x)G_n^{(b)}$ for $0\leq x\leq 1$ is a physically meaningful solution to (23), corresponding to having the volume fraction x of the system in the volume V in the form of phase (1). We might expect to use this for G_n in (24) and take derivatives with respect to x to determine the functions Ψ_n for which no change in G_n^* is required. This procedure bogs down in mathematical difficulties.

Let us instead turn to equations (55′). We again interpret the functions with asterisks to refer to infinite dilution. As z approaches z_γ from the two sides there are two solutions, $K^{(a)}_{m,0,n}$, and $K^{(b)}_{m,0,n}$, for every m and n, that satisfy (55′) with the same values of K^*. It follows that:

$$\sum_{m\geq 0}\frac{(-z)^m}{m!}(\sum\{\kappa\}_k)\int\int\cdots\int_V K^*_{k,\kappa,m}\times[K^{(a)}_{m+\kappa,0,n}-K^{(b)}_{m+k,0,n}]d\{m\}=0. \quad (67)$$

The functions,

$$\psi_k^{(\gamma,\{n\})}=K^{(a)}_{k,0,n}-K^{(b)}_{k,0,n}, \quad (68)$$

and the sets;

$$\Phi_\gamma(\{n\})=\psi_0^{(\gamma\{n\})},\ \cdots,\ \psi_k^{(\gamma,\{n\})}, \quad (69)$$

for any $\{n\}$ are therefore solutions to the homogeneous Eq. (66) at the activity z_γ at which phases (1) and (2) can coexist in the system.

CONCLUSION

The essential results may be summarized as follows. One may define distribution functions, F_n, as being proportional to the probability density that a set, n, of molecules are found at the coordinate postion $\{n\}$. The logarithms of these functions are $-W_n\{n\}/kT$, in which $W_n\{n\}$ is the potential of average force between the molecules at the position $\{n\}$. These potentials depend on the activity set z of the different molecular species present, and vary with z continuously from the true potential energy, at zero activity, but with discontinuities at the phase transitions.

The function, $W_n(z,\{n\})$ may be represented as a sum of terms, each depending on the coordinates, $\{\nu\}_n$, of a subset ν of molecules of the set n, summed over all subsets:

$$W_n=(\sum\{\nu\}_n)w_\nu(z,\{\nu\}_n). \quad (70)$$

At zero density, at least, one usually assumes that only the functions w_ν for $\nu\leq 2$, are non zero, corresponding to having the forces between molecules the sum of those between pairs only.

One considers a possible variation in the various functions, $w_k(z,\{k\})/kT$. A set, $\Phi(z)$, of functions, $\psi_0(z)$, $\psi_1(z,(i))$, $\cdots$, $\psi_k(z,\{k\})$, $\cdots$, may be defined by

$$\psi_k(z,\{k\})=\delta[w_k(\rho,\{k\})/kT], \quad (71)$$

where $\delta(w_k/kT)$ is the variation in w_k/kT. This set of functions, depending on the activity parameter z, represents a self-consistent set of

variations of w_k/kT, of which the set at one particular activity, most naturally that at zero activity, may be regarded as arbitrary.

In order to compute the set $\Phi(z)$, from a knowledge of the functions at some other activity, say $\Phi(z-y)$, a transformation matrix $A_z(y)$ may be employed which transforms $\Phi(z-y)$ into $\Phi(z)$. The elements, $a_z(y, \{k\}, \{m\})$, of this matrix, given by Eqs. (43), (30), and (21), consist of combinations of the distribution functions at the activity z, to which the transformation is made, multiplied by powers of y, the difference of activities. The limit of the transformation matrix, as the activity difference y becomes zero, is, of course, the unit matrix. The matrix multiplication involves both summation over all sets of molecules, and integration over the coordinates of each set.

The product of the two matrices $A_z(y)$ and $A_{z-y}(-y)$ is the unit matrix. This is a special case of the more general relation that

$$A_z(y)A_{z+z}(x)=A_{z+z}(x+y).$$

These matrix equations are equivalent to a set of sums of integral equations, (55) and (55′), relating the distribution functions at different activities of the system. The equations are convergent if the activities are such that only single phases are present in the system, even if the activity pairs are those at which different phases are stable.

One member of these equations, (53), permits a computation of the activity or free energy of the system in terms of the interactions of one molecule with its neighbors in the system.

If z is an activity for which the system exists in a single phase only, and z_γ an activity at which two phases, (a), and (b), can coexist, then there are function sets Φ_γ characteristic of z_γ which satisfy the transformation equation

$$A_z(z-z_\gamma)\Phi_\gamma=0.$$

In particular if $z=0$, $A_0(-z_\gamma)\Phi_\gamma=0$, Eqs. (66) and (62), show that there exist a set, Φ_γ, of variations of the potential of average force in the two phase system which can occur without variations in the temperature or potentials between the molecules at infinite dilution. The transformation matrix, $A_{z\gamma}(y)$, to this activity, z_γ, of the phase transition, has elements such that the summations and integrations diverge. The solutions, Φ_γ, to the homogeneous equation, $A_0(-z_\gamma)\Phi_\gamma=0$, are differences of certain combinations of the distribution functions of the two phases (a) and (b) which are at equilibrium at the activity z_γ, Eqs. (68), (30), and (21).

The Contribution of Restricted Rotation to Electron Scattering by Gases

J. KARLE
U. S. Naval Research Laboratory, Washington, D. C.
(Received January 22, 1947)

Several formulae have been derived expressing the contribution to the intensity of electron scattering of restricted rotation in the vapors of ethane, ethylene, biphenyl, and their derivatives. The probability distribution of the restricted rotator about its axis of rotation is expressed in terms of the barrier height, V_0. It has, therefore, been possible to evaluate the effect of barriers of known magnitude on scattering patterns. The possibility of evaluating the potential barrier using electron diffraction is discussed.

IT is well known from statistical thermodynamic studies[1] that many molecules exhibit restricted internal rotation at normal temperatures. This type of motion is of interest in the field of electron diffraction by gases because of its effect on the interpretation of scattering patterns in structure determinations, and also because of the possibility of using these patterns for evaluating the magnitude of the restricting potentials. Two methods are commonly used for interpreting the patterns from molecules which may possess restricted internal rotation. In both cases theoretical intensity curves are calculated and are compared to the experimentally observed patterns. These curves are based either on a rigid model (which obviously neglects the internal motion) or on a model undergoing small vibrations according to the theory developed by R. W. James[2] for x-ray diffraction by gas molecules. This theory arises from a normal coordinate treatment which is generally quite unwieldy for polyatomic molecules and so its prescribed effects are introduced into the analysis in an empirical way. Another approach which has been tried[3] is to treat the molecule as a rigid structure with an additional internal librational degree of freedom. In this way the concept of a potential barrier hindering free rotation may be directly introduced and its effect evaluated. This procedure is justified in molecules possessing barriers of the order of 3 kcal., as for instance derivatives of ethane, since in such cases the librational motion is far more important than the other vibrational degrees of freedom, especially at higher temperatures. On the other hand, some derivatives of ethylene may have barriers as high as 40 kcal. In this case the effect of the librational motion would be negligible at ordinarily attained experimental temperatures. In addition this motion and the energy quantum associated with it would approach the same order of magnitude as that of the other vibrations and could not be readily considered separately.

P. Debye[4] has investigated the effect of the various types of internal motion, namely, vibration and free and hindered rotation, on electron scattering by gas molecules. His theory for hindered rotation concerns 1,2 di-substituted ethanes and does not consider those cases for which classical statistics may not satisfactorily apply. In this article a quantum-mechanical distribution function for the angular distribution of the restricted rotator about its equilibrium position will be developed, and the theory extended to include the more completely substituted ethanes and also the derivatives of biphenyl and ethylene. For molecules undergoing hindered rotation, an increase in temperature may cause profound changes in their electron scattering patterns long before there are any considerable number of them undergoing free rotation, that is in states whose energy is greater than the barrier. This variation with temperature may be used to evaluate the hindering potential.

The theory to be developed will apply to the case in which the molecules of the gas occupy mainly the lower lying levels and the amplitude of the hindered rotation is not too large. The

[1] A discussion of the method and a compilation of the results may be found in G. Herzberg, *Infrared and Raman Spectra* (D. Van Nostrand Company, New York, 1945).
[2] R. W. James, Physik. Zeits. **33**, 737 (1932).
[3] (a) J. Y. Beach and K. S. Palmer, J. Chem. Phys. **6**, 639 (1938). (b) J. Y. Beach and A. Turkevich, J. Am. Chem. Soc. **61**, 303 (1939).
[4] P. Debye, J. Chem. Phys. **9**, 55 (1941).

other extreme, the case of free rotation, has already been investigated.[4,5]

DEVELOPMENT OF THEORY

The expression for the intensity of coherent molecular scattering from a rigid molecule is

$$\sum_{i=1}^{N}\sum_{j=1}^{N} f_i f_j \sin sr_{ij}/sr_{ij}, \quad (i \neq j) \tag{1}$$

where N is the total number of atoms in the molecule, f_i is the atomic scattering factor for electrons for the ith atom, r_{ij} is the distance between the ith and jth atoms and $s=4\pi \sin(\theta/2)/\lambda$ where θ is the angle of scattering and λ is the wave-length of the electrons. We are concerned with the contribution from varying interatomic distances which may be expressed by integrals of the type

$$\int \sin(sr_{ij})P(r_{ij})dr_{ij}/sr_{ij}. \tag{2}$$

The interatomic distances, r_{ij}, affected by the internal rotation and their probability distribution functions, $P(r_{ij})dr_{ij}$, will be expressed in terms of the angle of internal rotation, ϕ. By solving the Schroedinger equation for the restricted rotator undergoing small vibrations, the probability distribution of the rotating group as a function of angle ϕ for each of the lower states can be found. The distribution of the gas molecules among these states is determined by the Boltzmann distribution law. The probability functions $P'(\phi)d\phi = P(r_{ij})dr_{ij}$ may be obtained from multiplying the probability distribution within each of the hindered rotational states, as obtained from the Schroedinger equation, by a factor governing the frequency of occurrence of each of these states, as obtained from the Boltzmann law, and adding these products.

The effect of hindered rotation on electron scattering will first be developed for substituted ethanes of the type X_3CCY_3. They are symmetric top molecules and therefore lend themselves readily to theoretical treatment. It has been shown[6] that for symmetric top molecules the Schroedinger equation for rotational motion is separable into an equation containing the variables governing the motion of the molecule as a whole, and one in terms of the variable concerned with the internal motion. We are interested in the latter which is

$$d^2\psi/d\phi^2+8\pi^2 I(E-V)\psi/h^2=0, \tag{3}$$

where I is the reduced moment of inertia equal to $I_1I_2/(I_1+I_2)$, where I_1 and I_2 are the moments of inertia about the axis of the molecule of the two ends rotating with respect to each other, and ϕ is the variable of internal rotation. The other quantities have the usual significance. The potential function, V, is assumed to have the form

$$V=V_0(1-\cos\sigma\phi)/2, \tag{4}$$

where V_0 is the barrier height and σ is the number of minima in the potential function, for instance three for ethane. When ϕ is small, we get

$$V=V_0(\sigma\phi/2)^2. \tag{5}$$

On substituting (5) into (3) the Schroedinger equation for the simple harmonic oscillator is obtained. It is

$$d^2\psi/d\phi^2+8\pi^2 I[E-V_0(\sigma\phi/2)^2]\psi/h^2=0. \tag{6}$$

The normalized solutions to this equation are[7]

$$\psi_n(\phi)=N_n \exp(-\alpha\phi^2/2)H_n(\alpha^{\frac{1}{2}}\phi), \tag{7}$$

where

$$N_n=\{(\alpha/\pi)^{\frac{1}{2}}/2^n n!\}^{\frac{1}{2}},$$
$$\alpha^2=2\sigma^2\pi^2 I V_0/h^2,$$

and H_n is the Hermite polynomial of order n. Since we are concerned with the situation in which only the first few states are occupied significantly, we may add to the distribution function for these lower states the distributions for the higher harmonic oscillator states since their Boltzmann factors are so small that their contribution is essentially equal to zero. The advantage in including them arises from the fact that the infinite sum may be readily written in compact form.

The probability distribution function in terms

[5] J. Karle, J. Chem. Phys. **13**, 155 (1945).
[6] H. H. Nielsen, Phys. Rev. **40**, 445 (1932).

[7] There are also vibrations of small amplitude which may be considered as centered not only about $\phi=0$, but also about $\phi=2\pi n/\sigma$ as n goes from 1 to $\sigma-1$. These lead to wave functions and a distribution function which assume significant values in the vicinity of these σ values of ϕ. For our purposes the desired results may be obtained from considering only the distribution about $\phi=0$ since the others make an identical contribution to the scattering problem.

of the contributions from the various states is

$$(\alpha/\pi)^{\frac{1}{2}}(1-\exp[-h\nu/kT])\exp(-\alpha\phi^2) \times\sum_{n=0}^{\infty} H_n^2(\alpha^{\frac{1}{2}}\phi)\exp(-nh\nu/kT)d\phi/2^n n!, \quad (8)$$

where $\nu=\sigma(V_0/2I)^{\frac{1}{2}}/2\pi$, T is the absolute temperature, and k is the gas constant. The quantity $1-\exp[-h\nu/kT]$ normalizes the Boltzmann factors. Mehler[8] in studying the parabolic cylinder function, D, obtained the generating function,

$$\exp[(-[1-t]/[1+t])\rho^2/2]/(1-t^2)^{\frac{1}{2}} =\sum_{n=0}^{\infty} t^n D_n^2(\rho)/n!. \quad (9)$$

The following relation exists between the parabolic cylinder function and the Hermite polynomials,

$$D_n^2(\rho)=2^{-n}H_n^2(\rho/2^{\frac{1}{2}})\exp(-\rho^2/2). \quad (10)$$

On substituting (10) into (9) it is found that

$$\sum_{n=0}^{\infty} t^n H_n^2(\rho/2^{\frac{1}{2}})\exp(-\rho^2/2)/2^n n! =\exp[-([1-t]/[1+t])\rho^2/2]/(1-t^2)^{\frac{1}{2}}. \quad (11)$$

By comparing (11) to (8) it is apparent that by setting $t=\exp[-h\nu/kT]$ and $\rho/2^{\frac{1}{2}}=\alpha^{\frac{1}{2}}\phi$ we get for the sum of (8)

$$(\alpha/\pi)^{\frac{1}{2}}[\tanh(h\nu/2kT)]^{\frac{1}{2}} \times\exp[-\alpha\phi^2\tanh(h\nu/2kT)]d\phi. \quad (12)$$

This is the normalized distribution function we have been seeking. The function $b\exp[-b^2\phi^2]d\phi/\pi^{\frac{1}{2}}$, where $b^2=\alpha\tanh(h\nu/2kT)$, is the probability of finding the rotating group between ϕ and $\phi+d\phi$. Expression (12) is equivalent to the distribution function obtained by Bloch[9] for the linear harmonic oscillator. If $h\nu$ is small with respect to kT we obtain the classical result from (12),

$$(\sigma^2V_0/4\pi kT)^{\frac{1}{2}}\exp(-\sigma^2V_0\phi^2/4kT)d\phi. \quad (13)$$

We may proceed now with the scattering problem and the next step is to express the interatomic distances which change with the internal rotation in terms of angle ϕ. The equilibrium distances which occur depend upon whether the molecule, X_3CCY_3, is at equilibrium in the staggered or eclipsed configuration. The staggered configuration is the more probable one and is considered first. Two types of distances appear,

$$r_1=(c_1+c_2\cos\phi)^{\frac{1}{2}}$$

and

$$r_2=(c_1-c_2\cos[\phi-\pi/3])^{\frac{1}{2}}, \quad (14)$$

where $c_1=(l_2^2+l_1^2)/2$, and $c_2=(l_2^2-l_1^2)/2$. The quantity l_1 is the smallest possible distance of approach of atoms X and Y if the rotating groups could rotate freely and l_2 is the largest possible distance between them.

The contribution from small variations in r_1 resulting from hindered rotation is obtained from evaluating the integral,

$$b\int \sin[s(c_1+c_2\cos\phi)^{\frac{1}{2}}] \times\exp(-b^2\phi^2)d\phi/\pi^{\frac{1}{2}}s(c_1+c_2\cos\phi)^{\frac{1}{2}}. \quad (15)$$

We express $\cos\phi$ as $1-\phi^2/2$ and find that

$$\sin[s(c_1+c_2\cos\phi)^{\frac{1}{2}}] \sim\text{I.P.}\exp[i(sl_2-sc_2\phi^2/4l_2)] \quad (16)$$

where I.P. refers to the imaginary part. Integral (15) becomes the imaginary part of

$$b\exp(isl_2)\int_{-\infty}^{\infty}\exp[-(b^2+iB)\phi^2]d\phi/\pi^{\frac{1}{2}}sl_2, \quad (17)$$

where $B=sc_2/4l_2$. The small variations in r_1 have been omitted in the denominator of the integrand. Integral (17) has the value $b\exp(isl_2)/sl_2(b^2+iB)^{\frac{1}{2}}$ and the imaginary part is

$$b[\cos(sl_2)\text{I.P.}(b^2-iB)^{\frac{1}{2}} +\sin(sl_2)\text{R.P.}(b^2-iB)^{\frac{1}{2}}]/sl_2(b^4+B^2)^{\frac{1}{2}}, \quad (18)$$

where R.P. refers to the real part. By setting $(b^2-iB)^{\frac{1}{2}}=\rho^{\frac{1}{2}}\exp(i\xi/2)$ it can be shown that

$$\text{I.P.}(b^2-iB)^{\frac{1}{2}}=-(b^4+B^2)^{\frac{1}{2}}\sin(\xi/2)$$

and

$$\text{R.P.}(b^2-iB)^{\frac{1}{2}}=(b^4+B^2)^{\frac{1}{2}}\cos(\xi/2), \quad (19)$$

where $\tan\xi=B/b^2=sc_2/4l_2b^2$. We thus obtain for the contribution from r_1

$$(\cos\xi)^{\frac{1}{2}}\sin(sl_2-\xi/2)/sl_2. \quad (20)$$

There are three r_1 terms occurring for X_3CCY_3. If only a rigid structure was considered, the contribution to the scattered intensity would be

[8] F. G. Mehler, J. f. reine u. angew. Math. 66, 161 (1866).
[9] F. Bloch, Zeits. f. Physik 74, 295 (1932).

$\sin(sl_2)/sl_2$. The effect of the restricted rotation is to shift the maxima and minima by angle $\xi/2$, which varies with s, and to introduce a damping factor, $(\cos\xi)^{\frac{1}{2}}$. When the same atoms oscillate at each end of the C−C bond the relation $l_2^2-l_1^2=4a^2$ holds where a is the radius of rotation. When this relation is substituted into (20) a result similar to Debye's is obtained.

The contribution from small variations in r_2 resulting from hindered rotation is obtained from the integral

$$b\int \sin[s(c_1-c_2\cos[\phi-\pi/3])^{\frac{1}{2}}]$$
$$\times\exp(-b^2\phi^2)d\phi/\pi^{\frac{1}{2}}s(c_1-c_2[\phi-\pi/3])^{\frac{1}{2}}. \quad (21)$$

For small values of ϕ we have $\cos(\phi-\pi/3)\sim 0.5+(3^{\frac{1}{2}}\phi)/2-0.25\phi^2$. If we define

$$\tau_1=s(c_1-c_2/2)^{\frac{1}{2}},$$
$$\beta=c_2/8(c_1-c_2/2)-3(c_2/[c_1-c_2/2])^2/32,$$

and

$$\gamma=3^{\frac{1}{2}}c_2/4(c_1-c_2/2)$$

(21) becomes

$$b\int_{-\infty}^{\infty} \sin[\tau_1(1-\gamma\phi+\beta\phi^2)]$$
$$\times\exp(-b^2\phi^2)d\phi/\pi^{\frac{1}{2}}\tau_1. \quad (22)$$

As in (17) the variation of r_2 about its equilibrium value is omitted from the denominator. Integral (22) may be expressed as

$$b\Big[\sin\tau_1\int_{-\infty}^{\infty}\cos(\gamma\tau_1\phi-\beta\tau_1\phi^2)\exp(-b^2\phi^2)d\phi$$
$$-\cos\tau_1\int_{-\infty}^{\infty}\sin(\gamma\tau_1\phi-\beta\tau_1\phi^2)$$
$$\times\exp(-b^2\phi^2)d\phi\Big]\Big/\pi^{\frac{1}{2}}\tau_1. \quad (23)$$

After further expanding the integrands and bearing in mind that odd integrands do not contribute to the values of the integrals, it is found that the problem reduces to evaluating

$$\int_{-\infty}^{\infty}\cos(\gamma\tau_1\phi)\exp[-(b^2+i\beta\tau_1)\phi^2]d\phi. \quad (24)$$

The real part of the integrand of (24) is the contributing portion of the integrand of the first integral in (23), and the imaginary part is the contributing portion of the integrand of the second integral in (23). Integral (24) has the value

$$\pi^{\frac{1}{2}}\exp[-\gamma^2\tau_1^2/4(b^2+i\beta\tau_1)]/(b^2+i\beta\tau_1)^{\frac{1}{2}}. \quad (25)$$

By defining $(b^2-i\beta\tau_1)^{\frac{1}{2}}=\rho^{\frac{1}{2}}\exp(-i\theta/2)$ we find that the real part of (25) is

$$\pi^{\frac{1}{2}}\cos[(\gamma^2\beta\tau_1^3/4[b^4+\beta^2\tau_1^2])-\theta/2]$$
$$\times\exp[-\gamma^2b^2\tau_1^2/4(b^4+\beta^2\tau_1^2)]/(b^4+\beta^2\tau_1^2)^{\frac{1}{4}}, \quad (26)$$

and the imaginary part of (25) is

$$\pi^{\frac{1}{2}}\sin[(\gamma^2\beta\tau_1^3/4[b^4+\beta^2\tau_1^2])-\theta/2]$$
$$\times\exp[-\gamma^2b^2\tau_1^2/4(b^4+\beta^2\tau_1^2)]/(b^4+\beta^2\tau_1^2)^{\frac{1}{4}} \quad (27)$$

where $\tan\theta=\beta\tau_1/b^2$. By combining (26) with the coefficient of the first integral in (23), and (27) with the coefficient of the second, we get the desired result, the contribution from r_2,

$$(\cos\theta)^{\frac{1}{2}}\sin[\tau_1-(\gamma^2\tau_1\sin^2\theta/4\beta)+\theta/2]$$
$$\times\exp[-\gamma^2\tau_1^2\cos^2\theta/4b^2]/\tau_1. \quad (28)$$

If distance r_2 were fixed at the equilibrium point, the contribution to the scattering would be $\sin\tau_1/\tau_1$. The hindered rotation introduces not only a shifting in the maxima and minima and a damping term, $(\cos\theta)^{\frac{1}{2}}$, but also an exponential damping term dependent upon s^2. There are six distances of the type r_2 in X_3CCY_3.

When equilibrium occurs in an X_3CCY_3 molecule in the eclipsed position, there are again two different types of interatomic distances affected by the hindered rotation,

$$r_3=(c_1-c_2\cos\phi)^{\frac{1}{2}}$$
and (29)
$$r_4=(c_1-c_2[\phi-2\pi/3])^{\frac{1}{2}}.$$

The contribution to the scattered intensity may be obtained in precisely the same fashion as for the molecule in a staggered configuration at equilibrium. The contribution from r_3 is

$$(\cos\zeta)^{\frac{1}{2}}\sin(sl_1+\zeta/2)/sl_1 \quad (30)$$

where $\tan\zeta=sc_2/4b^2l_1$. The contribution from r_4 is

$$(\cos\delta)^{\frac{1}{2}}\sin[\tau_2+(\mu^2\tau_2\sin^2\delta/4\omega)-\delta/2]$$
$$\times\exp[-\mu^2\tau_2^2\cos^2\delta/4b^2]/\tau_2, \quad (31)$$

where

$$\tan\delta=\omega\tau_2/b^2,$$
$$\omega=c_2/8(c_1+c_2/2)+3(c_2/[c_1+c_2/2])^2/32,$$
$$\tau_2=s(c_1+c_2/2)^{\frac{1}{2}},$$

and

$$\mu=3^{\frac{1}{2}}c_2/4(c_1+c_2/2).$$

Molecules of biphenyl and its derivatives, ethylene and its derivatives, and partially substituted ethanes also exhibit hindered rotation. In general those molecules are not symmetric tops and therefore the internal rotational motion cannot be separated from the over-all rotational motion to give Eq. (3). If the coupling is not too strong, and this may be determined by comparing the values of the principal moments of inertia, it is still legitimate to consider (12) as the correct distribution function arising from the lower lying levels.

For many biphenyl derivatives the equilibrium position probably occurs with the planes of the benzene rings at right angles. In this case the formula to be used is

$$\sin(sc_1^{\frac{1}{2}})\exp[-s^2c_2^2/16c_1b^2]/sc_1^{\frac{1}{2}}. \qquad (32)$$

If the planar configuration is correct for some biphenyl derivatives as it is for ethylene derivatives, formulae (20) and (30) apply. It should be born in mind that the two potential minima may not be the same.

In substituted ethanes the structure problem is rather complicated owing to the existence of a threefold potential which does not have identical minima.[10] For the case of H_2XCCXH_2, the *trans*-configuration has been found to be the more stable one.[3] The restricted rotation formula which applies to this model is (20). It is probably more nearly correct in using (20) to set $\sigma=3$ instead of one, even though it does not have identical minima. The potential barrier V_0 would still signify the energy required to break out of the *trans*-position, but its value might be different than that of the potential barrier at the *cis*-position.

The formulae for hindered rotation occasionally may not be reliable for V_0/RT less than 5 but often may be used for V_0/RT as low as 3. This estimate is based on the requirement that the distribution function $P'(\phi)$ should damp out fast enough to justify the replacement of $1-\cos\sigma\phi$ by $(\sigma\phi)^2/2$ in (4), and also damp out fast enough to allow the approximated interatomic distances as in (16) and (22) to yield valid results when s becomes as large as 20.

[10] For an excellent discussion of this problem see reference 1, p. 346.

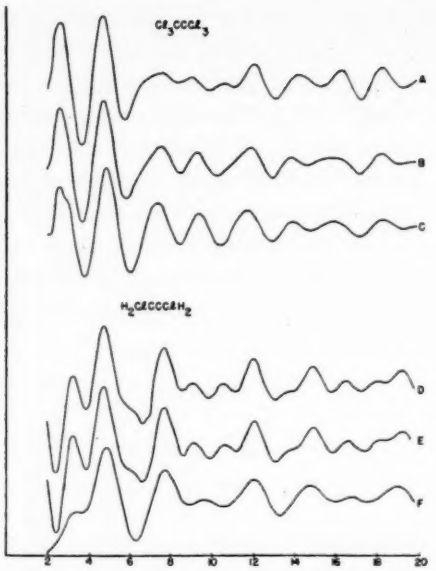

FIG. 1. Variation of scattering pattern with changes in V_0/RT for Cl_3CCCl_3 and $H_2ClCCClH_2$. V_0/RT is equal to ∞ in *A* and *D*, 5 in *B* and *E*, and zero in *C* and *F*. The hydrogen distances in $H_2ClCCClH_2$ were not included in the calculations. The abscissa is given in s units.

It is interesting to compare the effects of restricted rotation on distances whose equilibrium positions are *trans*, *cis* or intermediate. *Trans*- and *cis*- formulae are represented by (20) and (30), respectively, whereas (28), (31), and (32) represent various intermediate positions. The exponential damping factor in the latter three formulae should be noted. Owing to this term the contribution to the scattering from intermediate distances affected by hindered rotation is largely damped out, whereas that from the *cis*- and *trans*-positions is relatively unchanged. This may be related to the case of free rotation in which the contributions to the scattering arise from the vicinity of the *cis*- and *trans*-positions.

APPLICATION OF THEORY

Electron diffraction offers the possibility of determining the height of the potential barrier restricting rotation in certain molecules. One method, which is probably the least promising,

involves treating the barrier as an additional unknown in fitting theoretical intensity curves of assumed models to observed data. The difficulty with this method is that the number of variables ordinarily involved is too great to permit the establishment of a unique solution. Another method which is based on the radial distribution function has been suggested by Debye.[4] He has shown how the values of the radial distribution function in the vicinity of an equilibrium distance can be related to the probability distribution for that distance, e.g., (12).

Another approach to the problem of evaluating the barrier, which obviates to a large extent the ambiguity which arises in the first method suggested, is to study the changes introduced into the diffraction patterns when the sample of vapor is heated to successively higher temperatures. In favorable cases the ambiguity may be resolved owing to the fact that only a unique combination of structural parameters and potential barrier can fit the diffraction data over a range of temperatures.

Theoretical intensity curves for various values of V_0/RT are plotted for Cl_3CCCl_3 and $H_2ClCCClH_2$ in Fig. 1. Curves *A*, *B*, and *C* refer to Cl_3CCCl_3 and were based on an assumed model in which C−C=1.54A, C−Cl=1.76A and angle Cl−C−Cl was given the regular tetrahedral value. Curves *D*, *E*, and *F* refer to $H_2ClCCClH_2$ and were based on the same model as hexachloroethane by giving angle Cl−C−H the same value as was given to angle Cl−C−Cl. Curves *A* and *D* were calculated from the scattering formula for a rigid molecule, (1), the atomic scattering factors being set equal to the corresponding atomic numbers. Curve *A* was based on a staggered configuration and curve *D* on a *trans*-configuration. These curves represent the scattered intensity when the barrier is very large or the temperature is very low. Curves *B* and *E* were calculated for V_0/RT equal to 5. The contribution from the rigid portion of the molecules was calculated using formula (1). The contribution from the hindered rotation was obtained using formulae (19) and (27) multiplied by the atomic number of chlorine squared, and the proper frequency of occurrence of these terms for the molecules considered. The quantum correction was not introduced and σ was set equal to three. Curves *C* and *F* represent free rotation in the molecules. Formula (1) was used to calculate the contribution from the rigid portions of the molecules and the contribution from the freely rotating portions was calculated from the formulae in reference (5). Additional correction terms to the asymptotic formula of Debye were found to be negligible.

The effect of the internal motion on the scattering patterns of hexachloroethane and 1,2-dichloroethylene is vastly different. A great change in pattern has occurred in the range ∞ to 5 for V_0/RT in hexachloroethane whereas practically no change has occurred for dichloroethylene. If T is about room temperature then V_0/RT equal to 5 means that V_0 is equal to 3 kcal./mole. This is a customary order of magnitude.

We may conclude that electron scattering from some molecules may be sufficiently sensitive to changes in V_0/RT to permit an evaluation of their potential barriers. The possibility of a useful experiment depends upon the magnitude of the barrier, the vapor pressure and the heat stability of the substance as well as the pattern sensitivity. It is perhaps well to emphasize that the determination of the structure of some molecules may be greatly dependent upon proper evaluation of their hindered internal rotations.

Letters to the Editor

THIS section will accept reports of new work, provided these are terse and contain few figures, and especially few halftone cuts. The Editorial Board will not hold itself responsible for opinions expressed by the correspondents. Contributions to this section should not exceed 600 words in length and must reach the office of the Managing Editor not later than the 15th of the month preceding that of the issue in which the letter is to appear. No proof will be sent to the authors. The usual publication charge ($3.00 per page) will not be made and no reprints will be furnished free.

Effect of Temperature on the Mass Spectra of Hydrocarbons

R. E. Fox and J. A. Hipple
Westinghouse Research Laboratories, East Pittsburgh, Pennsylvania
February 26, 1947

SEVERAL years ago one of us reported a marked temperature effect on the relative peak heights observed in the mass spectra of hydrocarbons.[1] As this work has not previously been published, it would appear desirable to describe the experiment now in view of the recent interest expressed in it privately.

Figure 1 shows the ion source of the mass spectrometer tube used in the investigation. The thermocouple on the gas inlet block (3) should provide a fairly good measure of the temperature of the gas emerging from the small slit in it and crossing the electron beam. The ions formed by electron impact are then accelerated through the slits in electrodes (2) and (1) and pass into the conventional analyzer of the sectored-field type. The temperature of (3) was varied by adjustment of a furnace wrapped around the glass envelope of the ion source.

Using a mixture of isobutane and neon, the intensities of various ions in isobutane relative to Ne^{20+} were measured

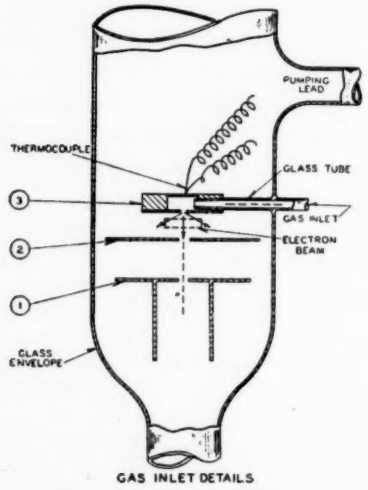

FIG. 1. Arrangement of ion source for studying the effect of temperature on the mass spectra of hydrocarbons.

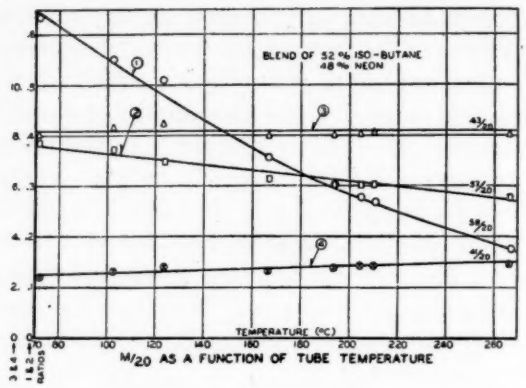

FIG. 2. Variation with temperature of several ions observed in isobutane (neon used as internal standard).

for various values of the temperature of (3). These data are plotted in Fig. 2. It is seen that there is a very marked dependence on temperature of the $C_4H_{10}^+$ ion. In fact, this ion is almost twice as abundant at 70°C as the $C_4H_9^+$ ion, becoming equal to it at approximately 180°C and is relatively less abundant at higher temperatures. Thus, the ratio of these two peaks may be used to measure the temperature of the source. The mass 58 peak in *n*-butane has a similar temperature dependence. Other hydrocarbons show an even greater variation of the spectrum with change of temperature. For instance the parent peak of 2,2,3-trimethylpentane is more than five times as large at 175°C than it is at 225°C. Other peaks in this spectrum show changes that are less pronounced.

[1] J. A. Hipple, reported at the St. Louis meeting of the American Institute of Chemical Engineers, November, 1944.

Decomposition of Solid Barium Nitrate by Fast Electrons*

Augustine O. Allen and John A. Ghormley
Clinton Laboratories, Oak Ridge, Tennessee
February 21, 1947

THE behavior of irradiated salts on solution is an almost unexplored subject, which has become of interest recently in connection with production of radioisotopes.

During 1944, the authors had occasion to irradiate ordinary C.P. grade barium nitrate crystals with a beam of 1.2-Mv electrons from a Van de Graaff generator. On dissolving the irradiated salt in water, copious effervescence occurred, and nitrite was found in the solution.

In one experiment, the salt was irradiated in a small closed glass vessel under helium; the energy dissipated was 1.1 watt-hr./g of salt. After irradiation, the vessel was evacuated and water was admitted; gas was evolved on solution to the extent of 0.9 cc/g of salt. Analysis showed the gas to contain 3 percent of hydrogen; the balance contained no acid gases and was presumed to be oxygen. The solution contained nitrite ion.

In a second experiment, the salt was irradiated while

TABLE I. Formation of gas and nitrite on solution of barium nitrate irradiated with 1.2 Mv electrons at a rate of approximately 1.5 watts/g.

Irrad. time, hr.	% NO_3^- converted to NO_2^-	Gas formed, cc/g (22° C, approx. 73 cm)	Calc. O_2 equiv. to NO_3^- found, cc/g (22° C, 73 cm)
2.8	5.5	5.9	4.9
6.0	10.5	10.1	9.0
9.6	13.0	12.8	11.5
13.0	18.0	16.4	16.0
17.3	21.1	19.0	18.9

spread out on a pan in the open air. The crystals initially turned yellow, but on further irradiation became milky, so that the color was obscured. Samples were taken from time to time and placed in a closed tube, to which water was admitted after evacuation. The gas was not analyzed, but the volumes produced were measured, and the nitrite content of the solutions was determined. Results of the measurements are shown in Table I. Energy was not absorbed uniformly by the salt during the irradiation because of variation of thickness of the salt layer and its distribution on the pan with respect to the electron beam; the rate of energy dissipation was estimated as roughly 1.5 watts/g salt. Solutions of irradiated salt (0.01–0.07M) showed a pH of 9 to 10, and were thus more alkaline than can be accounted for by hydrolysis of nitrite.

At 25 watt-hr./g, about 21 percent of the nitrate had been converted to nitrite. The conversion rate decreased with time, suggesting that a steady state might eventually be reached after 40 percent or more conversion.

Qualitative experiments showed that gas evolution on solution was not greatly reduced by heating the irradiated salt below the melting point, but was entirely prevented by fusion of the irradiated salt. Presumably the gas came out during fusion, but no direct observation was made on this point. Irradiation lowered the melting point of the salt, presumably because of the admixture of nitrite.

Narayanswamy[1] has reported the formation of nitrite near the surface of nitrate crystals illuminated by light of wave-length 2200–2500A. He ascribed the localization of the reaction at the surface to the escape of oxygen gas, assuming that recombination of the products should occur in the interior. In the present experiments, practically all the gas remained trapped in the crystal (as O atoms or O_2 molecules), so that thermal recombination must occur very slowly if at all. Localization of the photolysis must be ascribed to low penetration by the exciting light.

Existence of the photolysis has been ascribed[1] to dissociation of excited NO_3^- ions to NO_2^- ions and O atoms. Under electron bombardment, the same process probably occurs; in addition, many NO_3^- ions will be stripped of one outer electron, forming NO_3 radicals. This radical may later pick up an electron, with a probability of forming NO_2^- and O rather than NO_3^-; or it may decompose thermally to NO_2 and O. The NO_2 may remain as such in the crystal, and hydrolyze on solution to HNO_2+HNO_3; or may pick up an electron to give nitrite ion. The small amounts of hydrogen gas and of alkali are ascribed to reaction with water of electrons which were trapped during irradiation by barium ions, or at vacancies or imperfections in the crystal lattice.

The authors are pleased to acknowledge the help and counsel of Professor Milton Burton, in charge of radiation chemistry at the Metallurgical Laboratory when this work was performed, and Dr. F. J. Safford, in charge of operating the Van de Graaff generator.

* The work described herein was performed at the Metallurgical Laboratory of the University of Chicago under Contract No. W-7401-eng-37 with the Manhattan District.

[1] Narayanswamy, Trans. Farad. Soc. **31**, 1411 (1935).

Structure for Soap Micelles as Indicated by a Previously Unrecognized X-Ray Diffraction Band*

R. W. MATTOON, R. S. STEARNS, AND W. D. HARKINS
George Herbert Jones Chemical Laboratory, University of Chicago, Chicago 37, Illinois
March 10, 1947

MEASUREMENTS on a previously unrecognized x-ray diffraction band B_M suggest that in an aqueous solution the micelle of a soap, or similar colloidal electrolyte, consists of only *one* double layer of soap molecules (Fig. 1). The subscript M designates that an associated spacing d_M measures the approximate thickness of the micelle. Over a range of concentrations of a given soap d_M is apparently constant and about twice the length of the particular molecule involved (Table I).

McBain has considered that soap micelles exist in spherical highly ionic and lamellar weakly ionic forms; whereas, Hartley has considered them as spherical only. Evidence for the lamellar micelle as a stack of double layers of soap molecules, with "bound" water between the double layers, seemed to be given by the x-ray work of Hess, Kiessig, Philippoff, *et al.* (1937–1942). Similar experimental results have been discussed in two papers[1,2] from this laboratory in which extensive references to work on micelle structure are included.

It is now found that the spacing d_M', associated with the new diffuse band, is essentially constant for any given soap, as it should be if it represents the thickness of the double layer. The thickness increases from 36.5A for the 8-carbon atom soap to 58.1A for the 16-carbon atom soap (Table I). This is an increase of 21.6A caused by the addition of 16 C-atoms to the thickness of the double

TABLE I. Spacings in aqueous soap solutions calculated from the position of the peak of the micelle thickness band B_M.

Potassium soap	Bragg spacing[a] d_M ±1A	2 × length of molecule $2l$	Modified Bragg spacing[b] d_M' ±1A
Caprylate, KC_8	29.7	30	36.5
Caprate, KC_{10}	31.7	35	39.0
Laurate, KC_{12}	35.3	40	43.4
Myristate, KC_{14}	40.3	45	49.5
Palmitate, KC_{16}	47.3	50	58.1
Sodium lauryl sulfate[c]	37.3	47	45.9

[a] $d_M=\lambda/(2\sin\theta)$, valid for many diffracting layers.
[b] $d_M'=1.23\lambda/(2\sin\theta)$, valid in the limiting case for two diffracting centers (first maximum of $\sin x/x$). Note that $d_M<2l<d_M'$ for the simple potassium soaps.
[c] Kindly supplied by the Procter and Gamble Company.

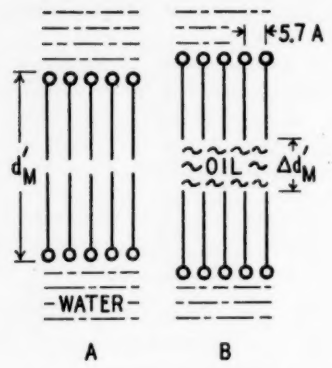

FIG. 1. Cross section of a highly idealized micelle. A. Thickness of micelle $d_M' \approx 50$A for potassium myristate, distance between nearest hydrocarbon chains $d_S' \approx 5.7$A (Bragg spacing $d_S = d_S'/1.23 \approx 4.6$A, molecular area $\sigma = (3)^{\frac{1}{2}} d_S'^2/2 \approx 27$A^2). B. Thickness of solubilized hydrocarbon layer $\Delta d_M' \approx 13$A for benzene.

layer. The increase in double the length of the molecule is 8×2.54, or 20.3A, which is the same within the limit of error of the d_M' measurements.

The short spacing d_S, with a constant Bragg spacing of about 4.6A, is essentially independent both of the length of the soap molecule and of the absence or presence of oil solubilized in the micelle. This distance corresponds to a molecular area of $27A^2$ in a plane perpendicular to the chains.

The lowest soap concentration at which the micelle thickness band B_M has thus far been measured is 1.3 percent by weight of potassium palmitate. The band B_I, related to the inter-micelle distance d_I, begins to be noticeable above concentrations of about 9 percent potassium laurate and about 7 percent potassium myristate. The d_I spacing, which steadily decreases with removal of water, is always larger than d_M'. The behavior of the three bands B_S, B_M, and B_I with respect to position, intensity, and width, all as a function of the particular soap and its concentration, seems to substantiate the following viewpoint. The micelle consists of *one* double layer of soap molecules from which the band B_M arises. As the concentration increases both the size and number of micelles probably increase. This means that the micelles are becoming closer together and a short-range order between micelles becomes more probable. This condition gives rise to the B_I band.

When a hydrocarbon is solubilized in a soap solution, the thickness d_M' of the micelle is increased an amount $\Delta d_M'$ (Fig. 1). This gives additional evidence that d_M' represents the thickness of the micelle. For example, potassium laurate solutions saturated with ethyl benzene give a $\Delta d_M'$ of about 6A; potassium myristate solutions saturated with *n*-heptane give about 11A and saturated with benzene about 13A. These relations will be presented in detail later.

In connection with this work the writers wish to thank Professor P. Debye for helpful advice.

* This investigation was carried out under the sponsorship of the Reconstruction Finance Corporation, Office of Rubber Reserve, in connection with the Government's synthetic rubber program.

[1] W. D. Harkins, R. W. Mattoon, and M. L. Corrin, J. Am. Chem. Soc. **68**, 220 (1946).

[2] W. D. Harkins, R. W. Mattoon, and M. L. Corrin, J. Colloid Sci. **1**, 105 (1946).

Sound Velocity and the Temperature Change of Molecular Association in Water

ALFRED WEISSLER
Naval Research Laboratory, Washington, D. C.
March 10, 1947

TWO empirical criteria for molecular association in liquids, proposed recently by Lagemann,[1] are based on sound velocity. Unfortunately, one of these incorrectly predicts an increase in association with increase in temperature, and the other makes no prediction.

Another quantity involving sound velocity appears better suited for providing information on temperature changes of molecular association. The molar sound velocity $R = Mv^{\frac{1}{3}}/d$ (where M is molecular weight, and v and d are sound velocity and density measured at the same temperature) was found by M. R. Rao[2] to be a temperature-independent constant for normal, non-associated liquids. But for water, and to a lesser extent such liquids as methyl alcohol and acetone, R increases considerably with temperature. It seems probable that R would remain constant even for these materials if the calculation utilized the effective M (which diminishes as association decreases) rather than the chemical-formula M. If this is true, increases in $v^{\frac{1}{3}}/d$ are a direct indication of decreases in extent of association.

This is illustrated in Fig. 1, where the relative association (taken as 1.0000 at 0°C), found from the ratio of

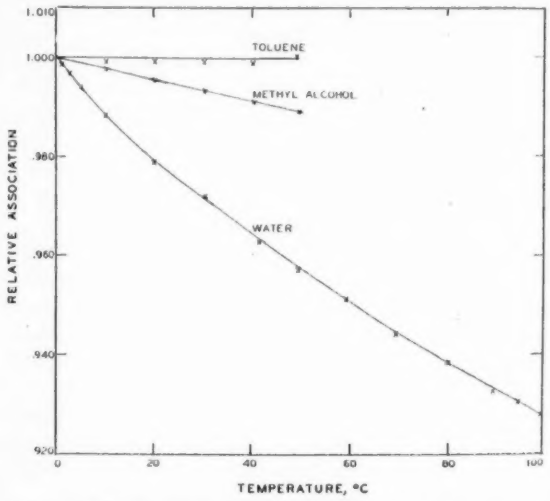

FIG. 1. Relative association of liquids as a function of temperature.

$v_0^{\frac{1}{3}}/d_0$ to $v_t^{\frac{1}{3}}/d_t$, is plotted as a function of temperature t. Water, which is highly associated, undergoes a decrease[3] of about 7.2 percent in association from 0° to 100°; while toluene, which is not associated, shows no appreciable change. Methyl alcohol occupies an intermediate position.

Correlation with the results of other methods is difficult. Over a dozen techniques have been used[4,5] to study the association of water, but the results disagree over a range of hundreds of percent. One detailed investigation,[6] based on Raman spectra, indicates that the association of water decreases by about 13.2 percent from 0° to 98°. However,

molecular aggregates which are stable for only 10^{-14} second will show up in Raman scattering, but the aggregates must be stable for 10^{-6} second in order to be detected by these sound velocity measurements. The latter method would therefore be expected to yield smaller values.

It may be noted, further, that absolute values of association cannot be obtained from the ratio of observed to calculated molar sound velocities. This is true because the bond increments for calculating R already include the associating tendency due to, for example, the $-OH$ group.

[1] R. T. Lagemann, J. Chem. Phys. **12**, 464 (1944).
[2] M. R. Rao, Ind. J. Phys. **14**, 109 (1940).
[3] The values used, for sound velocity in water, were those recently determined at one megacycle in this Laboratory by Miss Patricia E. Mortell.
[4] N. E. Dorsey, *Properties of Ordinary Water Substance* (Reinhold Publishing Corporation, New York, 1940), p. 166.
[5] O. Fruhwirth, Monats. f. Chemie **70**, 157 (1937).
[6] I. R. Rao, Proc. Roy. Soc. **A145**, 489 (1934).

Non-Ionic Detergents as Association Colloids Giving Long X-Ray Spacings in Aqueous Solution

JAMES W. MCBAIN AND SULLIVAN S. MARSDEN, JR.
Department of Chemistry, Stanford University, California
March 4, 1947

SOAPS and other ionic detergents in solution diffract x-rays so definitely as to demonstrate the presence of lamellar micelles. These lamellar micelles expand to take in layers of hydrocarbons when the latter are solubilized in the detergent solutions. It has not been known whether such lamellar colloidal particles exist in solutions of non-ionic detergents. It is the purpose of this note to establish that non-ionic detergents also exhibit similar long spacings on x-ray examination in aqueous solution.

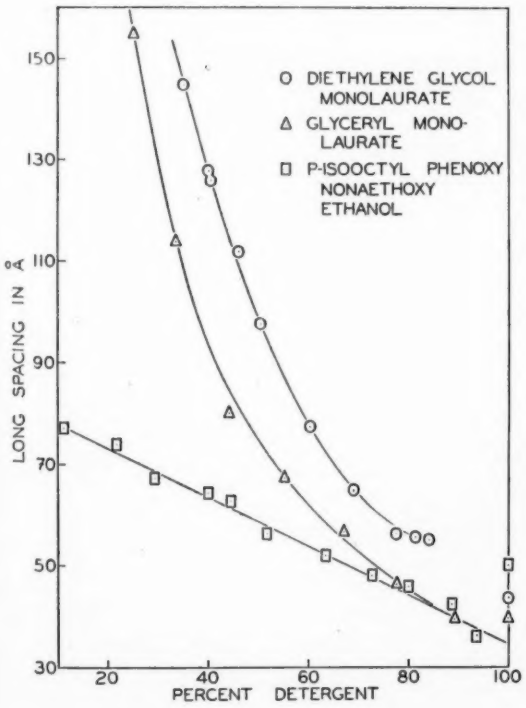

FIG. 1.

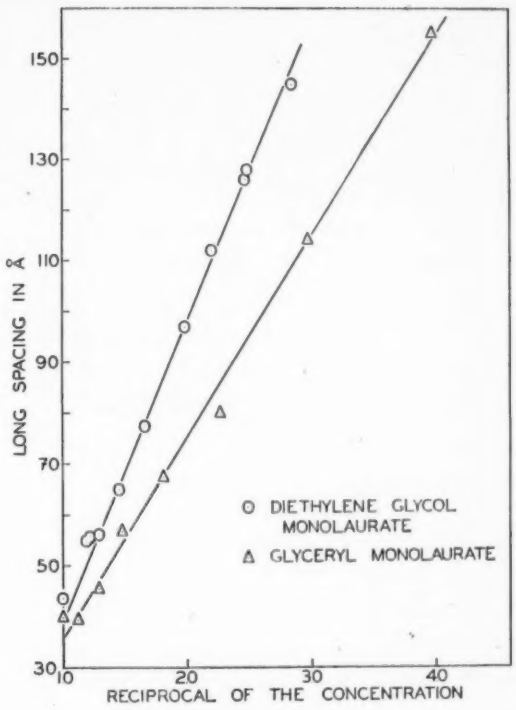

FIG. 2.

The spacings observed are of the order of 40 to 150A and their value depends upon the concentration, as shown in the accompanying graphs.

Para-isooctyl phenoxy nonaethoxy ethanol.—This is the condensation product of *p*-isooctyl phenol with ethylene oxide. Solutions of this material in water are all isotropic solutions exhibiting anomalous viscosity.[1] They produce x-ray diffraction patterns consisting of one or two orders of a very long spacing. There is also a broad halo due to side spacings with its maximum density at 4.5A. The long spacing of the solutions increases almost linearly with decrease in concentration, as shown in Fig. 1. This is similar to the now well-known behavior of ionic detergents in water. The liquid material itself does not give a pattern at room temperature but, when cooled to below its melting point, it gives a long spacing of 50A, which agrees well with the calculated value.

Diethylene glycol monolaurate.—This surface active agent is supplied by Glyco Products Company, Inc. In aqueous systems at concentrations from about 35 percent to 85 percent, it forms two phases: one is isotropic and gives no long spacing; the other is liquid crystal and gives a long spacing which varies as the reciprocal of the concentration of the diethylene glycol monolaurate (see Fig. 2). This is decidedly in contrast with the behavior of ionic detergents. The material is not a pure chemical; the impurities are not completely known and so their effect on the long spacing has not been determined.

Glyceryl monolaurate.—This is supplied by Glyco Products Company, Inc., as a white wax-like solid, and contains soap as a slight impurity. Its aqueous systems are also liquid crystalline and give long spacings which vary as the reciprocal of the concentration of the glyceryl monolaurate.

Additional work is being done in this laboratory on the preparation and examination of pure non-ionic compounds of this type. This, together with a detailed description of the above work, will be reported elsewhere.

[1] Karl Baedeker, Kolloid. Zeits. **94**, 161 (1941).

Errata: Lattice Energies, Equilibrium Distances, Compressibilities, and Characteristic Frequencies of Alkali Halide Crystals

[J. Chem. Phys. **5**, 143 (1937)]

MAURICE L. HUGGINS
Kodak Research Laboratories, Rochester, New York

March 7, 1947

IN columns 2 and 3 of Table I, M' should be 12.

In the fourth line of the second column on page 144, the equation should be $\epsilon = -\frac{9}{4}h\nu_{max}$.

In Eq. (3a), $(1+k_2)$ should be replaced by k_2.

In Eq. (3b), a in front of the bracket should be replaced by k_2.

The heading of column 7 of Table III should be $\frac{1}{\beta}\left(\frac{\partial\beta}{\partial T}\right)_P$.

The calculated compressibility values listed in columns 20 and 21 of Table III are incorrect. The correct values, together with the experimental values from column 19, are given below.

Formula	β exp. (ref. 16) 10^{-12} barye^{-1}	β (Eq. (2)) 10^{-12} barye^{-1}	β (Eq. (4)) 10^{-12} barye^{-1}
LiF	1.17	1.31	1.82
LiCl	3.41	3.35	3.27
LiBr	4.31	3.82	3.71
LiI	6.01	4.12	4.28
NaF	2.11	2.18	2.61
NaCl	4.263	4.56	4.29
NaBr	5.08	5.21	4.81
NaI	7.07	6.29	6.06
KF	3.30	3.17	3.66
KCl	5.63	6.16	6.01
KBr	6.70	7.13	6.81
KI	8.54	8.35	7.99
RbF	4.1	3.97	3.88
RbCl	6.65	7.00	6.25
RbBr	7.94	8.08	7.20
RbI	9.57	9.64	8.74
CsF	4.25	5.51	4.86
CsCl	5.95	5.89	5.57
CsBr	7.06	6.88	6.56
CsI	8.57	8.13	8.28